

UNIVERSITY OF CALIFORNIA SANTA BARBARA

The Life Cycle Energy-Water Usage Efficiency of Artificial
Groundwater Recharge Via the Reuse of Treated Wastewater

A DISSERTATION SUBMITTED IN PARTIAL SATISFACTION

OF THE REQUIREMENTS FOR THE DEGREE

OF

DOCTOR OF PHILOSOPHY

IN

ENVIRONMENTAL SCIENCE & MANAGEMENT

BY

ERIC DANIEL FOURNIER

COMMITTEE IN CHARGE

PROFESSOR ARTURO A. KELLER, CHAIR

ASSOCIATE PROFESSOR JAMES FREW

ASSOCIATE PROFESSOR ROLAND GEYER

SEPTEMBER 2015

THIS DISSERTATION IS APPROVED

BY

SIGNATURE: _____

JAMES FREW

SIGNATURE: _____

ROLAND GEYER

SIGNATURE: _____

ARTURO A. KELLER, COMMITTEE CHAIR

SEPTEMBER 2015

The Life Cycle Energy-Water Usage Efficiency of Artificial Groundwater Recharge Via the Reuse of Treated Wastewater

Copyright ©2015

BY

ERIC DANIEL FOURNIER

DEDICATIONS

THIS DISSERTATION IS DEDICATED TO THE MEMORY OF JULIO ARNOLD MUNIZ.

HE WAS MY BEST FRIEND.

ACKNOWLEDGEMENTS

I WOULD LIKE TO THANK MY FATHER PAUL, MY MOTHER PATRICIA, MY BROTHER BRYAN, AND MY GIRLFRIEND TESSA FOR THEIR CONTINUED SUPPORT OF MY EDUCATION. I WOULD ALSO LIKE TO THANK MY PHD COMMITTEE MEMBERS, DR. ARTURO KELLER, DR. JAMES FREW, AND DR. ROLAND GEYER FOR THEIR RESPECTIVE CONTRIBUTIONS TO THE DEVELOPMENT AND SUCCESSFUL COMPLETION OF THIS PROJECT. FINALLY, I WOULD LIKE TO THANK DR. CHARLES DANA TOMLIN FOR INSPIRING ME TO PURSUE A DOCTORATE IN THIS FIELD OF STUDY THROUGH HIS WORK, TEACHING, ELOQUENCE, AND INTEGRITY.

Curriculum Vitae of Eric Daniel Fournier

September 2015

Education

Bachelor of Science in Environmental Science, Bucknell University, Lewisburg, PA, June 2008, (Magna Cum Laude, Phi Beta Kappa)

Master of Environmental Science, Yale School of Forestry and Environmental Science, New Haven, CT, June 2010

Master of Arts in Geography, University of California Santa Barbara, Santa Barbara, CA, March 2015

Employment

2009-2010: Teaching Assistant, Geographic Information Science, Yale School of Forestry and Environmental Science, New Haven, CT

2010-2013: Teaching Assistant, Biogeochemistry, Landscape Ecology, Geographic Information Science, University of California at Santa Barbara, Santa Barbara, CA

Publications

Automating the Preprocessing of Heterogeneous Spatial Data Inputs to Multi-Criteria Site Suitability Analyses, *Environmental Software and Modeling*, Submitted 2015.

MOGADOR revisited: improving a genetic approach to multi-objective corridor search, *Journal of Environmental Planning and Design B*, 2015.

Minimizing impacts of land use change on ecosystem services using multi-criteria heuristic analysis, *Journal of Environmental Management*, 2015.

Spectroscopic investigations of Fe^{2+} complexation on nontronite clay, *Langmuir*, 2007.

Fellowships

Walton Family Foundation Sustainable Water Markets Fellow, Toyota Motor Company Doctoral Fellow, Forestry Scholarship, McKenna Foundation Research Fellow

Specializations

GIS, LCA, Genetic Algorithms, Stochastic Processes, Combinatoric Optimization

ABSTRACT

THE LIFE CYCLE ENERGY-WATER USAGE EFFICIENCY OF ARTIFICIAL GROUNDWATER
RECHARGE VIA THE REUSE OF TREATED WASTEWATER

BY

ERIC DANIEL FOURNIER

This dissertation investigates the dynamic energy-water usage efficiency of civil engineering projects involving the recharge of subsurface groundwater aquifers via the reuse of treated municipal wastewater. For this purpose a three-component integrated assessment model has been developed. The first component uses a cartographic modeling technique known as Weighted Overlay Analysis (WOA) to determine the location and extent of sites that are suitable for the development of groundwater recharge basins given a regional geographic context. The second component uses a novel Genetic Algorithm (GA) to address the multi-objective spatial optimization problem associated with locating corridors for the support infrastructure required to physically transport water from the treatment facility to the recharge site. The third and final component takes data about the anticipated recharge treatment source location, reuse destination location, and proposed infrastructure corridor location and uses them to populate a spatially explicit Life Cycle Inventory (LCI) model capturing all of the process energy consumption associated with the reuse system. Five case studies involving the planning of new basin scale artificial recharge systems within the state of California are presented and discussed.

Contents

o	INTRODUCTION	1
o.1	Research Objectives	2
o.2	The Energy-Water Nexus	3
o.3	Water Distribution Systems	6
o.4	Wastewater Treatment	8
o.5	Wastewater Recycling and Reuse	10
o.6	The Energy-Water Feedback Loop	13
i	SELECTING SUITABLE SITES	16
i.1	Selecting Suitable Sites for Artificial Groundwater Recharge Basins	17
i.2	Multi-Criteria Site Suitability Analyses	17
i.3	The MCSS Data Preprocessing Workflow	18
i.4	The MCSS Computational Workflow	19
i.5	The Software Toolset Repository Architecture	21
i.6	An Example Implementation	23
i.7	The Geographic Unit of Analysis	23
i.8	Graphical User Interface	25

1.9	The WOSS Model Outputs	28
2	LOCATING OPTIMAL CORRIDORS	31
2.1	Locating Optimal Corridors for Water Distribution Infrastructure	32
2.2	The Multi-Objective Corridor Location Problem	33
2.3	Genetic Algorithms	34
2.4	The MOGADOR Algorithm	35
2.5	The MOGADOR Data Structure	37
2.6	Initializing the MOGADOR Algorithm	38
2.7	An Example Pseudo-Random Walk	41
2.8	Initializing Problems with Large Decisions Spaces	43
2.9	Initializing Problems with Concave Decision Spaces	45
2.10	Measuring Initialization Performance	46
2.11	The MOGADOR Algorithm Outputs	50
3	QUANTIFYING LIFE-CYCLE ENERGY-WATER RESOURCE UTILIZATION	51
3.1	Quantifying Life-Cycle Energy-Water Resource Usage Efficiency	52
3.2	Life Cycle Assessment and Inventory Modeling	52
3.3	Wastewater Treatment Processes	54
3.4	Water Distribution Infrastructure	56
3.5	WWEST Recycled Water Reuse Life Cycle Inventory Model	58
3.6	Parameterizing Pump Energy Requirements	59
3.7	Parameterizing Construction Material Requirements	64
3.8	Parameterizing Chemical Consumption Rates	65
3.9	Estimating Net Water Usage Efficiency	65
3.10	The WWEST Model Outputs	66

4	CASE STUDY RESULTS	67
4.1	Santa Barbara Region	68
4.2	Oxnard Region	80
4.3	San Diego Region	91
4.4	Santa Ana – San Bernadino Region	102
4.5	Fresno – Tulare Region	113
4.6	Evaluating the MOGADOR Algorithm’s Runtime Performance	127
4.7	Evaluating the MOGADOR Algorithm’s Solution Quality	127
4.8	Evaluating the MOGADOR Algorithm’s Solution Elevation Profiles	131
4.9	Evaluating the Life-Cycle Water-Energy Usage Efficiencies of Proposed Reuse Systems	132
	APPENDIX A	135
	REFERENCES	273

Listing of figures

1	Perspectives on the Energy-Water Nexus	5
2	Dimensions of the Energy-Water Nexus	6
3	Characteristics of Water Distribution Infrastructure	7
4	Energy Intensity of Water Distribution Infrastructure	8
5	Process Flow Diagram of Wastewater Treatment Methods	10
6	Appropriate End Use Categories for Different Levels of Treated Wastewater	11
7	Water Intensity of Energy Production	14
1.1	Conceptual illustration of the input data preprocessing operations and work- flow phases typical to most MCSS analyses	20
1.2	Control logic for MCSS input data preprocessing workflow.	21
1.3	Directory tree structure for the toolset repository. Filetypes required for in- put data and automatically generated as output data are shown.	22
1.4	Table of input data sources used in the case study MCSS model for artificial groundwater recharge applications.	24
1.5	An overview of Step #1 in the GUI based workflow: parameterizing the ref- erence grid.	26

1.6	An overview of Step #2 in the GUI based workflow: selecting the reference polygon from the overlay shapefile geometry.	27
1.7	An overview of Step #3 in the GUI based workflow: selecting the reference polygon from the overlay shapefile geometry.	28
1.8	Graphical Illustration of the WOSS Model Outputs for Reference HUC-10 Boundary	29
2.1	MOGADOR Algorithm Pseudocode.	37
2.2	MOGADOR Algorithm Data Structure	38
2.3	Pseudo-Random Walk Algorithm Pseudocode	40
2.4	Pseudo-Random Walk Example	42
2.5	Conceptual Illustration of a Multi-Part Pseudo-Random Walk	44
2.6	Conceptual Illustration of a Convex Multi-Part Pseudo-Random Walk	46
2.7	Observing the Role of the Fixed Parameter q in Determining Individual Path Randomness	48
2.8	Observing the Role of Problem Size on Initialization Runtime	48
2.9	Observing the Characteristics of Multi-Part Pseudo-Random Walks	50
3.1	WWEST Model System Boundaries	59
4.1	Santa Barbara Region Overview	69
4.2	Santa Barbara Region Search Domain	70
4.3	Santa Barbara Region Destination Search Inputs: Slope Scores	71
4.4	Santa Barbara Region Destination Search Inputs: Geology Scores	71
4.5	Santa Barbara Region Destination Search Inputs: Landuse Scores	72
4.6	Santa Barbara Region Destination Search Outputs: Composite Scores	72
4.7	Santa Barbara Region Destination Search Outputs: Candidate Regions	73
4.8	Santa Barbara Region Proposed Corridor Endpoints	73
4.9	Santa Barbara Region Accessibility Based Objective Scores	75

4.10	Santa Barbara Region Land Use Disturbance Based Objective Scores	75
4.11	Santa Barbara Region Slope Based Objective Scores	75
4.12	Santa Barbara Region Corridor Analysis Results	77
4.13	Santa Barbara Region Top 100 Corridors Basin Wide Overview	78
4.14	Santa Barbara Region Proposed Corridor Elevation Profile	79
4.15	Oxnard Region Overview	82
4.16	Oxnard Region Search Domain	83
4.17	Oxnard Region Destination Search Inputs: Slope Scores	83
4.18	Oxnard Region Destination Search Inputs: Geology Scores	84
4.19	Oxnard Region Destination Search Inputs: Landuse Scores	84
4.20	Oxnard Region Destination Search Outputs: Composite Scores	85
4.21	Oxnard Region Destination Search Outputs: Candidate Regions	85
4.22	Oxnard Region Proposed Corridor Endpoints	86
4.23	Oxnard Region Accessibility Based Objective Scores	87
4.24	Oxnard Region Land Use Based Disturbance Objective Scores	87
4.25	Oxnard Region Slope Based Objective Scores	88
4.26	Oxnard Region Corridor Analysis Results	89
4.27	Oxnard Region Top 100 Corridors Basin Wide Overview	89
4.28	Oxnard Region Proposed Corridor Elevation Profile	90
4.29	San Diego Region Overview	93
4.30	San Diego Region Search Domain	94
4.31	San Diego Region Proposed Corridor Endpoints	95
4.32	San Diego Region Accessibility Based Objective Scores	96
4.33	San Diego Region Land Use Disturbance Based Objective Scores	97
4.34	San Diego Region Slope Based Objective Scores	98
4.35	San Diego Region Corridor Analysis Results	99

4.36	San Diego Region Top 100 Corridors Basin Wide Overview	100
4.37	Santa Diego Region Proposed Corridor Elevation Profile	101
4.38	Santa Ana – San Bernadino Region Overview	103
4.39	Santa Ana – San Bernadino Region Search Domain	104
4.40	Santa Ana – San Bernadino Region Destination Search Inputs: Slope Scores	105
4.41	Santa Ana – San Bernadino Region Destination Search Inputs: Geology Scores	105
4.42	Santa Ana – San Bernadino Region Destination Search Inputs: Landuse Scores	106
4.43	Santa Ana – San Bernadino Region Destination Search Outputs: Compos- ite Scores	107
4.44	Santa Ana – San Bernadino Region Destination Search Outputs: Candidate Regions	107
4.45	Santa Ana – San Bernadino Region Proposed Corridor Endpoints	108
4.46	Santa Ana – San Bernadino Region Accessibility Based Objective Scores . .	109
4.47	Santa Ana – San Bernadino Region Land Use Disturbance Based Objective Scores	109
4.48	Santa Ana – San Bernadino Region Slope Based Objective Scores	110
4.49	Santa Ana – San Bernadino Region Corridor Analysis Results	111
4.50	Santa Ana – San Bernadino Region Top 100 Corridors Basin Wide Overview	112
4.51	San Bernadino Region Proposed Corridor Elevation Profile	112
4.52	Fresno – Tulare Region Overview	114
4.53	Fresno – Tulare Region Search Domain	115
4.54	Fresno – Tulare Region Destination Search Inputs: Slope Scores	116
4.55	Fresno – Tulare Region Destination Search Inputs: Geology Scores	116
4.56	Fresno – Tulare Region Destination Search Inputs: Landuse Scores	117
4.57	Fresno – Tulare Region Destination Search Outputs: Composite Scores . .	118
4.58	Fresno – Tulare Region Destination Search Outputs: Candidate Regions . .	119

4.59	Fresno – Tulare Region Proposed Corridor Endpoints	120
4.60	Fresno – Tulare Region Accessibility Based Objective Scores	121
4.61	Fresno – Tulare Region Land Use Disturbance Based Objective Scores	122
4.62	Fresno – Tulare Region Slope Based Objective Scores	123
4.63	Fresno Region Corridor Analysis Results	124
4.64	Fresno Region Top 100 Corridors Basin Wide Overview	125
4.65	Fresno Region Proposed Corridor Elevation Profile	126
4.66	Algorithm Runtime Performance for Each of the Five Case Study Regions for Three Population Sizes	128
4.67	Algorithm Convergence Rates for Each of the Five Case Study Regions for Three Population Sizes	129
4.68	Comparison of the Along Path Distance and Cumulative Objective Scores be- tween the Solution Corridors and the Euclidean Shortest Corridors	130
4.69	Comparison of the Along Corridor Elevation Profiles for each of the Solution Corridors	131
4.70	Comparison of the Net Water Usage Efficiencies of Reuse for each of the Case Study Regions Measured in Terms of Both the Withdrawals and Consump- tion of Water for the Production of Energy Required for Reuse	134

*We have arranged a civilization in which most crucial
elements profoundly depend upon science and technology.*

Carl Sagan (1934-1996)

0

Introduction

0.1 RESEARCH OBJECTIVES

THE OVERARCHING RESEARCH OBJECTIVE of this dissertation can be stated as follows: develop an integrated modeling framework, incorporating data depicting local geographic context, that is capable of quantifying the life-cycle energy-water usage efficiency of proposed new infrastructural systems supporting the reuse of treated municipal wastewater for the purpose of artificial groundwater recharge. In order to achieve this goal the following three canonical problems were identified and addressed in sequential order:

1. Given multiple independent objectives – propose a systematic method for selecting sites that are suitable for the development of new artificial groundwater recharge infrastructure.
2. Given multiple independent objectives – propose a systematic method for routing optimal corridors for new water distribution infrastructure linking a designed treated effluent source to a designated recharge destination.
3. Given a fixed influent flow rate, a set of mean influent pollutant concentrations, a set of maximum effluent pollutant concentrations, and the topological structure of the effluent distribution network – propose a systematic method for determining the life-cycle energy-water usage efficiency of an integrated wastewater reuse system

The remainder of this Chapter (o) provides an in-depth background discussion of the both the academic and social relevance of the stated research objective. Subsequent Chapters (1-3) are organized with respect to the various independent research activities that were undertaken to address each of the three canonical problems listed above. The final Chapter (4) provides an in depth analysis of a set five case study implementations that were developed to assess the framework's efficacy in satisfying the stated research objective.

0.2 THE ENERGY-WATER NEXUS

Nearly all modern industrialized societies rely upon energy generation technologies which are derivative of a thermodynamic process known as a heat engine. In a typical heat engine the chemical energy stored within a fuel source such as coal, petroleum, or natural gas, must be first be released as ambient thermal energy through the process of combustion. The heat engine then, by virtue of its design, converts this ambient thermal energy into mechanical energy for the purpose of performing some sort of meaningful work – i.e. generating electricity.

The history of the advancement of the human species is a story which can be cast in terms of the progressive discovery new, higher density chemical energy stores and their enhanced exploitation via the development of new, ever more sophisticated heat engines^{34,35}. Interestingly however, is the fact that nowhere in our history has there ever occurred a single substantial deviation in the choice of the working fluid that actually performs the crucial energy conversion process within a heat engine: water. For all of the advances which have been made in terms of improved fuel processing, boiler and combustion chamber design, etc., so long as our energy economy continues to rely upon carbon based fuels, water will continue to remain stubbornly positioned as a critical component of nearly all major commercial scale energy systems.

As interesting aside, although much of the current rhetoric which is used to support a large scale shift towards renewable energy technologies focuses on the benefits of decarbonization; another key benefit of renewable energy technologies, which may be of equal or greater value going on into the future, is the dramatically reduced water intensity relative to that of traditional heat engine based systems. For example, just as photovoltaic electricity generation systems are associated with minimal carbon emissions, so too do they not require substantial inputs of water to facilitate their operation. This is something to watch

out for in the future, particularly in the context of long term infrastructure scale planning excises such as the one that shall be introduced as part of this dissertation.

Another technological system which can also be viewed as a foundation pillar of modern industrialized societies is the mechanized disposal of human and animal wastes via engineered sewage conveyance and treatment processes³. Here again, the advancement of the human species might alternatively be cast in terms of the progressive improvement in the reliability and efficiency of these systems over time. Furthermore, just as the advancement of our energy system appears to be bounded by the physical properties of the water, so too has the advancement of wastewater management been similarly constrained.

For example, in terms of water treatment processes, the upper bound on process efficiency is determined by *The Second Law of Thermodynamics*. This law states that, for any closed system, there is a tendency for the entropy of that system to increase over time⁴³. *Ceteris paribus*, wastewater, a heterogeneous mixture, possesses higher entropy than pure water does. This means that any attempt to purify a polluted wastewater stream must necessarily incur the cost of some energy input to facilitate the requisite reduction in entropy.

In terms of water distribution processes, the key physical determinant of energy efficiency stems from the density of water. At 1000 kg/m^3 , considerable energy must be expended whenever large quantities of water must be moved over a distance or lifted against an elevation gradient. Many treatment processes utilize pressurized sieving techniques where water is physically pushed through a porous membrane in order to forcibly remove dissolved pollutant species. As a consequence of this practice, the energy inputs required to overcome the previously mentioned entropic gradient are often supplied for the immediate purpose of moving quantities of water from place to place.

The energy-water nexus is a term which has emerged from within the academic research community to describe these types of dynamic interrelationships which are inherent to our energy and water systems. There are two perspectives from which the energy-water nexus

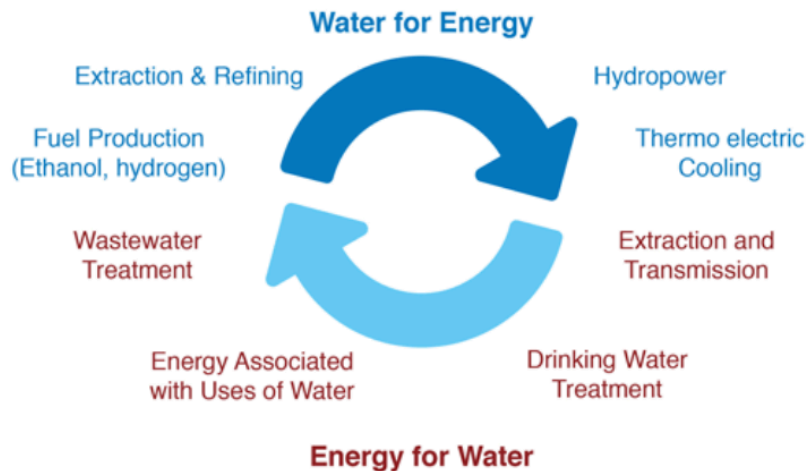


Figure 1: Perspectives on the Energy-Water Nexus⁶⁰

can be alternatively studied. The first emphasizes the *water for energy* dimension, and is generally concerned with the study of processes and technologies that are involved with the direct withdrawal and consumption of water for the production of both primary and final energy resources. The second of these perspectives, focuses alternatively on the *energy for water* dimension; investigating processes and technologies which consume energy for the purpose of transmitting or purifying freshwater resources.

Here in the United States, approximately 50% of total annual freshwater withdrawals are used for the cooling of thermoelectric power plants. Alternatively, roughly 4% of the nation's total energy consumption is dedicated to the transmission and purification of water and wastewater. While these national figures speak to the overall significance of this issue, the situation becomes more acute when one begins to consider different regional contexts.

The criticality of the energy-water nexus becomes greatly exacerbated in those areas where either water is scarce, energy is scarce, or both. Unfortunately, the state of California suffers from both of these conditions to varying degrees, making the energy-water nexus a frequent source of regional interest within both the academic research and socio-political

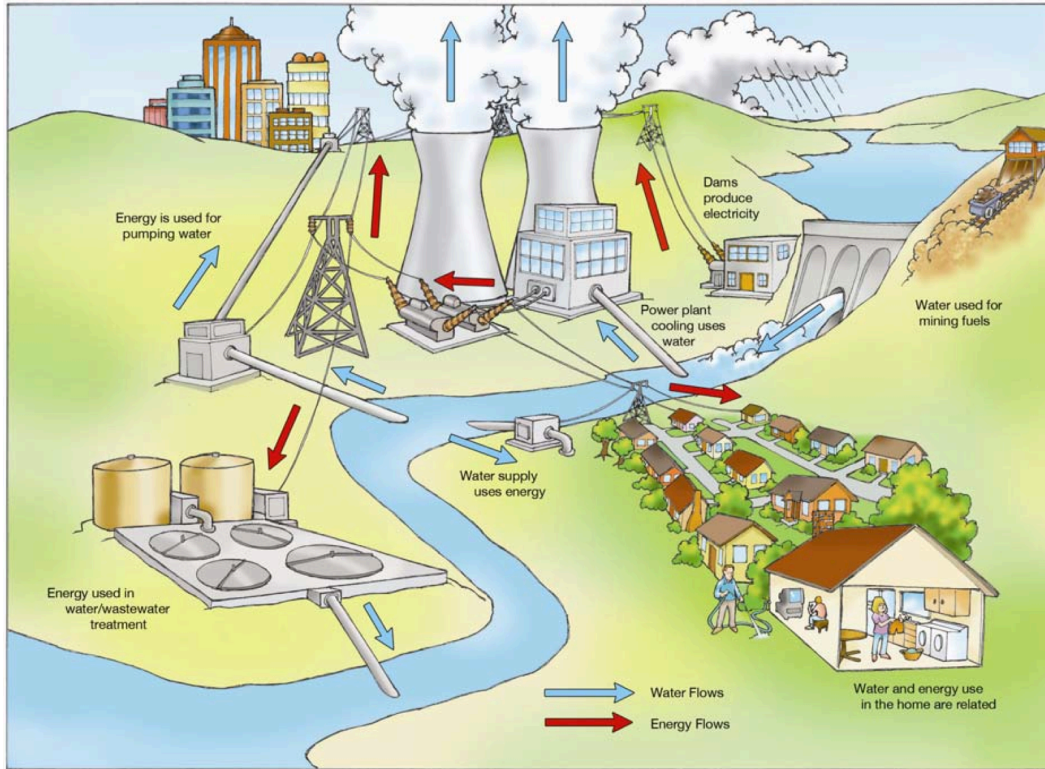


Figure 2: The dimensions of the energy-water nexus⁶⁰

circles. For example, in a 2005 report published by the California Energy Commission (CEC) it was found that 19% of the electricity and 32% of the natural gas consumed within the entire state were used for purpose directly related to the supply and treatment of freshwater resources⁴⁰.

0.3 WATER DISTRIBUTION SYSTEMS

One of the main drivers for of this tremendous energy consumption within the state of California is the large scale transfer of freshwater resources between physically distinct hydrologic basins. California is crossed latitudinally by a massive network of interconnected hydraulic engineering projects including pipelines, aqueducts, reservoirs, and pump stations⁶⁷. These systems, which have been funded by a mixture of Federal, State, and Local

agencies, were designed to reconcile discontinuities between the spatial and temporal distributions of the supply and demand for freshwater resources within the state³⁰.



Figure 3: The geographic extent of water distribution infrastructure in the state of California⁶⁷

Inter-basin transfers typically involve the movement of water against a considerable elevation gradient. Due to water’s previously mentioned high density, there are substantial energetic costs associated with operating the infrastructure required to facilitate these transfers. For example, the bar graph to the right of Figure 4 compares the energy intensity of

several different sources of municipal water within the state of California⁸¹. According to this research water resources which are supplied via inter-basin transfer, either through branches of the State Water Project or through the Colorado River Aqueduct, rank very poorly in terms of energy usage efficiency relative to a number of other water supply systems.

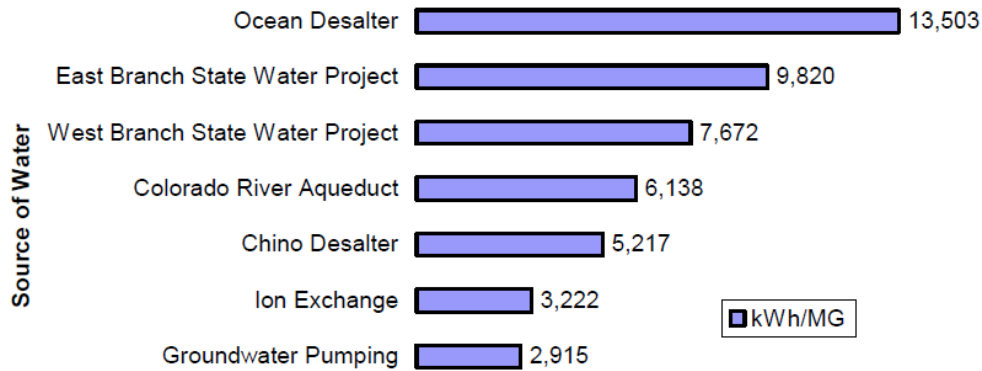


Figure 4: The geographic extent of water distribution infrastructure in the state California⁴⁶

0.4 WASTEWATER TREATMENT

The term *wastewater treatment* refers to a set of physical and chemical processes that have been individually designed and are collectively composed for the purpose of removing a suite of physical, chemical, and/or biological contaminants from a quantity of water⁵⁴. The operational goal of a wastewater treatment process is typically defined in terms of a set of desired effluent pollutant concentrations that are sufficiently low to enable that effluent to be used for a specific end-use application⁴. Crucially implicit in this definition therefore, is the notion that the precise combination and configuration of the individual, atomic treatment processes, will vary on the basis of the purity requirements associated with the anticipated end-use application. Figure 5 provides a high level view of the separate treat-

ment processes that are typical to modern wastewater treatment facilities; assigning them to a somewhat informal hierarchy consisting of: primary treatment, secondary treatment, and tertiary treatment⁴.

The collection of processes described in Figure 5 represent the required suite of treatment operations necessary to produce effluent water that is suitable for groundwater recharge applications (also known as: indirect potable reuse) given a normal stream of influent municipal wastewater. Typically, wastewater treatment plants (WWTPs) – normal in the sense that they are producing treated effluent from generic municipal sources for release into natural surrounding environs – are only required to provide up to a secondary treatment level⁴. This level of treatment, on the diagram provided in Figure 5, corresponds to the fourth row of processes from the top. As the figure shows, providing treated effluent for reuse applications necessitates the implementation of as many as seven additional layers of tertiary treatment in order to manage issues such as suspended colloids, disinfection, and phosphorous removal⁷⁶.

This hierarchy of treatment processes depicted in Figure 5 is only meant to be representative of the types of processes that are typically required for reuse applications. In reality however, neither the rigid segregation of treatment processes nor the association of each treatment level with a set of designated end-uses have been precisely codified into a coherent regulatory framework at the Federal level. In general, primary and secondary treatment are Federally mandated as part of the generic WWTP under provisions of the Clean Water Act^{23,12}. However, tertiary treatment processes and requirements for their application in the context of different desired end-use applications, are, at present, regulated at the state or local levels in a more ad-hoc manner. Figure 6 attempts to illustrate the complexity of this landscape by mapping treatment levels to different end-use types, with annotations where additional restrictions may apply^{23,65}.

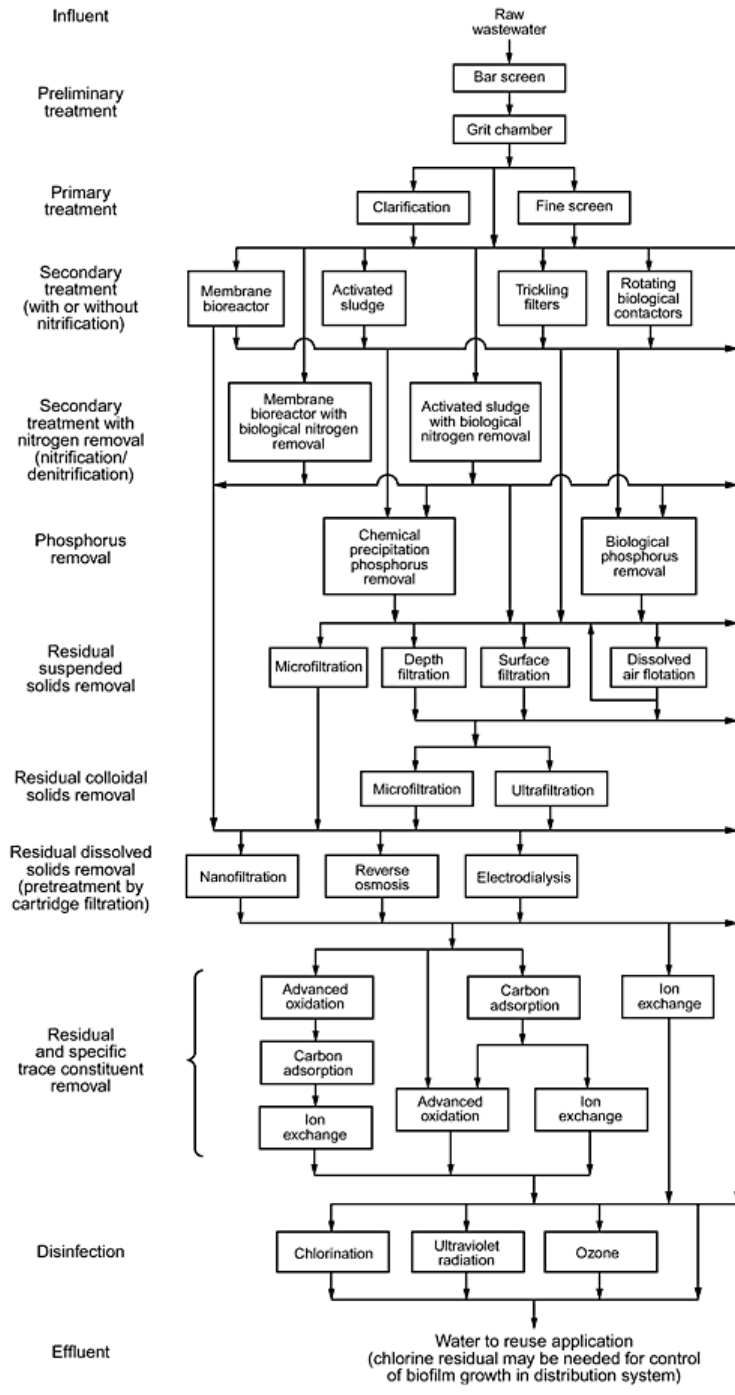


Figure 5: Process flow diagram of various wastewater treatment methods⁴

0.5 WASTEWATER RECYCLING AND REUSE

Over the past ten years the reuse of treated wastewater has emerged as the fastest growing source of new water supply for municipal water districts in the Western United States^{27,80}.

<i>Types of Use</i>	<i>Treatment Level</i>		
	<i>Disinfected Tertiary</i>	<i>Disinfected Secondary</i>	<i>Undisinfected Secondary</i>
Urban Uses and Landscape Irrigation			
Fire protection	<input checked="" type="checkbox"/>		
Toilet & urinal flushing	<input checked="" type="checkbox"/>		
Irrigation of parks, schoolyards, residential landscaping	<input checked="" type="checkbox"/>		
Irrigation of cemeteries, highway landscaping		<input checked="" type="checkbox"/>	
Irrigation of nurseries		<input checked="" type="checkbox"/>	
Landscape impoundment	<input checked="" type="checkbox"/>	<input checked="" type="checkbox"/> *	
Agricultural Irrigation			
Pasture for milk animals		<input checked="" type="checkbox"/>	
Fodder and fiber crops			<input checked="" type="checkbox"/>
Orchards (no contact between fruit and recycled water)			<input checked="" type="checkbox"/>
Vineyards (no contact between fruit and recycled water)			<input checked="" type="checkbox"/>
Non-food bearing trees			<input checked="" type="checkbox"/>
Food crops eaten after processing		<input checked="" type="checkbox"/>	
Food crops eaten raw	<input checked="" type="checkbox"/>		
Commercial/Industrial			
Cooling & air conditioning - w/cooling towers	<input checked="" type="checkbox"/>	<input checked="" type="checkbox"/> *	
Structural fire fighting	<input checked="" type="checkbox"/>		
Commercial car washes	<input checked="" type="checkbox"/>		
Commercial laundries	<input checked="" type="checkbox"/>		
Artificial snow making	<input checked="" type="checkbox"/>		
Soil compaction, concrete mixing		<input checked="" type="checkbox"/>	
Environmental and Other Uses			
Recreational ponds with body contact (swimming)	<input checked="" type="checkbox"/>		
Wildlife habitat/wetland		<input checked="" type="checkbox"/>	
Aquaculture	<input checked="" type="checkbox"/>	<input checked="" type="checkbox"/> *	
Groundwater Recharge			
Seawater intrusion barrier	<input checked="" type="checkbox"/> *		
Replenishment of potable aquifers	<input checked="" type="checkbox"/> *		
<i>*Restrictions may apply</i>			

Figure 6: Appropriate End Use Categories for Different Levels of Treated Wastewater⁴⁶

There are a variety of reasons for this growth trend. For example, some districts enjoy the degree of self determinism that ownership of a reuse system affords them; particularly in cases where they are beholden to a the whims of a third party water wholesalers or are junior water right holders within their basin. In general however, the primary driving force behind the increased interest in reuse has been down to the fact that treated municipal wastewater is perceived to be an efficient means of new water supply for a number of low quality end use cases^{45,14}.

If one looks at existing reuse systems, these assumptions regarding system efficiencies ap-

pear to be valid. This is because the vast majority of reuse systems which have been implemented to date have taken advantage of favorable circumstances such as where the destination location for the treated effluent is positioned in fairly close proximity to the WWTP. An illustrative example of such a situation might be the use of wastewater which had been subjected to basic secondary treatment for the irrigation of a nearby cemetery or golf course. These types of reuse systems can be thought of as low hanging fruit because the only additional energy process based energy expenditures associated with their operation come from whatever tertiary treatment processes must be added into the WWTP operations to meet the effluent purity requirements associated with the designated end-use.

More recently however, many municipalities have begun to actively investigate the possibility of expanding both the scale and extent of their reuse operations: capturing larger fractions of their WWTP plants' throughput and distributing the treated effluent to a more diverse portfolio of end-use recipients. Among these proposed new end-use applications, perhaps the most attractive has been for artificial groundwater recharge.

An artificial groundwater recharge operation is one which takes some stream of input water, it need to necessarily be treated wastewater, and either passively or forcefully introduces it to the subsurface aquifer¹⁰. The goal of this process is typically undertaken to remedy a condition of overdraft wherein the aquifer has been subjected to increased rates of withdrawals, decreases rates of natural infiltration, or both⁶⁹. Typically artificial groundwater recharge systems adopt one of two approaches in terms of the mechanism by which they physically deliver the water back to the subsurface. The first approach is passive – involving the construction of one or more large scale infiltration basins into which water is pumped and then allowed to percolate into the subsurface through a porous media under the force of gravity⁵⁸. The second approach is active – involving the construction of one or more pump wells through which water is forced into the subsurface under the action of a mechanized pump⁵⁸.

Due to the considerable cost associated with pump operation as well as the limited recharge capacity associated with each individual wellhead, recharge basins have, up until this point, proven to be far and away the more attractive of the two options in terms of existing facilities. The primary exemption to this rule being locations where the reason that the recharge operations have been undertaken is create a target increase in subsurface hydrostatic pressure for the purpose of mitigating the encroachment of brackish water into the aquifer – which can often occur in coastal regions – or for the purpose of halting or redirecting the movement of some subsurface groundwater pollutant plume⁶⁴.

Despite the fact that artificial recharge basins take advantage of the force of gravity to introduce the water back into the subsurface they can still be expected to be associated with fairly large operational energy requirements. This is because, for a host of practical engineering as well as political and economic constraints, recharge basins tend not to be constructed as close to the source of their supply water as one might initially think. As a result, considerable amounts of energy must be continually invested to pump water, often against an elevation gradient, from its source of production to the recharge basin where it will ultimately be consumed for the purpose of artificial groundwater recharge.

0.6 THE ENERGY-WATER FEEDBACK LOOP

The suggestion that all forms of artificial groundwater recharge are likely to be associated with non-trivial process based energy demands leads to an interesting question regarding the net life-cycle energy utilization efficiency of reuse systems. This question stems from an understanding of the water usage intensity of various electricity generation technologies can vary significantly and is often much higher than one might initially expect.

For example, Figure 7 plots the water usage intensity – measured in terms of units of water consumed per unit of electric power produced – for a suite of electricity generation

technologies that make up a substantial portion of the municipal energy generation portfolio here in the United States⁶. As Figure 7 illustrates, depending upon the details of how electricity is produced in a given region, artificial groundwater recharge operations that utilize heavily treated municipal wastewater as their source feedstock have the potential to be associated with significant process energy related water consumption levels at the point of electricity production.

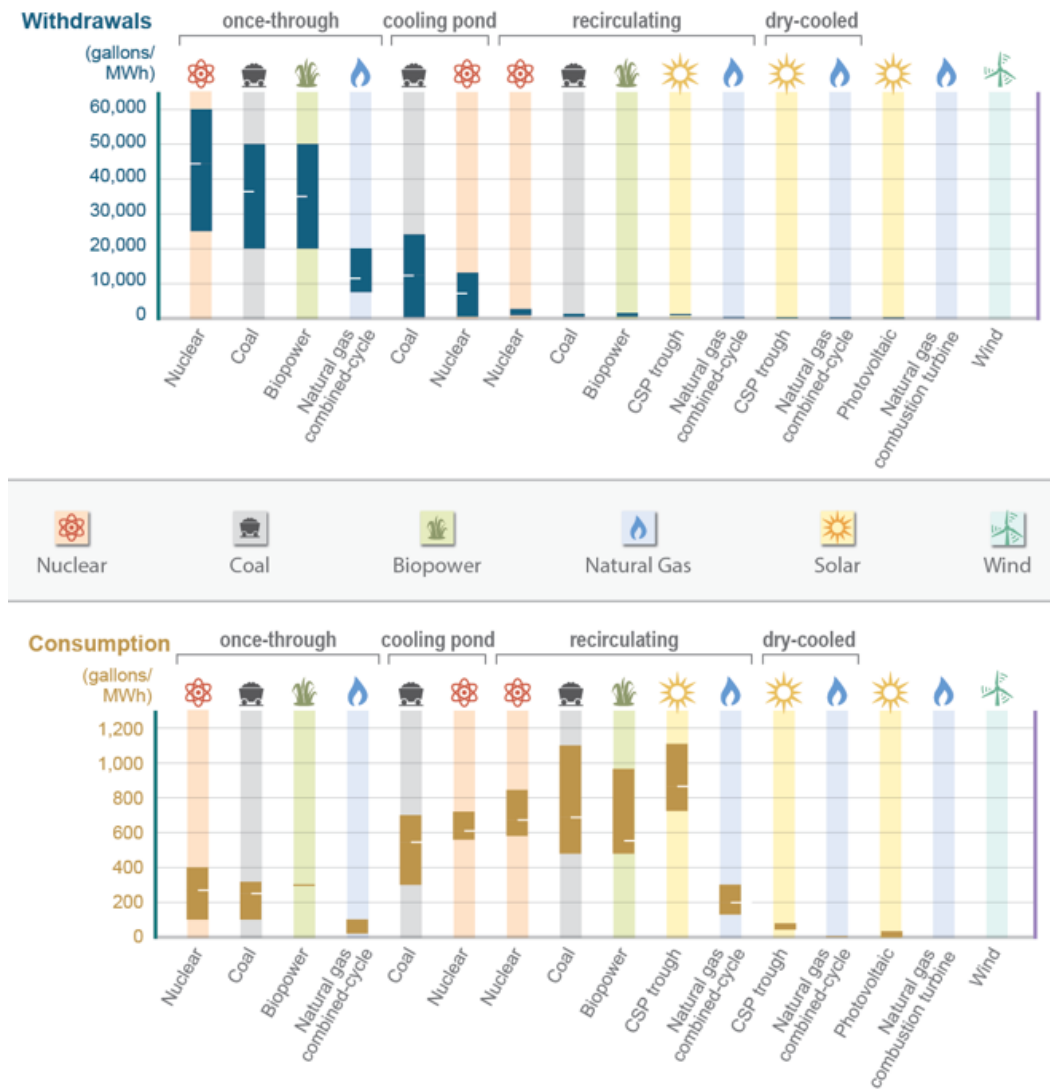


Figure 7: The water consumption intensity, measured in terms of water consumed per unit of electric power produced, for various electricity generation technologies⁶

In light of the presence of this significant feedback loop, the hypothesis that this dissertation has been designed to test is whether or not there exists a specific set of circumstances in which it may be possible for municipal wastewater reuse systems involving a substantial artificial groundwater recharge components to produce a situation where they are saving some water locally, but at the cost of consuming more water regionally. This hypothesized negative net water savings, at the regional scale, would therefore be the result of water consumption which is embedded in the energy that must be imported to facilitate the reuse and recharge operations.

*Do not lose your faith – for a mighty fortress is our
mathematics. It shall rise to the occasion. It always has.*

Stanislaw Ulam (1909-1984)

1

Selecting Suitable Sites

1.1 SELECTING SUITABLE SITES FOR ARTIFICIAL GROUNDWATER RECHARGE BASINS

THE FIRST PRINCIPLE CHALLENGE which must be overcome in an attempt to quantify the life-cycle energy water usage efficiency of a proposed new water reuse system involving artificial groundwater recharge is the need to develop of a systematic method for selecting sites that are suitable for the construction of the requisite recharge basins. This problem of *selecting suitable sites*, relative to one or more criteria of suitability, is one which is extremely common within the domain of Geographic Information Science (GIScience). And indeed, the need to develop consistent methodologies and capable tools for achieving this purpose were among the core research goals which initially stimulated the early development of the field^{78,77?}.

1.2 MULTI-CRITERIA SITE SUITABILITY ANALYSES

One methodology which has emerged as a reliable means of approaching this type problem, and the one which was adopted for the purposes of this dissertation, is a procedure known as multi-criteria site suitability (MCSS) analysis. MCSS analyses mathematically combine two or more input geographic data layers that each correspond to some independent measure of site suitability for a given landuse application⁹. The output of this MCSS computation is a single geographic data layer in which the value at each location represents a composite measure of overall site suitability relative to all of the independent criteria, simultaneously^{38,22}.

MCSS analyses are typically conducted using geographic information that has been stored in a continuous raster format. This means that prior to conducting this type of analysis each of the input geographic data layers that are to be used must be preprocessed relative to some reference raster format so as to ensure the feasibility and consistency of the

MCSS computation. For example, in order for the computation to be feasible: all of the input data layers must have the same number of cells and occupy that same geographic extent. Similarly, in order for the computation to be consistent: the ordinality and the scaling of the values in each raster must accurately reflect the relative weighting and directionality of each independent suitability criterium.

Geographic information system (GIS) software packages are commonly used to conduct both these types of data preprocessing operations as well as the MCSS computation itself⁵². This is because they provide pre-built functions which facilitate the import of spatial data layers from disparate sources as well as the manipulation of geographic data layers such that they satisfy the previously mentioned feasibility and consistency constraints. Often, the MCSS analyses itself is not the endpoint goal of a given research effort however. Many times, MCSS analyses are used as inputs to some other, more complex, numerical optimization model¹⁸. This situation is frequently encountered in the fields of operations research (OR) and location science (LS) where MCSS outputs are used to derive network topologies or linear programming constraints for optimization problems related to vehicle routing, flow maximization, or facility location^{45,19}.

1.3 THE MCSS DATA PREPROCESSING WORKFLOW

The generic data preprocessing workflow for MCSS analysis involves one or more of the three phases illustrated conceptually in Figure 1.1. First, all of the input spatial data layers must be checked to determine whether or not they possess the same coordinate system. If they do not, a single reference coordinate system must be chosen by the analyst to function as the standard for all of the input layers. The choice of this reference coordinate system is generally driven by the scale of spatial domain involved as well as the desired tradeoff between distance versus areal measurement error. The output of this *Reproject* operation is a

set of duplicate data layers that are all projected as the reference coordinate system.

The second phase of the workflow involves clipping the various input data layers on the basis of their overlap with some reference spatial extent. This reference extent may correspond to the boundaries of a single input layer or may be arbitrarily designated by the analyst. The output of this *Clip* operation is a set of duplicate data layers that all have the same spatial extent as the reference extent.

The third and final phase of the workflow involves rasterizing all of the input layers such that they have the same cell size and cell alignment. During this phase, input data layers that are stored using a different geographic data model must be algorithmically converted into a raster based representation. As part of this algorithmic conversion process, a reference cell size, usually corresponding to the largest cell size contained within the input data layers, is used as a reference. The output of this *Rasterize* operation is a set of duplicate layers that all share the same cell size and cell alignment as the designated reference.

1.4 THE MCSS COMPUTATIONAL WORKFLOW

Instead of executing the MCSS data preprocessing steps manually for each of the five case study regions that were going to be investigated as part of this dissertation, the decision was made to implement a more generic data preprocessing software framework which enable any researcher – not necessarily the author of this dissertation – to conduct a similar analysis for any region in which sufficient input data was available. These tools, which shall be described in subsequent sections, were implemented in the the MATLAB[®] programming environment and have been made publicly available as a source code repository hosted at: <https://github.com/ericdfournier/WOSS>. The control flow logic which guided their development is described in the pseudocode in Figure 1.2.

Prior to the initiation of any MCSS analysis the researcher must provide a set of raw spa-

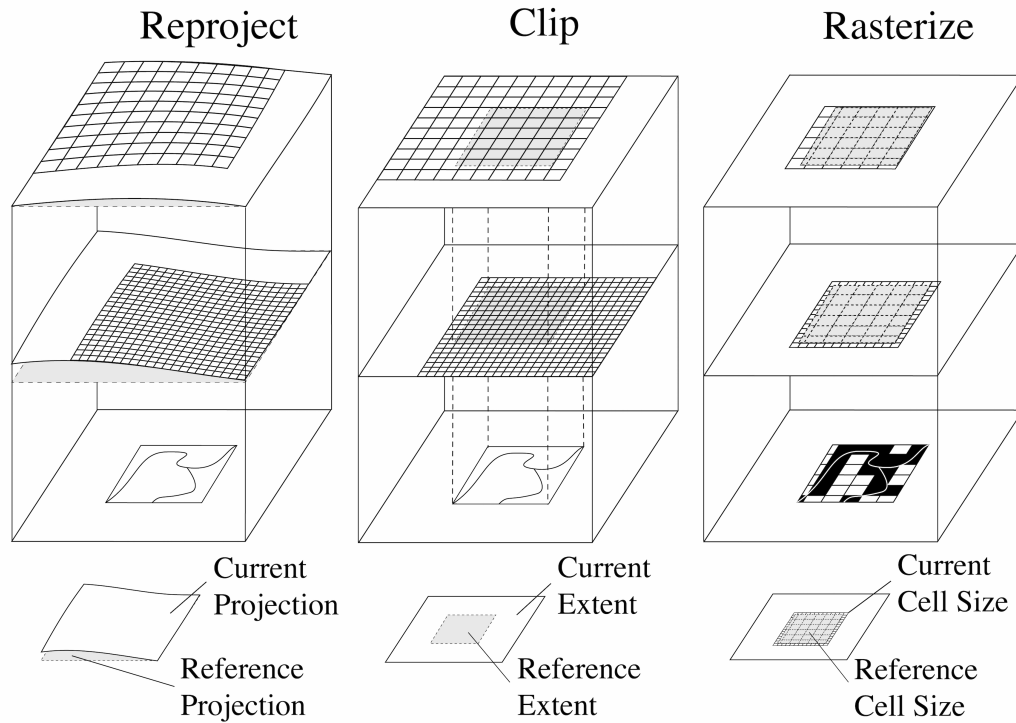


Figure 1.1: Conceptual illustration of the input data preprocessing operations and workflow phases typical to most MCSS analyses

tial data input files and designate a set of spatial reference criteria. Once these requirements are met, all of the input spatial data files are then subjected to a sequence of conditional statements. Depending upon the result of these conditional statement evaluations various transformation functions are then sequentially applied to the input data files so as to produce a set of outputs whose projection, spatial extent, cell size, and cell alignment all match a set of designated spatial reference criteria.

The current version of the toolset only supports the reprojection of input spatial data layers that are represented using geographic coordinates – i.e. data stored in latitude & longitude coordinate space. This constraint not only limits the directionality of the reprojection operation but also greatly simplifies the spatial interpolation routines required for the rasterization process. The authors plan to lift this restriction in future versions of the toolset as the MATLAB[®] language’s native support for forward map projection as well as

```

1: procedure PREPROCESS INPUT DATA
2:   for all input do
3:     if  $input_{prj} \neq reference_{prj}$  then
4:        $input = Reproject(input)$ 
5:     else if  $input_{ext} \neq reference_{ext}$  then
6:        $input = Clip(input)$ 
7:     else if  $isRaster(input_{type}) \neq True$  then
8:        $input = Rasterize(input)$ 
9:     else if  $input_{cs} \neq reference_{cs}$  then
10:       $input = Resize(input)$ 
11:    end if
12:     $output = input$ 
13:  end for
14:  return output
15: end procedure

```

Figure 1.2: Control logic for MCSS input data preprocessing workflow.

the automated parsing of standard formatted spatial reference data strings improves.

Following the preprocessing of the spatial data inputs, the next phase of the MCSS modeling process is the user guided reclassification of the data values in each layer into a quantitative measure of suitability for the land use application in question. Routines are provided in the toolset to facilitate this process. Among these are an automated histogram equalization based reclassification procedure which assigns suitability values ensuring an even distribution of all the values contained within some range across all of the areas within the spatial data layer. Other tools allow the user to manually specify the range of the bins used for the reclassification of raw input data values to site suitability rankings.

1.5 THE SOFTWARE TOOLSET REPOSITORY ARCHITECTURE

The directory structure of the WOSS toolset repository is illustrated in Figure 1.3. Below the top level root directory are four standalone files: (1) a *LICENSE.md* file, (2) a *README.md* file, (3) a *GUI.m* file and (4) *GUI.fig* file. The first two files contain the software license and general repository usage guidance, respectively. The third and fourth, are

the source code files supporting the standalone graphical user interface that visually guides a user through this same data preprocessing workflow.

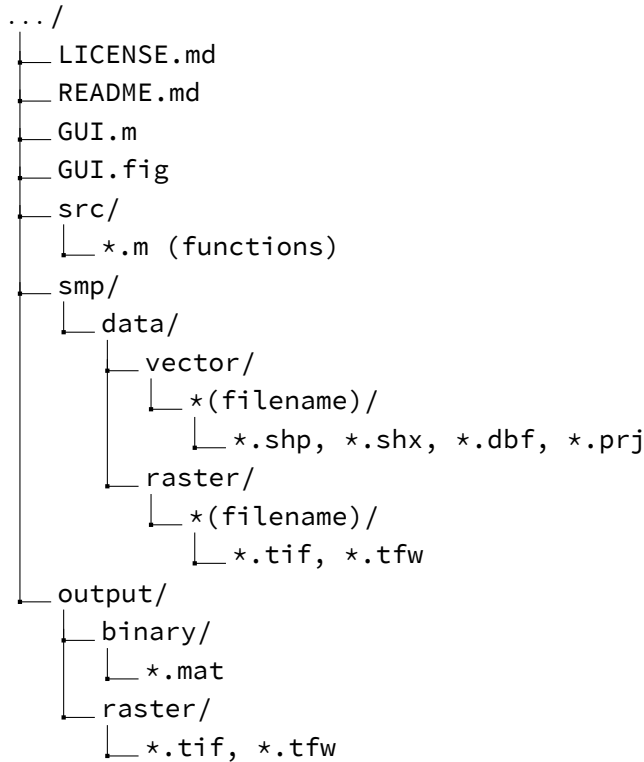


Figure 1.3: Directory tree structure for the toolset repository. Filetypes required for input data and automatically generated as output data are shown.

Also below the top level root directory are the following three subdirectories: (1) *src/*, (2) *smp/*, (3) *output/*. The *src/* directory contains the MATLAB[®] source code m-files comprising the toolset's various functions. The *smp/* directory contains MATLAB[®] .m-file scripts that can optionally be called to automate the execution of multiple data preprocessing workflows. The */smp/data/* directory contains two sub-directories: *vector/* and *raster/*. Each of these houses the corresponding sub-directories, one for each vector and raster based raw input spatial data files provided by the user. The tiles used for each of these **(filename)* sub-directories are automatically assigned to the outputs generated by the tool. The supported vector input filetype is the ESRI shapefile format. Alternatively, the supported

raster input file type is the open source GeoTiff format. Finally, the *output/* directory contains two sub-directories: *binary/* and *raster/*. These subdirectories comprise the default destination locations for all of the outputs generated by the toolset tools. Outputs can be produced in either the mat-file MATLAB[®] ASCII-binary format or in the same GeoTiff format as the input raster data.

The toolset supports the use of composite raster data sets which are made up of multiple, possibly overlapping, individual raster data tiles. It does this by performing a bounding box intersection test for each input raster data tile with the reference spatial domain. For those tiles whose bounding boxes are found to intersect that of the reference domain, values are iteratively compiled into a new composite mosaic data layer made up of, potentially several, individual tiles. This makes it possible to use input raster data layers that are of arbitrarily high resolution covering large geographic domains.

1.6 AN EXAMPLE IMPLEMENTATION

The raw input datasets which were selected for the example implementation were collected from several publicly available sources. A brief topical description of each source as well as a link to its source web repository is given in Figure 1.4. In addition to these raw input data sources, a number of derived data products are generated automatically from the digital elevation model (DEM) for use in this particular case study analysis. These derived products include: slope & aspect.

1.7 THE GEOGRAPHIC UNIT OF ANALYSIS

The geographic unit of analysis selected for this example implementation is the US Geologic Survey (USGS) Hydrologic Unit Code (HUC) level five watershed. Specifically, the level five watershed areas contained within the administrative boundaries of the state of

Type	Category	Source
Vector	Resource Areas	Cal-Atlas
Vector	County Boundaries	Cal-Atlas
Vector	Surface Geology	Cal-Atlas
Vector	Road Network	Cal-Atlas
Vector	STATSGO Soils	USGS
Vector	State Park Boundaries	Cal-Atlas
Vector	Stream Reaches	National Map
Vector	Street Network	Cal-Atlas
Vector	Surface Water Storage	Cal-Atlas
Raster	Crop Data Layer	USDA
Raster	Digital Elevation Model	National Map
Raster	NLCD Landcover	National Map

Figure 1.4: Table of input data sources used in the case study MCSS model for artificial groundwater recharge applications.

California. According to the USGS:

*The United States is divided and sub-divided into successively smaller hydro-logic units which are classified into four levels: regions, sub-regions, accounting units, and cataloging units. The hydrologic units are arranged or nested within each other, from the largest geographic area (regions) to the smallest geographic area (cataloging units). Each hydrologic unit is identified by a unique HUC consisting of two to twelve digits based on the levels of classification in the hydro-logic unit system.*⁶⁸

The level five designation within this HUC framework is comprised of closed contiguous regions possessing an average area of 588 square kilometers. These level five HUC designated areas are often referred to as the HUC-10 watersheds because of their use of a ten digit unique numerical identification code. Within the state of California, there are 1,040 individual HUC-10 watersheds. These watersheds are non-overlapping and have been derived algorithmically from the national elevation dataset by USGS scientists according to

the method described by⁶⁸.

1.8 GRAPHICAL USER INTERFACE

The WOSS toolset can be interactively parameterized via the the GUI depicted in Figure 1.5. The GUI is presented as a three step workflow, with each step building iteratively upon the product of the previous one to generate a final composite output. The first step involves the user providing the directory location of the shapefile from which the reference geometry will be selected. The user is presented with the option of specifying an alternative *Overlay Shapefile* that can be used to aid in the selection of this reference area. The second step involves the use of this overlay shapefile to generate an interactive map window that will appear to the user once it is time for the reference boundary to be selected. It should be noted that the reference shapefile always provides the source data from which the actual selection is made.

Next, the user is then prompted to input parameter values for two fields. The first corresponds to the grid density that will be used to generate all of the output layers. The default setting for this parameter is 1,169.99. This grid cell density roughly corresponds to cells that are (100 m x 100 m) or 10,000 m² within the latitude range bounding the state of California. The second input parameter value corresponds to the attribute field name in the reference shapefile that will be used for the output reference grid encoding. The attribute field must be of numerical type.

Once the user correctly provides all of these inputs they are then allowed to move onto the second step of the workflow which by clicking on the *Select Reference Boundary* button. During this step a map axis is generated in which the geometry information for the overlay shapefile is drawn on screen as shown in Figure 1.6. The user may then select their desired reference polygon by simply clicking on the appropriate location within the map.

Browse	Edit Reference Shapefile Path	
Browse	Edit Overlay Shapefile Path	
Enter Grid Cell Density (Cells/Degree Latitude)	1116.99	
Enter Reference Shapefile Attribute Field	Field Name	
Select Reference Boundary		

Figure 1.5: An overview of Step #1 in the GUI based workflow: parameterizing the reference grid.

The latitude longitude coordinates corresponding to this selection are automatically used to extract the containing polygon from the reference shapefile. This polygon is then automatically converted to a reference grid with the cell density and attribute field encoding parameters designated by the user.

The third step of the GUI based workflow, shown in Figure 1.7, involves the user providing the directory locations of the various spatial data inputs that are to be processed. These inputs should be organized according to the general directory layout described in the preceding section. Once these top level directory locations have been provided, the names of the raw input data layers are automatically populated into the accompanying tables and the users are prompted to provide one more parameter value for each vector and raster data category. For the raw input raster datasets, the users are requested to input to the table the numerical encoding of any *NaN* values. If none is present the field may simply be left blank. For the raw input vector datasets, the users are requested to input the text encoded name of the attribute fields on the basis of which the output grid layers will be encoded. Here again, as with the generation of the reference grid, these attribute field names should correspond to numerically encoded values.

Following successful completion of the various data processing steps the user is then

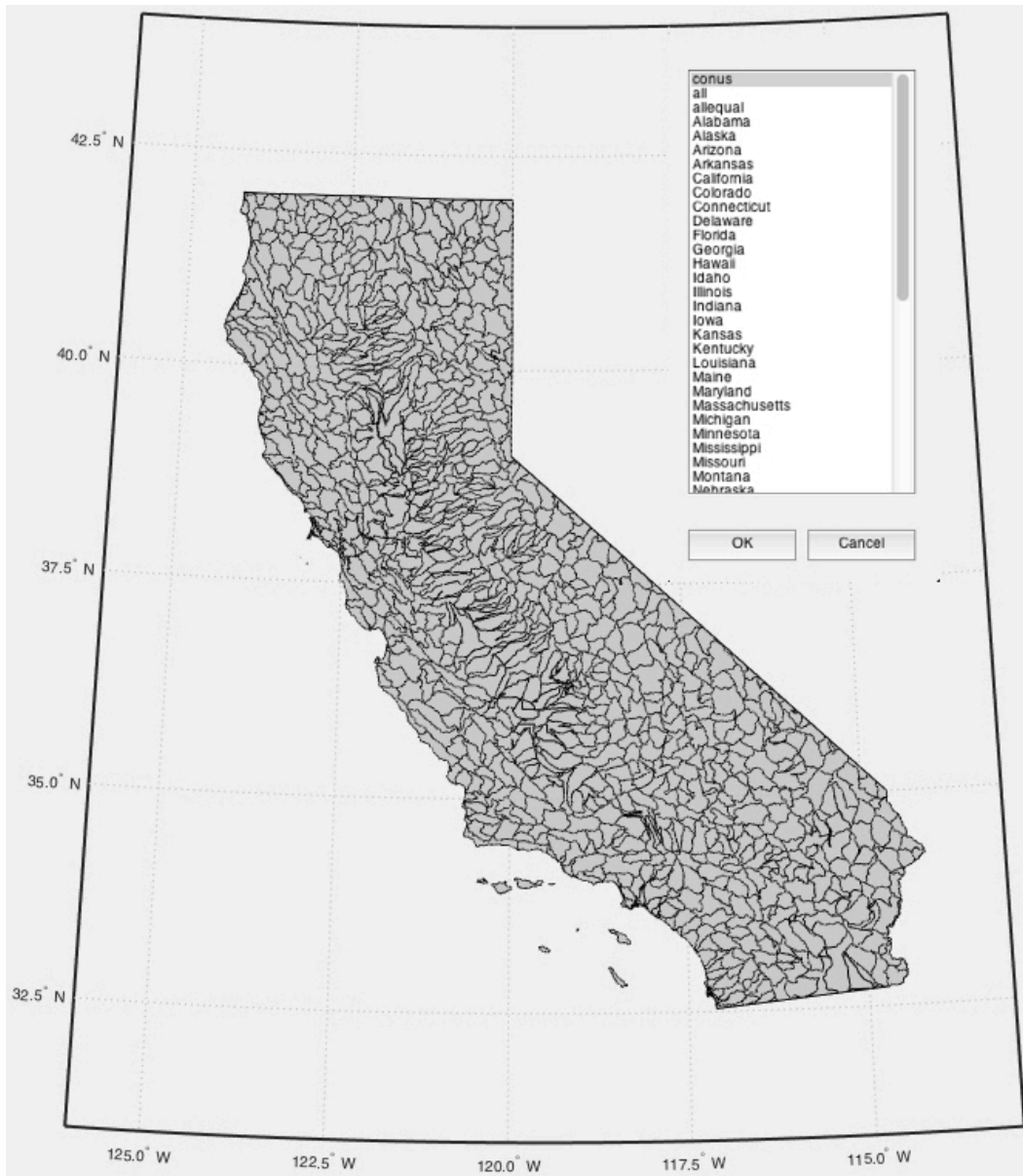


Figure 1.6: An overview of Step #2 in the GUI based workflow: selecting the reference polygon from the overlay shapefile geometry.

allowed to choose whether they want to save the output layer stack directly into the MATLAB workspace via the *Extract Data to Workspace* button, or to disk in a file encoded as either as a set of GeoTiff (.tiff) formatted rasters or a single MATLAB binary (.mat) via the *Extract Data to File* button.

Browse		Edit Top Level Raster Data Directory Path	
	Raster Sub-Directory Name	Raster NaN Code (Optional)	
1			
2			
3			
4			

Browse		Edit Top Level Vector Data Directory Path	
	Vector Sub-Directory Name	Vector Attribute Name	
1			
2			
3			
4			

Extract Data to File	Extract Data to Workspace
-----------------------------	----------------------------------

Figure 1.7: An overview of Step #3 in the GUI based workflow: selecting the reference polygon from the overlay shapefile geometry.

1.9 THE WOSS MODEL OUTPUTS

Figure 1.8 illustrates a set of sample outputs that were generated by the data preprocessing components of the toolset for an example HUC-10 reference boundary. The reference boundary can either be selected manually, by calling a function which prompts the user to click on map with all of the HUC-10 boundaries drawn on it, or automatically, by specifying the 10-digit code corresponding to the desired HUC-10 watershed. The toolset processes generate an output layer stack – the individual component layers of which are illustrated in the colored inset map panels. Only layers for which there is at least one non-empty data value are included in the generated outputs. Thus, the number of output components may vary depending upon the coverage of the input data layers relative to the domain of the reference boundary. For vector data inputs, the values which are contained in the output are those corresponding to a single attribute field selected by the user. This field must

be either a real or coded numeric data type as the raster data format does not support the native representation of categorical variables.

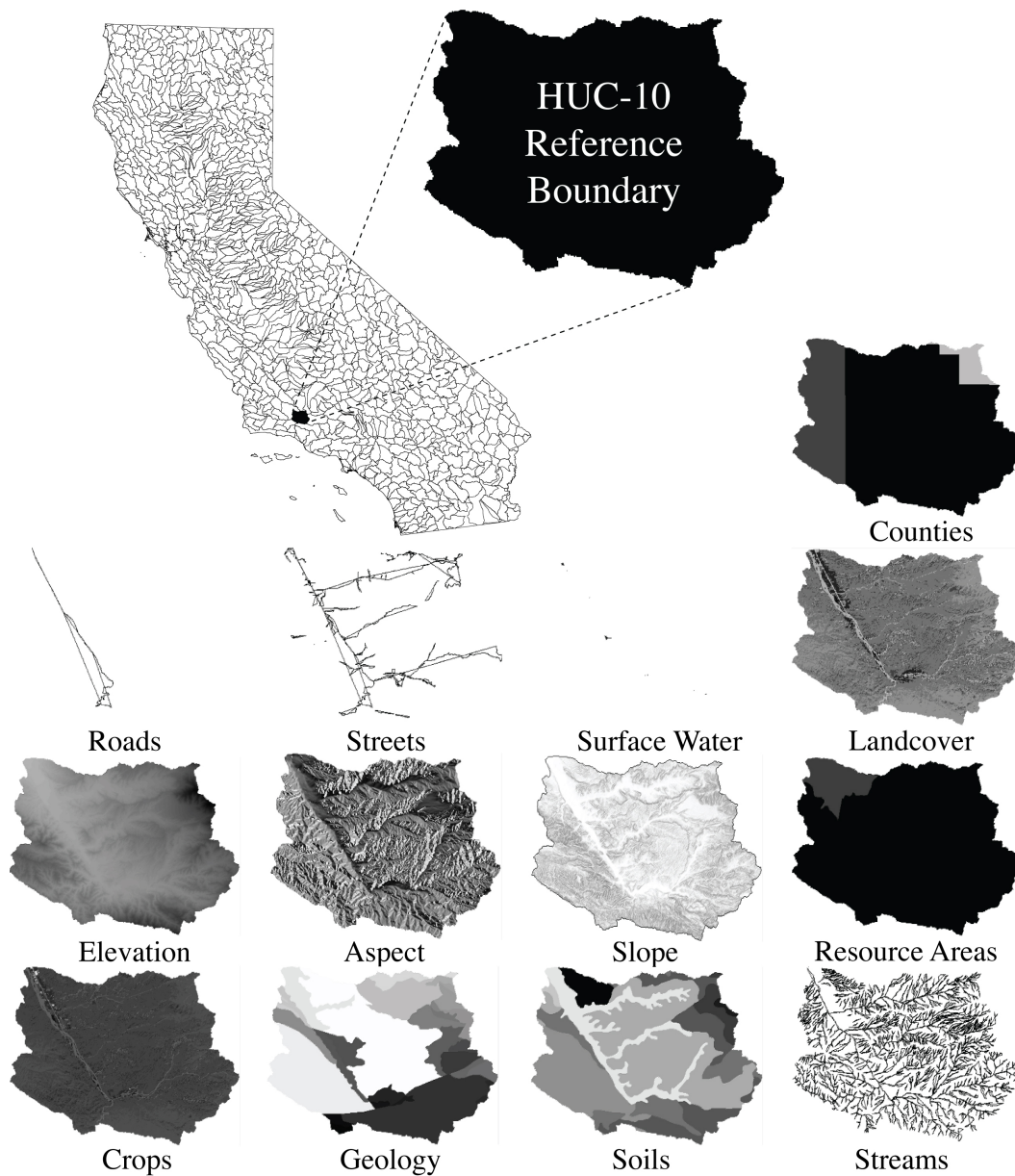


Figure 1.8: Graphical Illustration of the WOSS Model Outputs for Reference HUC-10 Boundary

The toolset structure allows for the automated repetition of this data preprocessing workflow for a large number of reference boundaries. In this case study implementation, for example, the toolset was used to prepare a single such output layers stack for each of the

1,040 individual HUC-10 reference boundaries contained within the state of California. With these outputs, a corresponding the MCSS analysis could then be easily conducted for any or every such HUC-10 watershed in the State.

[A computer] takes these very simple-minded instructions – 'go fetch a number, add it to this number, put the result there, perceive if it's greater than this other number' – but executes them at a rate of, let's say, 1,000,000 per second. At 1,000,000 per second, the results are indistinguishable from magic.

Steve Jobs (1955-2011)

2

Locating Optimal Corridors

2.1 LOCATING OPTIMAL CORRIDORS FOR WATER DISTRIBUTION INFRASTRUCTURE

THE SOURCE OF LOCATION for the delivery of treated wastewater for artificial groundwater recharge applications is always the Wastewater Treatment Plant (WWTP). WWTPs are overwhelmingly located at low elevation points within the hydrological basins that they serve; as this feature ensures a minimum energy input requirement to deliver wastewater from its distributed sites of generation (i.e. the many homes and businesses distributed geographically throughout the basin) to a single centralized point of treatment. In this way, a system design based upon a single centralized WWTP is best able to take advantage of the use of gravity to provide the motive force for the wastewater's journey through the system. As a side note, an question which may become of substantial future interest is how a more prominent role of reuse may alter our thinking about the optimal design of water treatment collection and conveyance infrastructure. Specifically, it remains an open research question as to whether or not the existing paradigm, with large centrally location treatment facilities, would persist as the most favorable solution if one were charged with designing an integrated wastewater treatment and reuse system from the oft.

The salient output of the first model component – WOSS – is the designation of one or more suitable sites for the placement of either a gravity fed surface spreading infiltration basin or a pump driven subsurface recharge well. In this way, we are left with one or many – in the case of multiple suitable sites – combinations of point source and destination locations. The next modeling challenge which must be overcome therefore is the development of a scheme for generating plausible pathways which connect the source locations to the various destinations. The implicit assumption here being, that in order to deliver the treated wastewater from its source of production, the WWTP, to the end point of use, the recharge site, new water conveyance infrastructure must be constructed.

At this stage it is important to pause to consider whether or not the construction of new water conveyance infrastructure is in fact a necessary condition of all or any water reuse projects. There are two perspectives from which a response to this objection can be framed. The first is technical in nature. If no new conveyance structure is implemented, two fundamental technical requirements must be met. The first is that the point of reuse must be situated favorably with respect to the existing potable water conveyance system such that it can be readily be connected to, and withdraw from it, large quantities of water for recharge purposes. The second is that the treated wastewater which is to be reused must be returned to a sufficiently high standard of quality such that it can be reincorporated directly back into the potable water supply. This second constraint, while technically feasible given sufficient financial resources, leads naturally to the other category of potential objections to the development of a reuse project without the addition of new conveyance infrastructure: namely, the social stigma associated with co-mingling so-called reclaimed *black water*, with the potable freshwater supply. There is a considerable body of research in the social sciences which suggests that a majority of people harbor a very basic, if somewhat irrational, prejudice against the direct reuse of reclaimed water for potable applications.

2.2 THE MULTI-OBJECTIVE CORRIDOR LOCATION PROBLEM

The multi-objective corridor location problem can be formally written as Equation 2.1⁸⁶. The problem involves the simultaneous minimization of the sums of w independent objective functions \hat{O}_w evaluated at the set of discrete locations x_n comprising a corridor of length n . A valid corridor x_n is subject to the constraint that all of its nodes must be contained within the feasible search domain Ω . Additional, optional constraints, as in Equation 2.2, are often imposed upon the structure of x_n and shall be discussed in greater detail in

subsequent sections.

$$\text{Minimize : } \prod_{n=1}^n \left\{ \hat{O}_1(x_n), \dots, \hat{O}_w(x_n) \right\} \quad (2.1)$$

$$\text{S.t. : } x_n \in \Omega \quad (2.2)$$

Where:

x_n = The set of discrete row column indices defining a corridor of length n

Ω = The set of discrete row column indices defining the feasible decision space

O_w = The true but unknown forms of w continuous objective functions

\hat{O}_w = The estimates of O_w defined over the discrete set Ω

As a subset of SPPs, corridor location problems tend to be defined in the context of networks with large numbers of nodes and highly structured topologies³³. These shared characteristics arise from the fact that corridor location problems are typically posed in the context of continuous geographic space – a feature which requires that the requisite underlying network structure be generated algorithmically⁷¹. In practice, this is frequently accomplished by automating the conversion of a geographically referenced raster grid into a set of nodes by referencing the the centroids of the cells within the raster in a process similar to that described by⁴¹. Once the nodes in the network have been created they can then connected to one another by automatically generating arcs using some standard mode of node connectivity; again, using methods similar to those described by¹⁹.

2.3 GENETIC ALGORITHMS

Genetic Algorithms (GAs) are a family of search heuristics that mimic the process of natural selection to derive one or more near optimal solutions to a given optimization prob-

lem.³¹ GAs constitute a subset of Evolutionary Algorithms (EAs) which encode solutions using data structures that are analogous to biological chromosomes²⁵. This feature allows the search for new, better solutions to be accomplished via the iterative application of genetic operations such as crossover, mutation, selection, etc.³² GAs have been developed and profitably used in a wide variety of problem domains from engineering and economics to chemistry and physics. General purpose reviews of the application of GAs to various problems are available from the following references.^{29,88,21} For a more specialized reviews regarding state of the art applications of multi-objective genetic algorithms see the excellent book from Coello & Lamont and, more recently, from Zhou *et al.*^{20,86}

2.4 THE MOGADOR ALGORITHM

MOGADOR is an acronym stands for: *Multiple Objective Genetic Algorithm for Corridor Selection Problems*.⁸⁵ The algorithm was introduced as a novel genetic approach to the problem of multi-objective corridor search.^{55,85} Its development was intended to service need for a robust method of siting optimal corridors relevant to a variety of environmental planning and design applications.^{7,16,87} A need which persisted despite numerous previous efforts to adapt general purpose, deterministic, SSP solution techniques for use in corridor location.^{36,42,51} The continued need for refined algorithmic approaches to the location of optimal corridors within a broad range of application domains is evidenced by the continued appearance of closely related publications during the intervening years.^{2,56,57,63,66,79}

Relative to other traditional shortest path finding routines, the MOGADOR algorithm has been observed to possess a number of favorable characteristics. First among these is the ability of MOGADOR to accommodate large problem statements (large Ω) and or those which require the simultaneous evaluation of large numbers of independent objectives (large w)^{59,85}. Another useful feature of the MOGADOR algorithm is its ability to generate

an entire solution set from a single run – as opposed to the single solution per run which is typical of traditional SPP algorithms^{17,28,37,85}. Lastly, but perhaps most importantly, is that when properly parameterized, each of the solutions generated by the MOGADOR algorithm can be said to be non-inferior to every other⁸⁵. In this way, the output solution set approximates the so called Pareto optimal solution set for the given problem statement²⁶.

In order to proceed with our discussion of the MOGADOR algorithm, some basic terminology must first be defined. In the context of the MOGADOR algorithm a single gene x is comprised of a pair of row column indices (r, c) to a geographically referenced 2-D array comprising the feasible search domain Ω . An individual I_m is comprised of a sequence of row column index vectors x_n which collectively form a valid pathway between a predefined set of source $^s x$ and destination $^d x$ locations. In this way, each individual represents a feasible solution to the proposed corridor location problem. A population P_g is comprised of m individuals. And, finally, an evolution E_b is comprised of g populations.

Figure 2.1 provides a pseudocode description of the MOGADOR algorithm. Its structural components are fairly typical among GAs in general. The search process begins with a stochastic routine for generating of an initial seed population P_1 . Following the initialization of this seed population, the fitness F_1 of each individual in the seed population is computed by summing the objective function scores corresponding to each set of nodes comprising each individual. Upon the completion of this initialization phase, the algorithm then enters a loop wherein successive genetic operations are applied to the initial seed population. In the case of MOGADOR, these operators include: the selection individuals for reproduction on the based upon their fitness, the crossover of selected individuals that share at least one common feature, and finally, the mutation of crossed over individuals so as to maintain a degree of random variation within the population. At the end of each loop iteration a new population is generated, its fitness evaluated, and a convergence parameter computed on the basis of the observed rate of improvement in population fitness

across previous iterations. If convergence is achieved ($c_g < {}^t c$) the loop is broken and the algorithm terminates returning: the evolutionary history of the population $P_{r:g}$, the corresponding fitness values each individual within the population $F_{r:g}$, and the convergence parameter history $C_{r:g}$.

```

1: procedure MOGADOR
2:    $g = 1 \leftarrow$  initialize loop iterator
3:    $c_g = 0 \leftarrow$  initialize convergence parameter
4:    $P_g = \text{initializeSeedPopulation}(m, \Omega)$ 
5:    $F_g = \text{computePopulationFitness}(P_g, \hat{O}_w)$ 
6:   while  $c_g < {}^t c$  do:
7:      $g += 1 \leftarrow$  update loop iterator
8:      $S_g = \text{selectIndividualsFromPopulation}(P_g)$ 
9:      $X_g = \text{crossoverSelectedIndividuals}(S_g)$ 
10:     $P_g = \text{mutateCrossoverIndividuals}(X_g)$ 
11:     $F_g = \text{computePopulationFitness}(P_g)$ 
12:     $c_g = \text{computeConvergenceParameter}(F_{r:g})$ 
13:  end
14: end while
15: return:  $P_{r:g}, F_{r:g}, C_{r:g}$ 
16: end procedure

```

Figure 2.1: MOGADOR Algorithm Pseudocode.

2.5 THE MOGADOR DATA STRUCTURE

The optimal data structure for use in concert with the MOGADOR algorithm is a nested list of lists. Such a list based data structure is well suited to this context as there can be a high degree of variability in the number of elements produced by the different stochastic genetic operators. Figure 2.2 illustrates a small but valid example such a nested list of lists data structure as used in the context of the MOGADOR algorithm. Note, for example, how the number of row column index vectors n in the first individual I_1 equals 5, while the number of index vectors in subsequent individuals $I_{2:4}$ belonging to the same population, ranges between 3 and 6. The source of this variation has to do with the stochasticity inher-

ent to the population initialization routine. Similarly, note how the number of populations g in the first evolution E_1 is 3 while the number of populations in the second evolution is 4. The source of this variation has to do with the stochasticity in the crossover and mutation processes. Indeed, the only level of the data structure's hierarchy at which a constant number of elements is required is at the population level. Meaning, in other words, that each population P_g contained within evolutions E_b must all possess the same number of m individuals. This requirement ensures that the behavior of the genetic operators is consistent between separate evolutions.

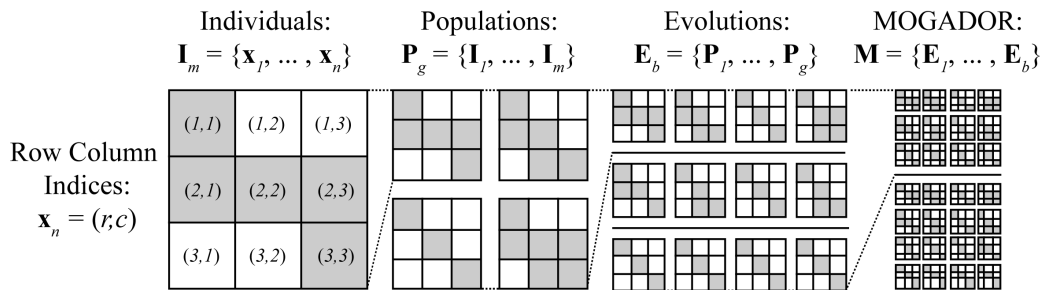


Figure 2.2: MOGADOR Algorithm Data Structure

2.6 INITIALIZING THE MOGADOR ALGORITHM

A novel population initialization procedure has been developed for use in conjunction with the MOGADOR algorithm which improves the global quality of the output solution set while simultaneously reducing overall computational effort. At its core, this novel pseudo-random walk algorithm works by repeatedly sampling a dynamically parameterized bivariate Gaussian distribution. The generic form of the probability density function for the bivariate Gaussian distribution can be written as Equation 2.3⁴⁴. Here, the bivariate Gaussian PDF $f(\tau)$ is function of two inputs. [1] The first is a mean vector μ , comprised of the

means (μ_1, μ_2) of two continuous random variables (τ_1, τ_2) . [2] The second is a covariance matrix Σ , comprised of the pairwise covariances σ for all possible combinations of the continuous random variables (τ_1, τ_2) .

$$f(\tau) = \frac{1}{\sqrt{(2\pi)^2 |\Sigma|}} \exp \frac{-1}{2} (\tau - \mu)^T \Sigma^{-1} (\tau - \mu) \quad (2.3)$$

Where:

τ = The set of correlated continuous random variables (τ_1, τ_2)

μ = The set of mean values (μ_1, μ_2) for (τ_1, τ_2)

Σ = The pairwise covariance structure $\begin{bmatrix} \sigma(\tau_1, \tau_1), & \sigma(\tau_1, \tau_2) \\ \sigma(\tau_2, \tau_1), & \sigma(\tau_2, \tau_2) \end{bmatrix}$ for (τ_1, τ_2)

Each sampled value for τ_1, τ_2 can be reduced to a unit vector and interpreted as a set of row column index deltas. The repeated sampling of the distribution therefore provides a simple yet powerful technique for generating randomized positional changes within a 2-D lattice. Additionally, as shall be discussed in the subsequent sections, the ability to dynamically adjust the parameters of the bivariate Gaussian PDF at any time during the sampling process provides a mechanism by which one is able to functionally constrain the randomness of the walk; hence the term: pseudo-random walk.

Figure 2.3 provides a pseudocode representation of the proposed pseudo-random walk procedure. Structurally, the routine consists of two nested while loops. At each iteration h of the outer loop a single step x_n along an individual walk I_m is taken. This loop continues until the location of the current step is equal to that of the destination $^d x$. At each iteration u of the inner loop a candidate next step Δx_u is produced by random sampling the parameterized bivariate Gaussian PDF $f(x_u)$. Candidate next steps are only considered valid if they are contained within the current valid connected set V_n . The current valid connected set is comprised of all neighboring nodes that not been previously visited and that are inclusive

to the search domain Ω . If the candidate step is found to be valid the inner loop terminates, the outer loop iterates, and the walk process continues. If the valid set is ever found to be empty the outer loop iterator b is reset and the entire process is restarted.

```

1: procedure PSEUDO-RANDOM WALK
2:    $n = 1 \leftarrow$  initialize outer loop iterator
3:    $x_n = s_x \leftarrow$  initialize individual at source
4:    $I^* = \text{computeEuclideanShortestPath}(s_x, d_x)$ 
5:   while  $x_n \neq d_x$  do:
6:      $V_n = \text{computeValidConnectedSet}(x_{i:n}, \Omega)$ 
7:     if  $V_n = \emptyset$  then:
8:        $n = 1 \leftarrow$  reset outer loop iterator
9:       continue
10:    end if
11:     $u = 1 \leftarrow$  initialize inner loop iterator
12:     $\mu_n = \text{computeOrientationVector}(x_n, d_x)$ 
13:     $d_n = \text{computeMinimumBasisDistance}(x_n, I^*)$ 
14:     $n = n + 1 \leftarrow$  update outer loop iterator
15:    while  $x_n \notin V_n$  do:
16:       $\Sigma_u = \text{computeCovarianceMatrix}(d_n, u)$ 
17:       $\Delta x_u = \text{sampleBivariateGaussianDistribution}(\mu_n, \Sigma_u)$ 
18:       $x_n = x_{n-1} + \Delta x_u$ 
19:       $u = u + 1 \leftarrow$  update inner loop iterator
20:    end while
21:  end while
22:  return:  $x_{i:n}$ 
23: end procedure

```

Figure 2.3: Pseudo-Random Walk Algorithm Pseudocode

In the process of sampling the parameterized bivariate Gaussian distribution the following three pieces of information are used to functionally constrain the probabilities associated with each candidate next step Δx_u . [1] At the start of each walk the set of array indices corresponding to the Euclidean shortest path I^* from the source to the destination are generated using Bresenham's line algorithm¹¹. Using this set of indices the minimum distance d_n from the current position to the nearest point along this Euclidean shortest path is determined. [2] Next, at each step an orientation vector is computed indicating the orientation

of the destination location relative to the current position. [3] Finally, each time the bivariate Gaussian PDF is sampled a counter variable u is iterated.

The orientation vector is interpreted as the mean of the bivariate Gaussian $PDF(\mu_n)$. Alternatively, the minimum distance and iteration variables (d_n, u) are processed as inputs to a generator function which produces the covariance matrix Σ_u . This composition of this generator function ensures that the degree of randomness inherent to the selection of each next step is directly related to number of iterations while at the same time being inversely related to the minimum distance from the current location to the Euclidean shortest path.

2.7 AN EXAMPLE PSEUDO-RANDOM WALK

In an effort to make this pseudo-random walk procedure more comprehensible, particularly with regards to the parameterization of the bivariate Gaussian PDF $f(x_u)$, an example implementation is provided in Figure 2.4. On the far left of Figure 2.4. the current status of an arbitrary pseudo-random walk is shown midway through completion. Also drawn, as a broken line, is an abstract representation of the Euclidean shortest path I^* connecting the source location $^s x$ to the destination location $^d x$. Show at bottom is the current value of the distance parameter $d_n \approx 7.1$. Just to the right of this, in the zoom inset area, the current valid connected set V_n is drawn with the previously visited indices (x_n, x_{n-1}) greyed out to illustrate their elimination from consideration as valid next steps in the walk process. Also shown in this inset are the row column unit vector deltas Δx_u associated with movement to each of the seven nodes contained within the current valid connected set. The small arrow pointing downwards and to the right depicts the current state of the orientation vector μ_n which describes the position of the destination location $^d x$ relative to the current walk location x_n . The current value of this vector ($\mu_n = [1, 1]$) can be thought of as indicating the row and column deltas associated the next step possible step most directly leading towards

the destination.

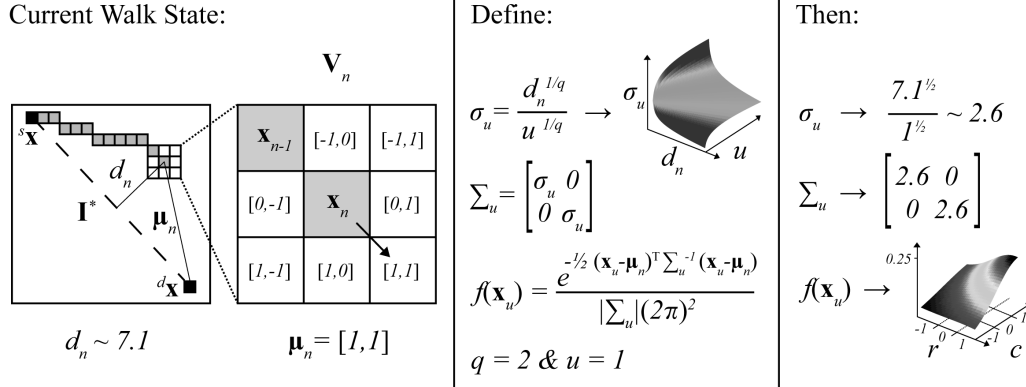


Figure 2.4: Pseudo-Random Walk Example

Continuing on to the right within Figure 2.4, three functions and two parameter values are defined. [1] First, the covariance term σ_u for the current sample iteration u is specified using a covariance generator function whose form enforces the relationship between distance, iteration count, and covariance previously described. A small demonstration plot of this function's form is provided. [2] Next, the covariance matrix Σ_u is defined by inserting the covariance term σ_u to the diagonal elements of an empty square 2-D matrix. This repeated use of the same covariance term guarantees that for any value of σ_u the output covariance matrix Σ_u will be positive definite. A square, symmetric, and positive definite covariance matrix is a hard requirement for the evaluation of the parameterized bivariate Gaussian PDF $f(\mathbf{x}_u)$. The final two variable definitions (q, u) are provided for the sake of computing illustrative values for the other parameters. Numerical evaluations of these expressions are given on the far right portion of the figure. Here again, a small demonstration plot showing the form of the evaluated bivariate Gaussian PDF $f(\mathbf{x}_u)$ is provided.

One aspect of this process which warrants further discussion is the role of the fixed parameter q in determining the degree of randomness exhibited by a given pseudo-random walk. The degree of randomness can be quantitatively defined as the range and extent to which the bivariate Gaussian PDF $f(\mathbf{x}_u)$ deviates from its uniform bivariate counterpart.

To illustrate this concept consider for example the characteristics of the PDF that would be required to produce a simple random walk using a similarly structured procedure. In such a case the value of $f(x_u)$ would have to be equal for all possible values of Δx_u . Due to the way in which the covariance generator function has been proposed, the q parameter can therefore be used to determine the maximum range of variation in σ_u which can be produced from any combination of (d_n, u) input values. In this way, q does not alter the structure of the bivariate Gaussian PDF $f(x_u)$ but rather only its magnitude. As a result, while the value of q must always be greater than zero to produce real outputs from the covariance generator function, its value is inversely related to the degree of walk randomness.

2.8 INITIALIZING PROBLEMS WITH LARGE DECISION SPACES

While the pseudo-random walk procedure can be used to generate an initial seed population for any MOGADOR problem statement; a number of circumstances have been identified in which the performance of the population initialization procedure can be further refined. [1] The first such situation involves problems with extremely large decision spaces – defined as being thousands grid cells or more on a side. [2] The second problem specifications where it is known, *a-priori*, that the Euclidean path connecting the source to the destination is not entirely feasible.

Historically, corridor location problems which have been posed in the context of extremely large decisions spaces (large Ω) have been considered infeasible both for conventional deterministic SPP optimization techniques as well as for heuristic approaches such as MOGADOR. With regards to MOGADOR, the source of this infeasibility stems from the huge runtime commitment associated with generating and processing populations containing a sufficient number of individuals so as to ensure that a sufficient amount of genetic diversity can be captured during the initialization phase to conduct a global search.

One strategy which can be employed to ensure enough genetic diversity is produced within the initial seed population without having to generate populations of unduly large size or populations with individuals characterized by a high degree of randomness, is the generation of so called multi-part pseudo random walks. This procedure can be thought of as somewhat analogous to orthogonal statistical sampling techniques such as Latin Hypercube sampling which are used to generate samples from a non-uniformly distributed population by first dividing it into equally probable subspaces^{53,83}. The implicit assumption here being that the fitness distribution of all possible corridors connecting a typical source and destination pair is similarly non-uniform.

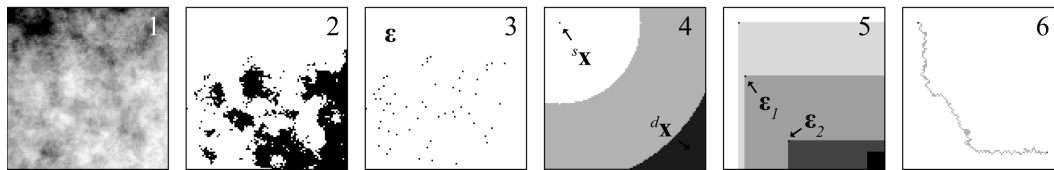


Figure 2.5: Conceptual Illustration of a Multi-Part Pseudo-Random Walk

The multi-part walk process is described by the sequence of panels moving from left to right within Figure 2.5. [1] The process begins with the far left panel which plots the value of the objective variables within the a square 2-D search domain. [2] The first step is to create a binary mask of feasible nodes by selecting objective surface values less than some arbitrary threshold. [3] The next step involves determining the cell indices for the set of centroid nodes ϵ computed from the connected components within this binary mask. [4] After this, these centroids are assigned rankings on the basis of their inclusion in bins of progressive Euclidean distance from the source location. [5] Next, the procedure requires the iterative selection of centroids ϵ_1, ϵ_2 , one from each successive distance bin, until the bin containing the destination location is reached. The centroid selection process can be unstructured, random within each bin, or structured (as shown), where the centroids considered eligible for selection each iteration is restricted to those orientated positively in the

direction of the destination. [6] Finally, the source is connected to the destination a series of pseudo-random walks constructed for sequential pairs of the selected centroids.

2.9 INITIALIZING PROBLEMS WITH CONCAVE DECISION SPACES

Another circumstance which has the potential to dramatically effect the performance of the pseudo-random walk procedure are problem specifications in which all or a portion of the Euclidean path connecting the source to the destination falls outside the feasible area of the search domain. Such a circumstance can be described as a concave problem, as the source and destination locations are not convex to one another within the boundaries of the decision space Ω . Concave problem statements have the potential to create a situation where at each iteration n of the pseudo-random walk process large values of μ must be attained before the covariance term is relaxed enough to allow for the sampling process to generate a Δx_μ that is contained within the valid set V_n . In a worst case scenario, the entire runtime improvement associated with the pseudo-random walk based population initialization procedure might be lost.

An approach which has been developed to address such cases is the so called concave multi-part pseudo random walk. It is similar to the standard multi-part walk in that the final walk is composed of a collection of pseudo-random walk sections. However, it differs from the standard walk procedure in that rather than partitioning the space on the basis of distance bands, it iteratively divides the decision space into a series of convex subregions. Here again, these convex sub region contain the centroids associated with connected regions of low objective variable values. The procedure is illustrated conceptually by the sequence of panels contained in Figure 2.6.

The concave multi-part walk process is described by the sequence of panels moving from left to right within Figure 2.6. [1] In the first panel, on the far left, we can see a problem that

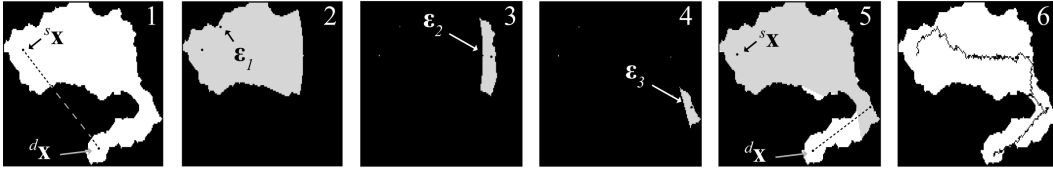


Figure 2.6: Conceptual Illustration of a Convex Multi-Part Pseudo-Random Walk

has been posed in such a way that the Euclidean path connecting the source to the destination is not feasible as it exits the boundaries of the search domain. [2] For brevity, the two subsequent steps are not shown as they are identical to steps 2-3 in the standard multi-part pseudo random walk procedure. These omitted steps involve the generation of candidate centroids from the connected components within the objective surface. The next illustrated step, shown in the panel second from left, involves computing all of the row column indices that are convex to the source location. Within this convex region a the first centroid ϵ_1 is selected. Here again, the process can be unstructured, where the entire convex region is searched, or structured, as shown, where the initial convex region is restricted to some maximum distance from the source. [3-4] From here, additional non-overlapping convex subregions are computed and candidate centroids iteratively selected from within them. [5] The centroid selection process concludes when the current convex region contains the destination location. [6] Finally, the source is connected to the destination, as in the simple multi-part case, by a series of pseudo-random walks constructed for sequential pairs of the selected centroids.

2.10 MEASURING INITIALIZATION PERFORMANCE

The stochastic processes inherent to the pseudo-random walk procedure, as well as to many other components of the MOGADOR algorithm, make it difficult to analytically derive performance characteristics. As a consequence, with MOGADOR, as with many other

GAs, features such as runtime performance must be evaluated through empirical observation. The following sections introduce the results obtained from several such empirical investigations related to the performance of the pseudo-random walk based population initialization procedure for the MOGADOR algorithm. For reference, all computations were performed using a desktop class hardware possessing a 2.3 GHz Intel Quad Core i7 processor (2nd Gen.) with 16 GB of system RAM.

The first of these investigations seeks to understand the role of the fixed parameter q , embedded in the pseudo-random walk covariance generator function, in determining the structural characteristics of output populations. In order to study this issue, a synthetic problem statement was created. This problem statement involves a square search domain of 100 nodes on a side – resulting in a total problem size of $\Omega = 10,000$ nodes. The value of the estimated objective function \hat{O}_w used to evaluate fitness was set as constant for all of the nodes in the search domain. In this way, the objective score is roughly equivalent to individual walk length in Euclidean space. Using this problem statement, twenty seed populations, all containing $m = 100$ individuals, were generated using monotonically increasing values of q beginning with $q = 0.5$ and concluding with $q = 10$. For each the generated populations, the average objective scores for all individuals as well as the standard deviation of the objective scores among individuals were evaluated. The results of this empirical investigation are presented in Figure 2.7.

As Figure 2.7 illustrates, increasing the value of the fixed parameter q causes the individuals within the a population to more closely approximate the Euclidean shortest path between the source and destination. Similarly, relaxation of this parameter results in an increase in the perceived randomness among the individual walks within a population. These attributes can be clearly observed in the two images to the right of Figure 2.7 which show the frequency with which every node within the search domain has been visited by any individual within two populations generated from different values of q .

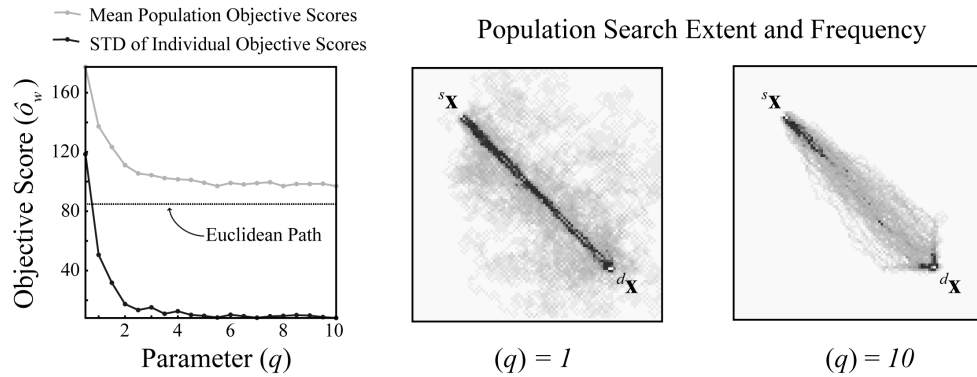


Figure 2.7: Observing the Role of the Fixed Parameter q in Determining Path Randomness

Another issue warranting empirical investigation is the relationship between runtime performance of the proposed initialization procedure and problem size. In order to study this issue a series of ten synthetic problem statements were constructed with near identical structural components; differing from one another only in terms of problem size. In each of these problem statements the source location was positioned one fifth of the way down and to the right from the top left of the search domain and, likewise, the destination location was positioned a constant one fifth of the way up from the bottom right corner of the search domain. For all of the different populations generated, the value of the fixed parameter q was set relatively high $q = 10$ to reduce computational effort.

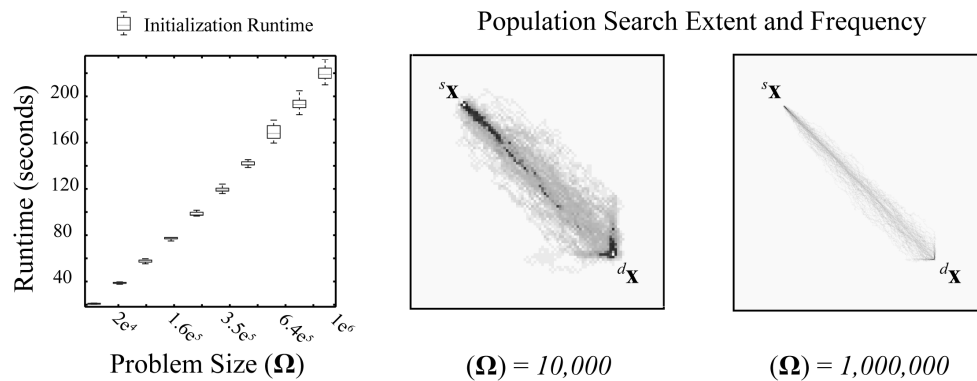


Figure 2.8: Observing the Role of Problem Size on Initialization Runtime

The plot to the left of Figure 2.8 illustrates the the distributional properties of the run-

times required to generate ten replicate populations for the ten problem statements of progressively increasing size – resulting in a total of $g = 100$ unique populations, each comprised of $m = 100$ individuals. Such repeated simulation is necessary as the proposed initialization routine is based upon a stochastic sampling process which can and will deliver variable runtimes for the repeated applications to the same problem context. One feature of note in this plot is the roughly linear relationship between the mean runtime and problem size for this type of pseudo-random walk based approach to the problem initialization procedure for the range of problem sizes considered. The two images to the right illustrate the effective search extent and frequency for the smallest and the largest populations generated during this investigation.

One of the considerations previously discussed related to the initialization of the MO-GADOR algorithm in the context of large problem statements was the need to ensure sufficient diversity within the seed population for the search process to be conducted at the global level. This problem is clearly evident in the population search extent and frequency image contained on the far right of Figure 2.8. In this example, the population clearly fails to explore a sufficiently large portion of the decision space to be considered as a form of global search. The solution which was previously proposed to this problem involved generating so called multi-part pseudo-random walks. The subsequent investigation therefore, compares the statistical characteristics of a set of populations generated from standard pseudo-random walk to another set of population generated from multi-part pseudo random walks. The results of this investigation are provided in Figure 2.9.

The runtime reductions which can be achieved from the use of the multi-part pseudo random walk procedure will principally occur in the context of relatively high value settings for the fixed parameter q . This is because while the various component segments of a multi-part walk may not deviate significantly from the Euclidean shortest path however, the randomized connection of multiple such segments produces composite individuals that

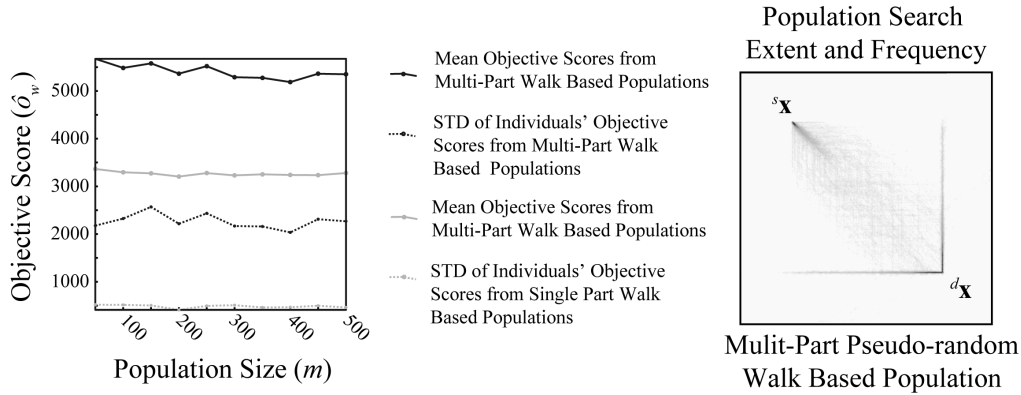


Figure 2.9: Observing the Characteristics of Multi-Part Pseudo-Random Walks

are significantly more diverse.

2.II THE MOGADOR ALGORITHM OUTPUTS

The output of the MOGADOR algorithm is the state of population at the time in which the algorithm has either achieved convergence or has been terminated upon reaching the specified limit for evolutionary iterations. This population contains the row-column subscripts for each individual corridor as well as the corresponding fitness values at each of the row column subscripts along the entire length of each individual corridor. These individuals are ranked on the basis of their aggregate cumulative fitness values. These values are computed by summing each objective value at each subscript location along the length of each individual corridor. Because this is a multi-objective context two individuals may have equivalent aggregate cumulative fitness scores yet the distribution of these scores across the various objectives may vary. This would represent a situation where those two individuals – as independent solutions to the multi-objective corridor location problem – are *Pareto optimal* or, alternatively stated, inclusive of the *non-dominated set*.

Either the rest of the world can't live like the developed world or we need, as a society, to think more about the technology of providing these services with less intensive use of at least certain resources. We need to do a more diligent job of good housekeeping.

Thomas E. Graedel (1940-)

3

Quantifying Life-Cycle Energy-Water Resource Utilization

3.1 QUANTIFYING LIFE-CYCLE ENERGY-WATER RESOURCE USAGE EFFICIENCY

THE THIRD MAJOR CHALLENGE associated with this dissertation's stated research objective involves the development of a systematic method for quantifying the life-cycle energy-water resource utilization efficiency of water reuse systems involving significant artificial groundwater recharge components. For this purpose, the decision was made to build upon a substantial body of previous research on this subject by utilizing an existing life-cycle inventory (LCI) database comprising energy and material process flow data collected from a large sample of existing WWTP operations and reuse facilities^{72,73,74}. The novel contribution of this dissertation to this body of work appears in the form of a new set of methods for the programmatic parameterization of the LCI model based upon the geographic context and spatial layout of the proposed reuse project under evaluation.

For example, by first determining suitable sites for recharge infrastructure and then elucidating near-optimal corridors for the distribution network supplying the treated wastewater from the WWTP, the research analyst is then able to gain a deeper and more fundamental understanding of the systems behaviors. For example, with a detailed corridor specification in hand, it then becomes possible to estimate process energy demands of the system from first principles rather than having to use vague reference data aggregated from a wide distribution of empirical measurements⁴⁶. As we shall demonstrate in subsequent sections, these new capabilities go a long way towards improving both the accuracy and the precision of the model's outputs.

3.2 LIFE CYCLE ASSESSMENT AND INVENTORY MODELING

Life-cycle assessment (LCA) is an environmental accounting framework that was developed to systematically quantify the material and energy inputs and outputs from a product, pro-

cess, or system throughout all its stages of life. It uses a cradle-to-grave or, in some cases, cradle-to-cradle perspective, to evaluate the design processes as well as the entire supply chain associated with manufacturing, transportation, the use phase, and waste management^{62,61}. Practically, process based LCA analyses, which shall be the focus of the remainder of this discussion, incorporate two distinct modeling phases. The first involves the development of a Life-cycle Inventory model is a cumulative record of all of the materials and energy flows required to deliver a single functional unit of the product or process in question. The second, optional, phase of LCA analyses is the Life-cycle Impact Assessment (LCIA) component. An LCIA model attempts to translate the raw energy and material flows contained within the LCI into different categories of environmental impacts such as global warming potential, ocean acidification, freshwater eutrophication, etc.

If we recall, the overarching goal of this dissertation project was to quantify the energy-water usage efficiency of artificial groundwater recharge projects involving the reuse of treated municipal wastewater. In order to accomplish this goal customized LCI models will be developed for five case study regions in which the distribution networks responsible for transporting the treated wastewater for its point of origin, the WWTP, to its destination point of consumption, an artificial groundwater infiltration basin positioned at a designated destination location, typically upstream within the regional watershed. The raw data supporting the creation of each of these custom LCI models was derived from the University of California at Berkeley supported WWESTweb Tool, which stands for: *WasteWater-Energy Sustainability web Tool*⁷². In each case study, the scope of this LCI modeling exercise was limited to the construction and operational requirements associated with the WWTP plant, the treated water distribution network, and the infiltration basin. This system boundary has been defined in such a way as to emphasize the dynamic contribution of the treated wastewater distribution to the LCI of a given functional unit of treated wastewater delivered to the sub-surface in the face of variable geographic context.

3.3 WASTEWATER TREATMENT PROCESSES

The phrase wastewater treatment encompasses a wide variety of different processes and operational facilities depending upon: the quality of the influent water, the volume of the influent water, and the desired quality/end-use application for the treated effluent water⁴⁸. In the United States the operation of WWTPs are regulated at both the State and Federal levels⁴⁷. At the Federal level the principle regulatory agency is the United States Environmental Protection Agency (USEPA) and the principle regulatory program is the National Pollutant Discharge Elimination System (NPDES)⁸⁰. According to the legal mandate of the NPDES program, WWTP operators – as well as a wide variety of other entities – are required to apply, at regular time intervals, for discharge permits which provide them with the legal right to release waters containing limited concentrations of regulated pollutants into the environment. Also under this mandate, the USEPA is required to distribute these permits and enforce non-compliance with their terms.

Since the inception of the NPDES program, the USEPA has worked to make readily accessible a centralized database of all registered permit holders within the United States. This database is interesting for the purposes of this project in that it contains spatially referenced information about the operational aspects of every operating WWTP in the U.S.²³ Crucially, this information includes data on maximum daily permitted flow rates and total maximum daily loads that can be used to parameterize the type of process based LCI model facilitated by the WWEST tool.

In terms of their basic physical layout and operational requirements, WWTPs are typically constructed with a tiered layout; comprising primary treatment, secondary treatment, and sometimes, various so called tertiary processes^{70,4,58}. Both primary and secondary treatment are terms that come with narrow legal definitions and are implemented at nearly all WWTP plants handling municipal sewage discharges. Tertiary treatment processes are

more loosely defined and encompass a suite of advanced treatment processes that are so costly that they tend to only be implemented at a minority of WWTP that are subject to a unique circumstances in terms of influent pollutant loadings/composition or requirements associated with designed high purity effluent end-use applications^{15,39}.

Primary treatment encompasses processes and equipment dedicated to the physical separation of non-soluble waste constituents present in the influent wastewater stream⁵⁴. Within a WWTP, a number of distinct processes are often lumped together as being part of the primary treatment. For example, when water first enters the WWTP it is guided through a series of progressively refined grates to screen out bulk pollutants such as anthropogenic trash or natural plant and animal detritus. Following from this bulk screening phase, the water is guided into a series of settling basins where its movement is slowed to crawl to facilitate the settlement of suspended pollutant materials such as sediment⁵⁴. Due to the slow rate at which this settling process proceeds, the physical infrastructure which supports it can comprise a significant fraction of the overall footprint of a WWTP; particularly for those with high flow volume processing requirements.

Secondary treatment encompasses processes and equipment dedicated to the biological – and sometimes chemical – degradation of soluble waste constitutes present in the influent wastewater stream⁵⁴. In most municipal WWTP secondary treatment is accomplished through a passively aspirated, aerobic biological digestion reactors. In these reactors large colonies of bacterial species are cultivated on high surface area media using the organic components of the influent wastewater stream as a feedstock for the continued growth⁵⁴. At the end of their life cycle, the bacteria fall to base of the reactor tank and must be continuously removed in the form of a product known as activated sludge.

Tertiary treatment encompasses processes and equipment dedicated to the removal of soluble inorganic and some organic chemical species – including some viruses and pharmaceutical agents – present within the influent wastewater stream⁵⁴. At present, tertiary treat-

ment processes are not mandatory for all WWTP facilities regulated under the NPDES program. In general, they tend to only be implemented at those specific locations in which a last and credible threat to public or environmental health has been identified and for which a targeted tertiary treatment process exists to address. In this way, mandates for tertiary treatment are typically instigated at the state or local level and done so on a case by case basis. Among the most common tertiary treatment processes include: reverse osmosis filtration, batch irradiation with ultra-violet light, the application of specialized chemical amendments, de-nitrification processes, and others⁵⁴.

For the purposes of this analysis and the customized LCI models which shall be constructed as part of the case study investigations, only primary and secondary treatment processes shall be included in the scope. This decision has been made to eliminate a substantial bias in the inventory models process flows that might be associated with the inclusion of specialized tertiary treatment procedures.

3.4 WATER DISTRIBUTION INFRASTRUCTURE

The immediate delivery and reuse of treated wastewater for various municipal and agricultural end-use applications is still a relatively new phenomenon^{5,8}. As such, the regulatory landscape surrounding such practices is still not well defined at the Federal level here in the United States⁴. Consequently, what regulations due exist, typically have been enacted at the State and local levels, with the most advanced frameworks, unsurprisingly, existing in those states such as Florida, California, and Arizona where the popularity of reuse as viable alternative source of freshwater supply, has been surging in recent years^{14,50,64,84}.

In all of the locations within the United States for which solid regulatory frameworks surrounding reuse currently exist, there are strong constraints governing the use of existing water distribution infrastructure for the transportation of treated wastewater from its point

of origin, the WWTP, to its point of end-use^{24,82,13}. These regulations, without exception, stipulate that treated wastewater, even if returned to a level of quality consistent with requirements for potable use, cannot be conveyed using existing distribution infrastructure carrying potable water for human consumption in municipal areas. Due to this regulatory constraint, all treated wastewater destined for some sort of municipal reuse must be carried through dedicated parallel distribution infrastructure¹⁴. In California, this infrastructure is easily identified at locations where treated wastewater is being reused due to the bright purple color of all the pipes. This color encoding is meant to be a strong visual reminder that the water being carried within them has not been deemed, from a regulatory perspective, as being fit for direct human consumption^{12,80}.

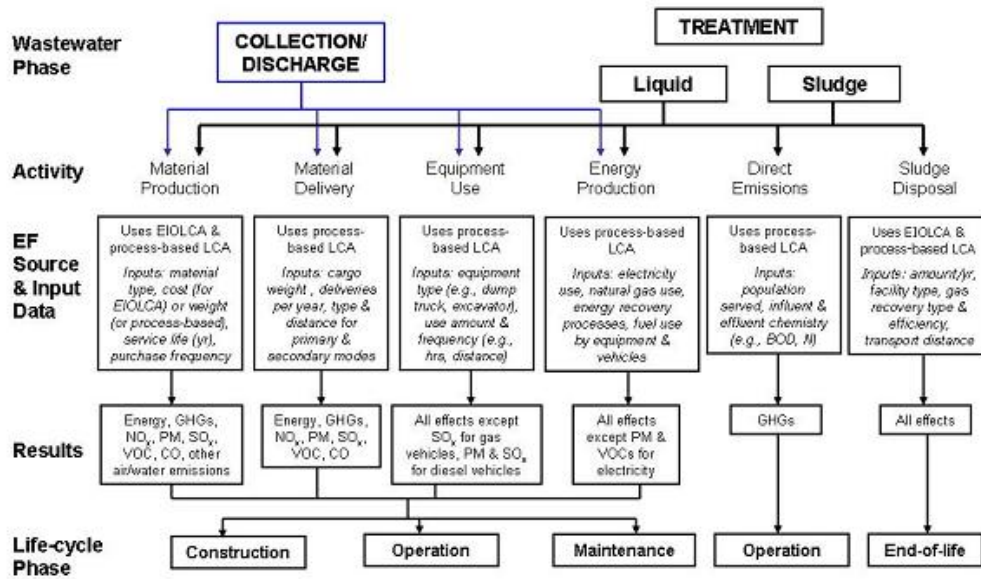
The requirement that treated wastewater, regardless of its standard of treatment and anticipated end use application, be transported using a separate parallel distribution network is expected to be a crucial factor in determining the overall life-cycle energy-water usage efficiency of large scale water reuse systems feeding into artificial groundwater recharge basins. The reasoning behind this expectation is based upon the interaction of the following two key factors. Firstly, water is a dense material, and thus it is very energy intensive to transport it over long distances and against steep elevation gradients. Secondly, artificial groundwater recharge basins typically require fairly large amounts of contiguous land area that are situated in fairly close proximity to highly developed urban and suburban communities. Municipal water resource management agencies are tightly constrained in terms of the operating budgets from which they are able to draw funds to procure new land holdings for the purpose of constructing artificial recharge basins. Thus, artificial recharge basins, primarily to economic constraints, are typically located fairly far afield from the WWTPs which feed them.

3.5 WWEST RECYCLED WATER REUSE LIFE CYCLE INVENTORY MODEL

The WWEST Recycled Water Reuse Life-cycle Inventory Model refers to an integrated life-cycle inventory database and modeling framework for understanding the environmental impacts of wastewater treatment and reuse processes that was developed by a team of academic researchers operating out of the University of California at Berkeley College of Engineering⁷⁵. The principal investigators behind the project are Doctor Arpad Horvath, Professor of Civil and Environmental Engineering, and Doctor Jennifer Stokes. Doctor Stokes completed the initial development work for the WWEST model as part of her doctoral dissertation research in the area of environmental impact assessment of civil infrastructure systems.

The LCI database underlying the WWEST toolset contains process flow information for the manufacture and operation of equipment and facilities involved in the supply, treatment, and distribution of municipal wastewater for the purpose of non-potable reuse. Figure 3.1 provides a schematic overview of the WWEST database model components and their respective input data sources.

The WWEST LCI database can be accessed in two ways. The first, which provides full access to all of the attribute fields contained within the database, is via an excel spreadsheet that has been distributed with a built-in set of computational macros. The second method exposes a more limited range of the data values contained within the database and is accessible via a streamlined web application, also known as WWESTweb. The principle difference between the WWEST excel model and the web application is in the extent to which each allows the user to customize the various parameters associated with a hypothetical water reuse project and its supporting infrastructure. In this sense, the excel based model is more appropriate for building an LCI model to quantify the process flows attributable to an existing facility or which is in a very advanced stage of design planning. Conversely, the



Data can be entered into WWEST in either metric or U.S. units. Some default information about system processes and materials are available in WWEST.

Figure 3.1: WWEST Model System Boundaries

WWESTweb framework is more appropriate for less well defined scenario based planning exercises, where the primary goal is to assess the relative impact of major system design alternatives that have only roughly been fleshed out.

3.6 PARAMETERIZING PUMP ENERGY REQUIREMENTS

The WWEST model requires a number of key input parameters to be supplied by the user before it can be run. These parameters correspond to various attributes of the proposed reuse system including: pipe length and material information derived from the distribution network topology, estimates of distribution process energy consumption figures, and process based chemical inputs associated with any required tertiary treatment phases.

In order to facilitate the systematic parameterization of the WWEST model a program-

matic workflow was developed which automates the calculation of a number of parameters from two input data sources: [1] the topology of the distribution network (i.e. the corridor solution from the MOGADOR optimization model) and [2] the expected daily flow rate derived from the maximum permitted flow value assigned to each WWTP facility through the NPDES permitting program.

To illustrate how this workflow functions, take for example the process of calculating the expected energy requirements associated with the distribution of the treated wastewater from its source at that WWTP to its destination at the reuse facility. Estimating the instantaneous power output associated with the operation of a pipeline based water distribution system begins with Equation 3.1⁴⁹.

$$P = \frac{Q * H_t * g * \rho}{E} \quad (3.1)$$

Where:

P = The instantaneous pump energy (W)

Q = The instantaneous flow rate (m^3/s)

H_t = The total head (m)

g = The gravitational constant (m/s^2)

ρ = The density of the fluid (Kg/m^3)

E = The pump efficiency factor (*unitless*)

The first term in this expression (Q), the instantaneous flow rate, can be computed by dividing the annual volume of water processed by the WWTP by the number of seconds in a year. The second term (H_t), the total system head, can be computed summing the individual static and dynamic head components as in the following Equations 3.2 and 3.3⁴⁹.

The last three terms (g, ρ, E) are constants that are characteristic to the system.

$$H_s = e_i - e_o \quad (3.2)$$

Where:

H_s = The static head component

e_i = The elevation at pipeline inlet

e_o = The elevation at pipeline output

Equation 3.2 describes how the static head can be computed as the difference between the elevations at the inlet and the outlet locations for the pipeline. When the corridor specification is known, this difference can be straightforwardly assessed by referencing the first and last subscript indices of the corridor to a raster based digital elevation model.

Computing the dynamic component (H_d) of the total system head is a significantly more complicated process; however, it can, nonetheless, be similarly automated from the same detailed knowledge of the pipeline corridor specification and its underlying elevation profile. Equations 3.3 through 3.7 illustrate the sequence of operations by which dynamic head (H_d) can be computed⁴⁹.

$$H_d = \frac{K_t * V^2}{2g} \quad (3.3)$$

Where:

H_d = The dynamic head component

K_t = The total system losses

V = The flow velocity

The dynamic head term is a representation of the frictional forces that arise from the movement of water through the pipeline. The cumulative effects of these forces are rep-

resented by the term (K_t), total losses, and are multiplied by the square of the velocity at which the water is flowing. The (K_t) can be parsed into two separate components, (K_p & K_f), as shown in Equation 3.4⁴⁹. These two terms represent the relative contribution of the friction associated with the movement of water over the textured surface of the pipeline's interior walls and the friction associated with the movement of water through a tortuous pipeline that has various connective fittings such as elbow joints and flow control valves.

$$K_t = K_p + K_f \quad (3.4)$$

Where:

K_p = The pipe loss component (*unitless*)

K_f = The fitting loss component (*unitless*)

Typically, the velocity term (V) is computed from the product of a specific flow rate (Q) and a pipeline cross sectional area (A) as in Equation 3.5. However, in the case of this analysis, the pipeline cross sectional area was solved for by specifying a maximum permissible flow velocity $V_{max} = 10$ (*m/s*) relative to some designated flow rate⁴⁹.

$$V = \frac{Q}{A} \quad (3.5)$$

Where:

A = The cross sectional area of the pipe (m^2)

The component of the total losses attributable to the cumulative friction encountered along the pipeline's pipe section walls (K_p) can be calculated from Equation 3.6 as the product of a friction coefficient (f) and the pipeline length (L) divided by the diameter of the

pipeline pipe sections (D)⁴⁹.

$$K_p = \frac{f * L}{D} \quad (3.6)$$

Where:

f = The friction coefficient of the pipe (*unitless*)

L = The cumulative length of all the pipe sections (m)

D = The diameter of each pipe section (m)

The friction component (f) of the pipeline loss term (K_p) can be computed from the empirically derived Equation 3.7 where (k) is a roughness factor that is characteristic to the pipe section material construction and (Re) is the Reynolds number, which is a dimensionless quantity that this associated to the smoothness with which a fluid flows and can be derived from the fluid's characteristic kinematic viscosity (ν) as in Equation 3.8⁴⁹.

$$f = \frac{0.25}{\left\{ \log_{10} \frac{k}{3.75 * D} + \frac{5.74}{Re^{0.9}} \right\}^2} \quad (3.7)$$

Where:

k = The roughness factor of the pipe material (m)

Re = The Reynolds Number of the fluid (*unitless*)

$$Re = \frac{V * D}{\nu} \quad (3.8)$$

Where:

ν = The kinematic viscosity of the fluid (m^2/s)

The fitting losses (K_f), which make up the second component of the total losses expression (K_t) and which ultimately feeds into the calculation of dynamic head (H_d), can be computed by using the corridor specification to cumulatively assess the need for various fitting components to facilitate pipeline deviations and flow control systems. The contribution of each fitting component to the total (K_f) factor is empirically defined and can be computed by iteratively summing the contribution of each fitting (K_n), multiplied by its appropriate fitting loss factor (K'_n), along the entire length of the pipeline corridor as in Equation 3.9⁴⁹.

$$K_f = \sum_{i=1}^n \{(K_i * K'_i) + \dots + (K_n * K'_n)\} \quad (3.9)$$

Where:

K_n = The individual fitting loss component (*unitless*)

K'_n = The individual fitting loss factor (*unitless*)

3.7 PARAMETERIZING CONSTRUCTION MATERIAL REQUIREMENTS

Once the pump energy associated with the corridor specification has been computed according to method laid out in Equations 3.1 - 3.9 the next step is to estimate the volume of reinforced concrete that must be poured to facilitate the construction of the requisite infrastructural components of the proposed reuse system. It is assumed for the purpose of this analysis that these new infrastructural components will principally be associated with the need to install one or more pumping houses which will be situated along the length of the corridor⁴⁹. The determination of the size of each of these facilities and their concomitant material footprints will be assessed on the basis of the total pump energy required for each corridor and the structure of the different elevation profiles. Consideration will be

given to economies of scale in terms of the efficiency that can be achieved through the operation of larger pump systems.

3.8 PARAMETERIZING CHEMICAL CONSUMPTION RATES

The third key set of parameters that must be provided to the WWEST model are the volumes of any consumable chemical substances that must be provided to facilitate the tertiary treatment processes associated with the proposed reuse system. Ideally, the determination of these parameters would be made on the basis of the relative quality of the influent wastewater to that of the effluent treated water. However, the data requirements for this level of specificity in the model parameterization are significant and thus were left outside the scope of this analysis.

3.9 ESTIMATING NET WATER USAGE EFFICIENCY

The final step towards the research program's overarching goal of estimating the life-cycle energy-water usage efficiency of proposed new reuse systems involves converting life-cycle energy consumption into predicted water consumption. This conversion can be accomplished by applying known water usage efficiency factors for a suite of energy generation technologies to the local grid mix responsible for producing the energy that will be supplied to the reuse system over its life-cycle. For the purpose of this analysis, the calculated metric will focus on the consumptive use of water for energy production as opposed to the non-consumptive use. This designation is important as the difference between the consumptive and non-consumptive water use profiles for a number of energy generation, and in particular, cooling technologies, can be non-trivial.

While the distribution of energy generation technologies is known from published statistics on the local grid mix associated with each of the five case study regions, a more granular

breakdown of the precise thermoelectric cooling technology used by each category of energy producer is not known. In the absence of this detailed information a range of energy usage efficiencies – corresponding to the min-max range of cooling technology efficiencies for each production method – will be generated by the analysis, providing bounds to our uncertainty in the final calculated values.

3.10 THE WWEST MODEL OUTPUTS

The final output of the WWEST based calculation will involve three numbers. The first corresponds to the volume of wastewater that is to be treated and recycled by the proposed reuse operation over the course of a given year. The second corresponds to the life-cycle energy requirements attributable to this volume of water reuse each year at the site in question. The third number will be the quantity of water that must be consumed in order to generate the energy associated with the system's annualized life-cycle energy requirements. By computing the ratio of the second number to the third we will thus be left with an estimated ratio depicting the life-cycle energy-water usage efficiency of the proposed reuse system. If this ratio is greater than one it means that the proposed system is highly efficient, with more water being saved within the local basin each year than is consumed – likely elsewhere, outside the basin – to produce the energy associated with its operation. Similarly, if this ratio is greater than zero but less than one, the system is only partly efficient. And finally, if this ratio is less than zero, the system is highly inefficient, with more water being expended to produce the energy required for the reuse operation than is saved by the operation of the reuse system. This third condition would essentially amount to a situation where water was being virtually imported into the basin in the form of the energy consumed by the reuse system.

In god we trust. All others bring data.

William Edwards Demming (1900-1993)

4

Case Study Results

4.1 SANTA BARBARA REGION

THE FIRST CASE STUDY REGION, comprising the coastal southern portion of Santa Barbara County, was selected to reflect the local interests of the institution supporting this dissertation research. Hydrologically, this case study region is distinctly enclosed by a steep coastal mountain range to the north and the Pacific Ocean to the south. This case study area is not connected to any of the major inter-basin water transfer projects within the state (i.e. The State Water Project, the Los Angeles aqueduct, etc.). As such, Santa Barbara municipal water managers must be both creative and self-reliant in terms of their long-term municipal water supply strategies.

Fortunately, from a freshwater management perspective, the region's unique physical geography also functions to limit the possibilities for increased population growth and urban development. Thus, the prospects for severe water shortages due to steep increases in demand are fairly unlikely. Despite this fact however, the recent drought conditions throughout the state have led to high wholesale water costs for the Santa Barbara district. This is because they are in competition with regional agricultural interests with long-term investments in costly orchard-based crops that cannot be left to fallow.

In terms of alternative water supply options within the region, Santa Barbara has recently renewed talks for the development of a local seawater desalination plant that had been put on hold following the 2008 economic recession. This willingness to reconsider a high-cost desalination-based alternative freshwater supply strategy suggests that large-scale municipal water reuse may also be put forth as a feasible alternative in the near-term future and thus, that such a prospective analysis of the tradeoffs associated with such a system would indeed be a valuable exercise.

4.1.1 REGIONAL CONTEXT

- HUC-8 Code: 18060013
- Total Area: 1,173.6 km^2
- Maximum Elevation: 1,376.7 m
- Minimum Elevation: $-0.7 m$
- Mean Slope: 13.98 %
- Standard Deviation of Slope: 11.07 %
- Dominant Soil Composition: Hydrologic Soil Group - B: 10 – 20% clay, 50 – 90% sand, 35% rock fragments



Figure 4.1: Santa Barbara Region Overview

4.1.2 SEARCH DOMAIN

The search domain used for both the weighted overlay site suitability analysis as well as the corridor location problem specification is depicted in Figure 4.2. The extent and dimen-

sions of this search domain is depicted in the statistics below.

- Grid Dimensions: 363 *cells* x 1351 *cells*
- Grid Cell Resolution: 100 *m* x 100 *m* (1 *ha*)
- Feasible Grid Cells: 117,363 *cells*



Figure 4.2: Santa Barbara Region Search Domain

4.1.3 DESTINATION SEARCH INPUTS

There are three key inputs to the weighted overlay analysis used to determine the location and extent of suitable sites for the implementation of artificial groundwater recharge basins within the region. The four layers which were generated as the discrete inputs to the WOA procedure are depicted in Figures 4.3 through 4.5. The first layer gives each cell in the search domain a score between 1 and 10 on the basis of the suitability of its slope for the implementation of a artificial groundwater recharge basin. Areas with steep slopes are given lower suitability scores. Areas with shallower slopes are given high suitability scores.

The second input to the WOA destination search process is based upon the permeability of the surface geology as shown in Figure 4.4. Permeability is a crucial parameter in determining the rate of infiltration that can be achieved by a recharge basin and thus the requisite size of a basin for the purpose achieving a specified total rate of recharge. The geology

score layer gives each cell in the search domain a ordinal score between 1 and 10 on the basis of the underlying surface geology layer's permeability constant.

The final input to the WOA destination search process is based upon the existing landuse as shown in Figure 4.5. The existing landuse can be a proxy measure of both the cost of procurement for the landholdings required to implement the artificial recharge basin as well as the regulatory and engineering difficulty associated with artificial recharge basin implementation. Here again, these scores are have been pegged to a 1 to 10 ordinal scale that aligns with those assigned to each of the other two score layers.

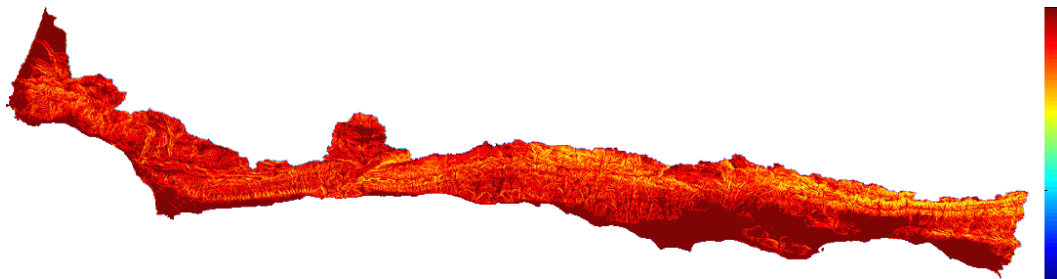


Figure 4.3: Santa Barbara Region Destination Search Inputs: Slope Scores

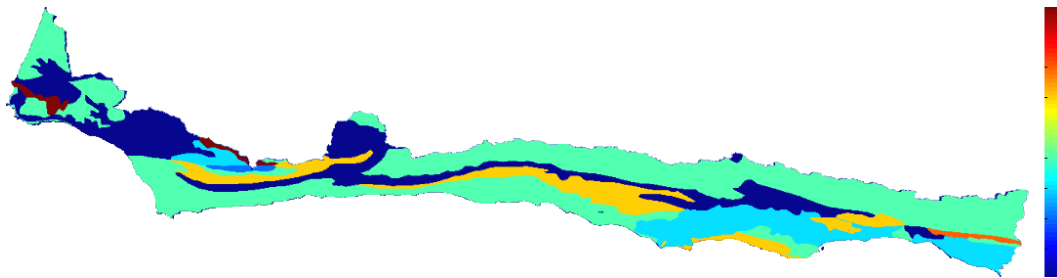


Figure 4.4: Santa Barbara Region Destination Search Inputs: Geology Scores

4.1.4 DESTINATION SEARCH OUTPUTS

The raw output of the WOA destination search process is a composite layer of which depicts a measure of overall suitability for the given landuse application on an ordinal scale

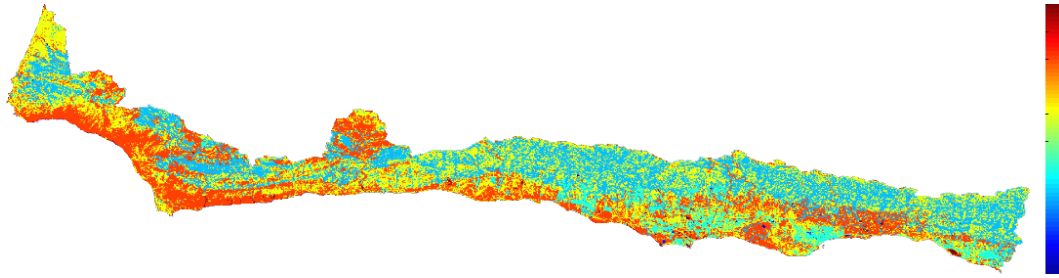


Figure 4.5: Santa Barbara Region Destination Search Inputs: Landuse Scores

as in Figure 4.6. This single composite suitability layer is then thresholded, selecting only those areas that have the highest composite suitability scores as shown in Figure 4.7. A set of morphological operations is applied to this threshold mask which ranks each connected area of high suitability in terms of its size. Larger connected areas of high suitability are considered better in this process and thus, in this way, a single destination location for the corridor search process can be automatically selected as the single largest area of high aggregate suitability with the study area.

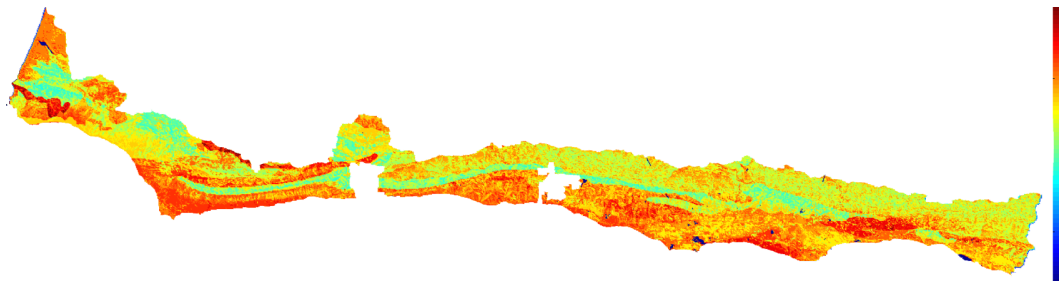


Figure 4.6: Santa Barbara Region Destination Search Outputs: Composite Scores

4.1.5 PROPOSED CORRIDOR ENDPOINTS

For the Santa Barbara case study region, the final output of the WOA analysis is shown in Figure 4.8 in red and mapped relative to the location of the source location for the corridor location analysis that corresponds to the location of the largest WWTP within the basin, in

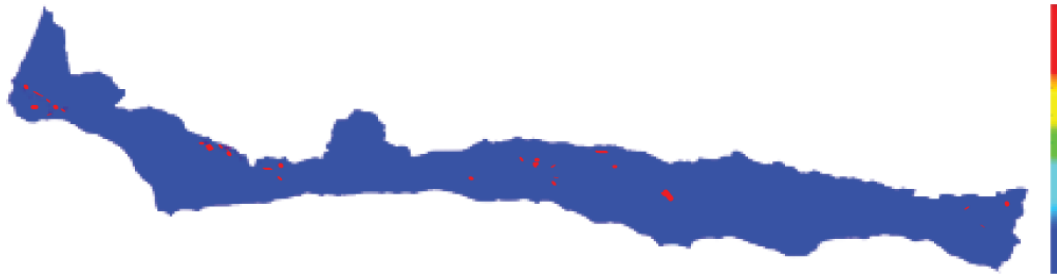


Figure 4.7: Santa Barbara Region Destination Search Outputs: Candidate Regions

green. These two points, plus the extent of the search domain, form the basis of the corridor location problem specification that is to be discussed in further detail in the subsequent section.

- Start Location: (313, 1083)
- End Destination: (248, 886)
- Shortest Euclidean Path Distance: 20,745 m (21 km)

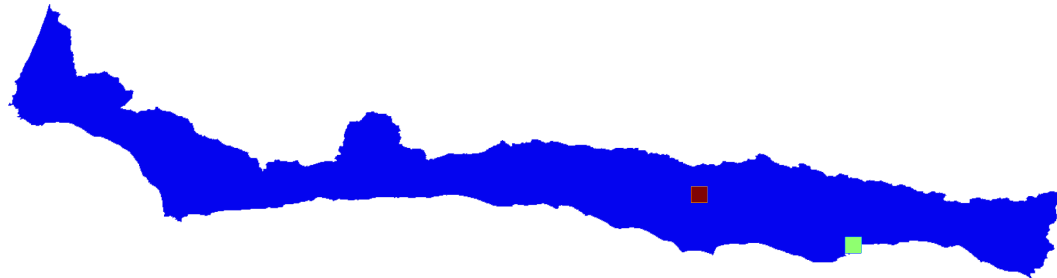


Figure 4.8: Santa Barbara Region Proposed Corridor Endpoints

4.1.6 PROPOSED OBJECTIVE LAYERS

For the corridor location problem specification used as the input to the MOGADOR algorithm, four key pieces of information are required. The first three correspond to the source location, the destination location, and the search domain boundaries that have been previously described. The fourth key input category corresponds to the objective score layers

which capture the cost associated with routing sections of a corridor over each grid cell in the search domain. For this analysis, the following three distinct objectives were developed.

The first objective category is based upon the accessibility of each location for the purposes of constructing and maintaining the water distribution infrastructure that the corridor is designed to support and is shown in Figure 4.9. It is fundamentally easier to get materials and people to a locations that are positioned along road networks. As a result, the underlying road network topology was used to encode a continuous objective score layer with values ranging from 1 to 10 that can be described as a measure of *Accessibility* and which favors those locations that are on and around roads.

The second objective category is based upon the existing land use regime within the regional search domain. The idea behind the composition of this objective can be thought of as somewhat of the converse of Accessibility in the sense that, regions which are already heavily developed are likely to be socially, politically, or economically challenging to implement corridors for large scale water distribution pipeline infrastructure. Using standardized USGS based land use classification, each grid cell in the search domain is given a nominal objective score value from 1 to 10 corresponding the relative level of *Disturbance* that would be associated with routing a corridor across it. This objective layer is depicted in the layer plotted in Figure 4.10.

The third objective category is derived from the underlying slope within the search domain. Steeper slopes are assigned a higher ordinal score, ranging from 1 to 10. This objective reflects the desire for corridors to be shorter in length and minimally accumulate slopes over their length. In this way, the slope score provides a mechanism for the corridor routing algorithm to preferentially favor corridors that would have minimal energy requirements in terms of the operational energy requirements of the anticipated water distribution infrastructure. This slope score objective layer is depicted in Figure 4.11.

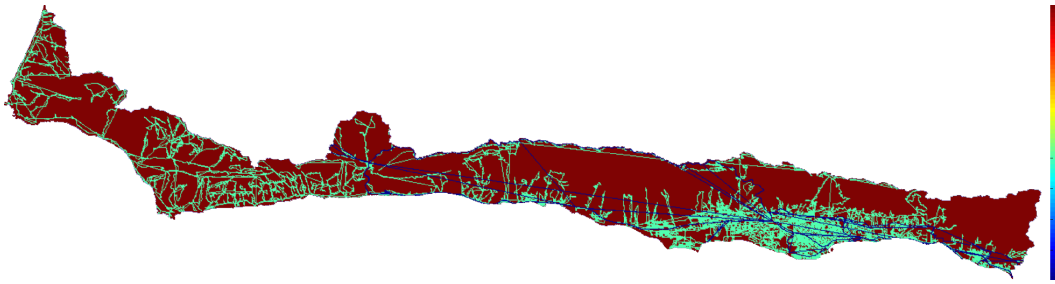


Figure 4.9: Santa Barbara Region Accessibility Based Objective Scores

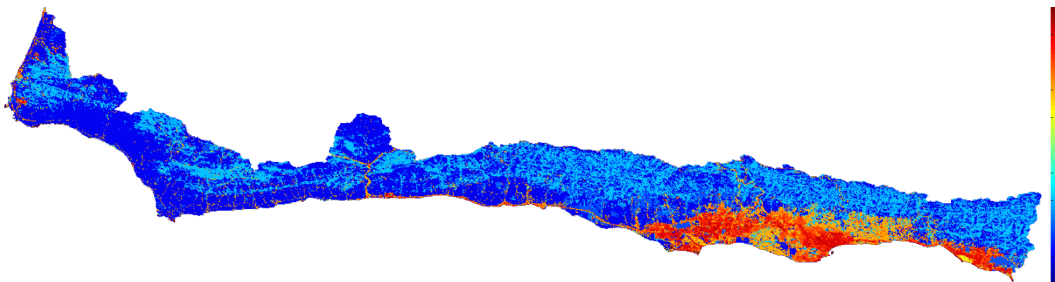


Figure 4.10: Santa Barbara Region Land Use Disturbance Based Objective Scores

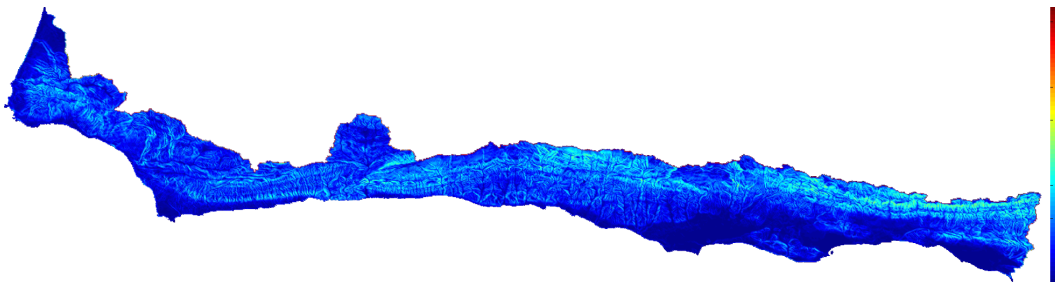


Figure 4.11: Santa Barbara Region Slope Based Objective Scores

4.1.7 PROPOSED CORRIDOR SOLUTIONS

Shown in Figure 4.12 are the outputs of a series of three runs of the MOGADOR algorithm for the Santa Barbara region problem specification. These three runs differ solely in terms of the number of individuals contained within the seed population. The size of this seed population determines the extent with which the input search domain is search and, consequently, the degree to which the output solution corridor is likely to approximate

the global optimal solution. The figure contains six panes made up of three rows and three columns. The columns depict, from left to right, and plan view of the final output solution set, and line plot of the break down of objective scores for the top 100 ranked individuals in the final output solution set, and, finally, a histogram plot of the frequency of total aggregate objective scores among the same top 100 individuals. Alternatively, the rows, moving from top to bottom, reflect the changing results as the population size is increased from 1,000 to 10,000 to 100,000.

As the histogram plots of the aggregate objective scores illustrate, with a population size of 100,000 the aggregate objective scores are quite low, and the quality of the final output solution set is very high. This improvement in solution quality comes at the expense of processing time/effort. This tradeoff shall be discussed in greater detail and illustrated comparatively across all of the five case studies at the end of this Chapter.

One interesting feature of this exercise which can be readily appreciated from this set of plots is the source of the improvement in the aggregate objective scores between the different runs. For example, note the height of the data series depicted by the blue line, corresponding to the accessibility score, in the three plots in the middle column. The progressive decrease in the values associated with this line indicates that the reduction in aggregate objective scores between the three runs can be attributed to a reduction in the Accessibility score. This is tantamount to saying that the search process is able to provide better solutions as it *finds the road network*. And indeed, this conclusion is reflected from a simple visual inspection of the output corridors plotted in the panels contained in the first column. Here it can be seen that in the 100,000 population size solution set, the pathway sections have become much more linear, and appear to correspond with the layout of different road segments which occupy the area in between the source and the destination.

Figure 4.14 provides an illustration of the top ranked final output corridor solution presented in the context of the full search domain. For all of the case studies the highest quality

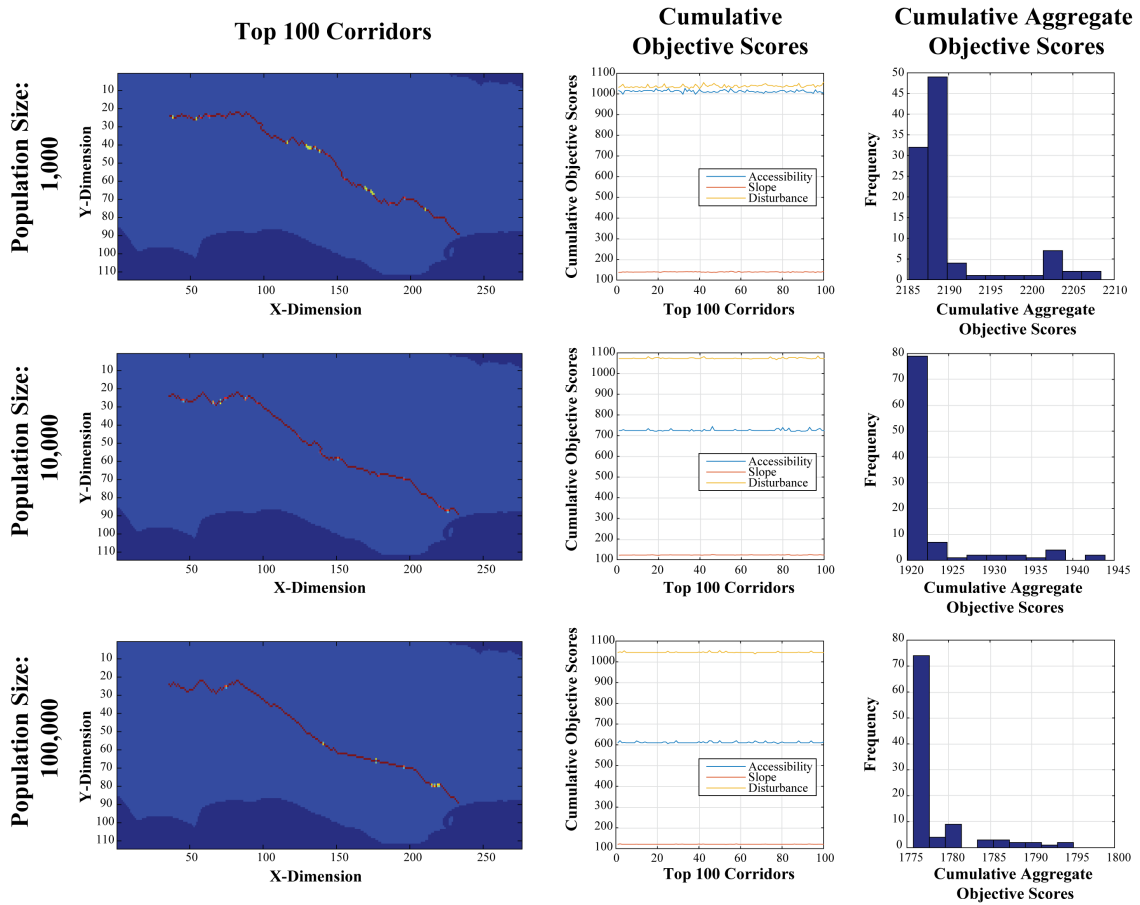


Figure 4.12: Santa Barbara Region Corridor Analysis Results

solution was developed by the model run containing the largest seed population. This was fully expected however and is in good agreement with the theoretical discussion of the role of the population initialization procedure in the behavior of the MOGADOR algorithm described in Chapter 3.

4.1.8 ALONG-CORRIDOR ELEVATION PROFILE

Figure 4.14 illustrates the along-corridor elevation profile that can be generated by superimposing the output corridor solution on top of a regional digital elevation model for the Santa Barbara region. As the Figure shows the total elevation gain between the source and

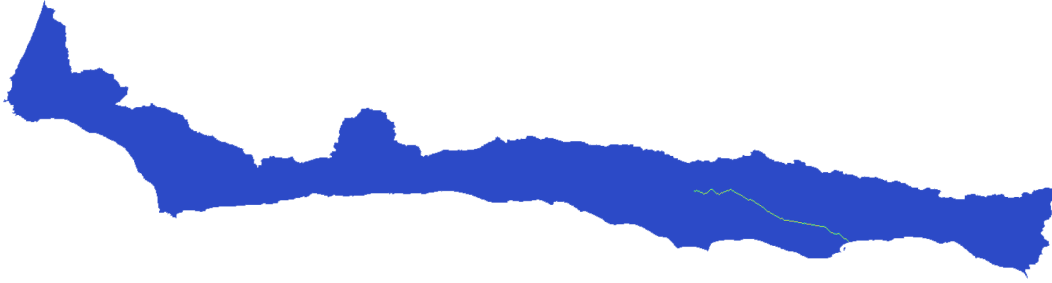


Figure 4.13: Santa Barbara Region Top 100 Corridors Basin Wide Overview

the destination location is a modest 200 meters across a distance spread of roughly 25 kilometers. While it may appear that the corridor has a significant amount of vertical fluctuations, these are minor in absolute terms, and stem from the fact that the slope score – the objective most directly related to the corridor elevation profile structure – was but only one of three in the multi-objective problem statement. These elevation fluctuations therefore can be thought of as the result of a profitable tradeoff between the accumulation of smoother slopes and more favorable values for the other two objectives.

Along Corridor Elevation Profiles (Smoothed)

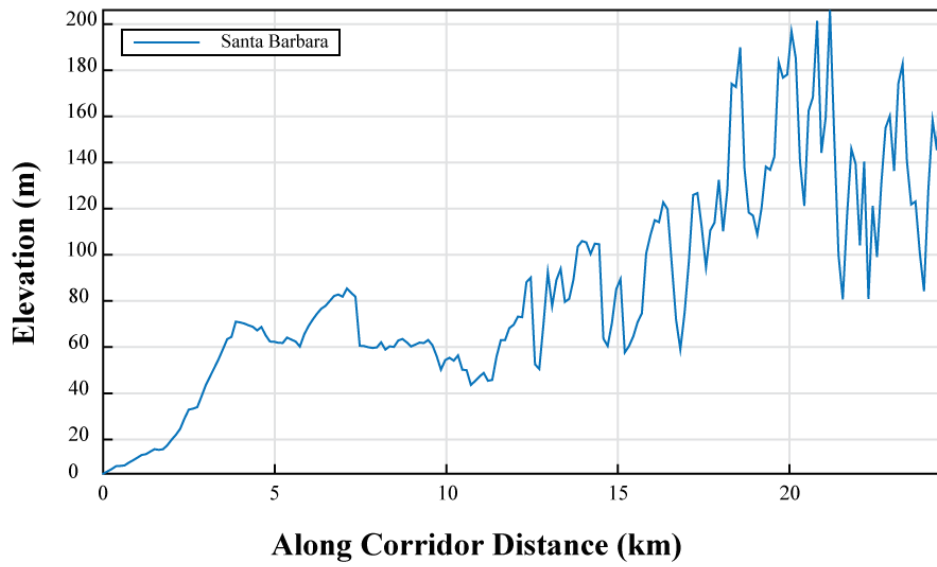


Figure 4.14: Santa Barbara Region Proposed Corridor Elevation Profile

4.2 OXNARD REGION

The second case study region consists of the HUC-8 zone containing the Oxnard plain and its immediate surrounding territories stretching as far inland as Ojai. This second case study region is located nearly adjacent to the first – separated only by a single HUC-8 basin. The reason for the choice of two case study regions in such close physical proximity is down to the recent implementation of a functioning large scale water reuse system by the municipal water management district there.

The majority of this HUC-8 zone's area is comprised of a broad low lying alluvial plain. This plain has found rich application within the agricultural sector, supporting the production of a wide variety of row crops as well as high value orchard stands. Over the past three decades, the region has also experience significant population growth with sprawling suburban communities encroaching into the more marginal farmlands or those held by smaller independent farmers. The combined freshwater demands of these two sectors have conspired to create a persistent imbalance between freshwater supply and demand in this coastal region.

Oxnard's struggle with freshwater management issues can be traced as far back as 1937 when the USGS identified that sustained groundwater pumping to support the irrigation of surface crops was contributing to the depletion of the underlying aquifer and inviting the intrusion of brackish seawater into the subsurface hydrologic strata. In response to this issue, the local municipal water authority enacted a program in which a portion of the regions' agricultural water was diverted towards a series of subsurface injection wells – strategically positioned along the coast – through which freshwater would be pumped to created an artificial pressure head barrier to prevent further intrusion of seawater, and thus further contamination of the aquifer.

This program has operated successfully for a number of decades now; achieving a func-

tional equilibrium between the level of groundwater pumping occurring within the basin and the amount of water that is delivered to the artificial intrusion barrier. More recently however, decreases in available freshwater supply due to a persistent statewide drought have forced municipal water managers in this region to think more proactively about developing alternative sources of water supply. This process began with the creation of a plant to substitute potable freshwater for reclaimed brackish water for use in the subsurface barrier injection wells.

The successful operation of this plant for a number of years inspired enough confidence among the water resource management authorities in this area to pursue and very recently achieve a goal of implementing a facility capable of reclaiming and reusing the growing volume of municipal wastewater being generated within the basin. This new facility, commissioned just this year, provides the capability to treat 100% of the wastewater generated in the basin to a potable standard through a complex treatment chain incorporating a sophisticated chain of tertiary treatment processes including: advanced micro-filtration, reverse osmosis, ultraviolet filtration, and ozonation. The long term plan for the water currently being produced by this facility is for groundwater recharge at higher elevation locations within the basin. As such, this locale represents the ideal candidate for evaluation in this study.

4.2.1 REGIONAL CONTEXT

- HUC-8 Code: 18070102
- Total Area: 5,188.3 km^2
- Maximum Elevation: 2,664.4 m
- Minimum Elevation: -0.05 m
- Mean Slope: 15.54 %
- Standard Deviation of Slope: 11.11 %

- Dominant Soil Composition: Hydrologic Soil Group - B: 10 – 20% clay, 50 – 90% sand, 35% rock fragments



Figure 4.15: Oxnard Region Overview

4.2.2 SEARCH DOMAIN

The search domain comprising the Oxnard study region is described in the statistics below and depicted graphically in the map panel contained within 4.16. Relative to the total land area contained within the Santa Barbara study region, the Oxnard domain is quite large, being nearly four times its total size.

- Grid Dimensions: *677 cells x 1586 cells*
- Grid Cell Resolution: *100 m x 100 m (1 ha)*
- Feasible Grid Cells: *518, 834 cells*

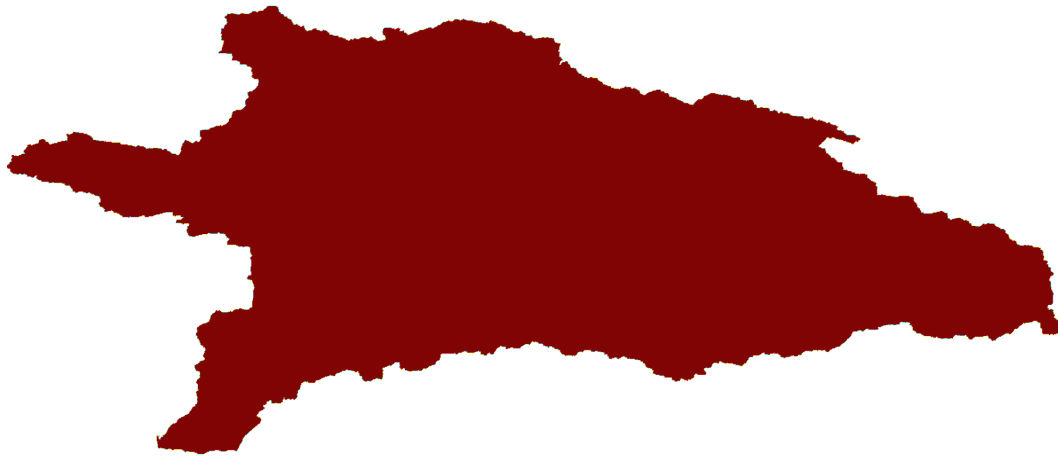


Figure 4.16: Oxnard Region Search Domain

4.2.3 DESTINATION SEARCH INPUTS

In Figures 4.17 through 4.19 the three key inputs to the Oxnard reuse destination search process are shown. A visual inspection of these three layers reveals that there is an obvious band of continuously high suitability stretching from the foot of the basin (at the lower left) along its lower portion nearly across its breadth (to the lower right). This corridor is flat low lying river bed. It possesses a highly permeable surface geology, a very shallow slope profile, and relatively low intensity land use applications.

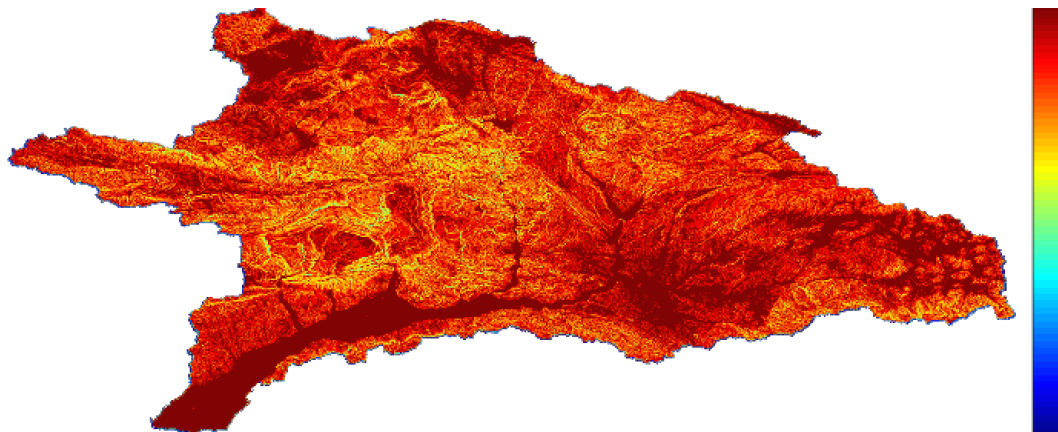


Figure 4.17: Oxnard Region Destination Search Inputs: Slope Scores

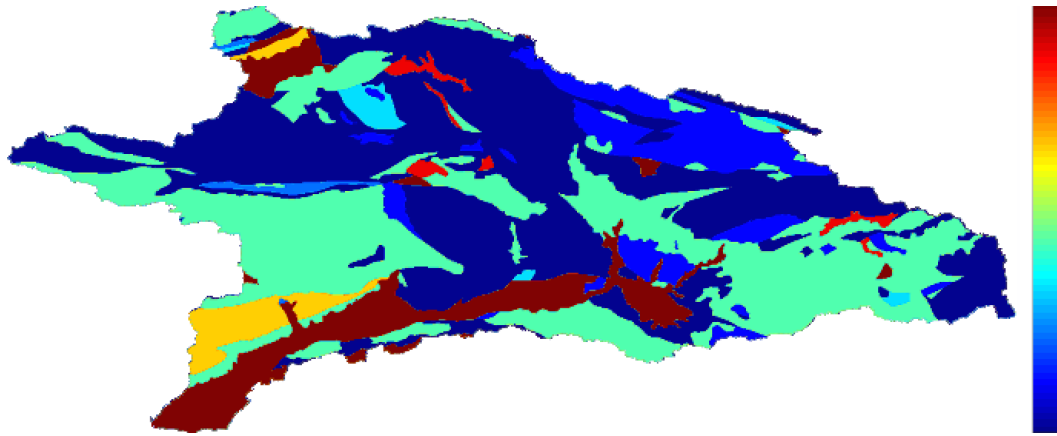


Figure 4.18: Oxnard Region Destination Search Inputs: Geology Scores

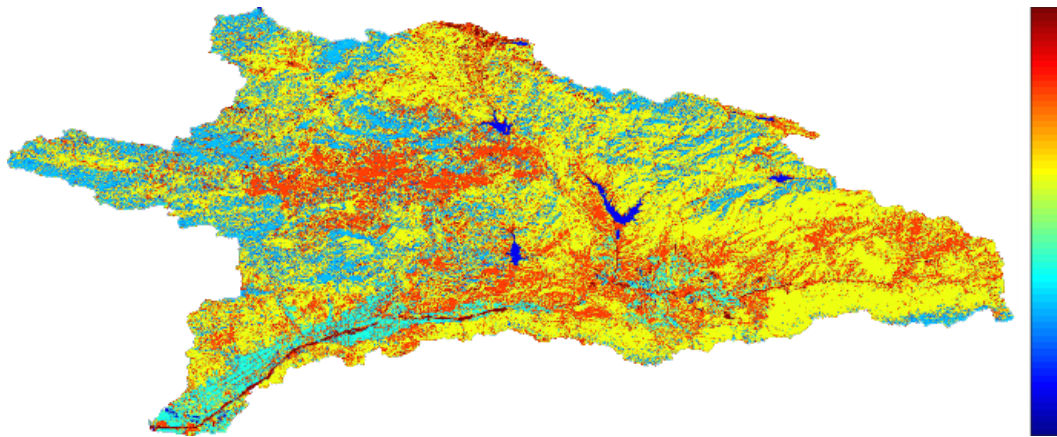


Figure 4.19: Oxnard Region Destination Search Inputs: Landuse Scores

4.2.4 DESTINATION SEARCH OUTPUTS

The layer showing the composite suitability of each cell within the study site for the site of a destination artificial water reuse facility is shown in Figure 4.20. As this figure shows, the area with the highest composite suitability is that which was mentioned previously as being clearly visible within each of the individual input suitability layers. The majority of the top ranked areas of contiguous high suitability are contained within this region, as shown in Figure 4.21.

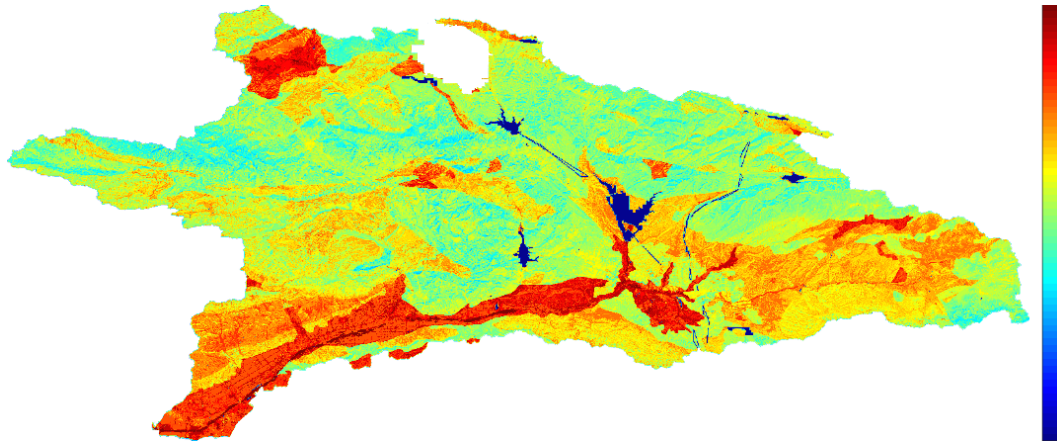


Figure 4.20: Oxnard Region Destination Search Outputs: Composite Scores

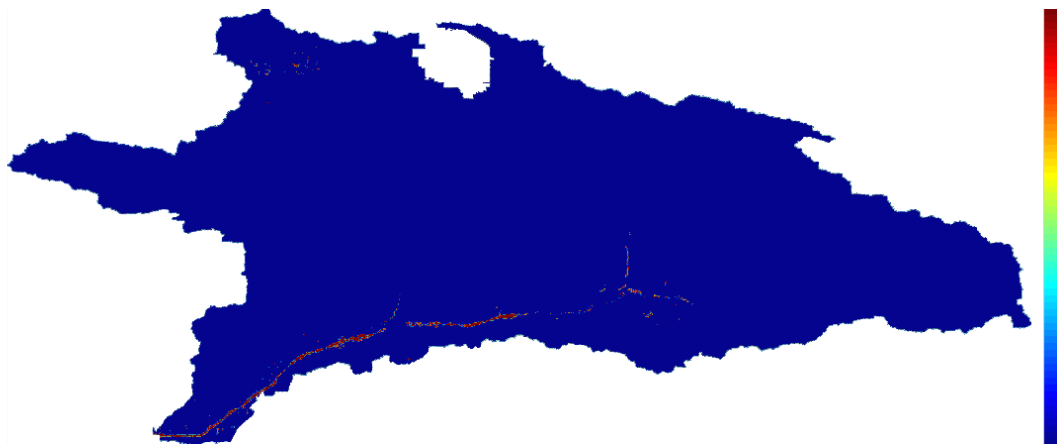


Figure 4.21: Oxnard Region Destination Search Outputs: Candidate Regions

4.2.5 PROPOSED CORRIDOR ENDPOINTS

For the Oxnard case study region, the final output of the WOA analysis is shown in Figure 4.22 in red and mapped relative to the location of the source location for the corridor location analysis that corresponds to the location of the largest WWTP within the basin, in green. These two points, plus the extent of the search domain, form the basis of the corridor location problem specification that is to be discussed in further detail in the subsequent section.

- Start Location: (656, 236)
- End Destination: (513, 532)
- Shortest Euclidean Path Distance: 32, 873 *m* (32 *km*)

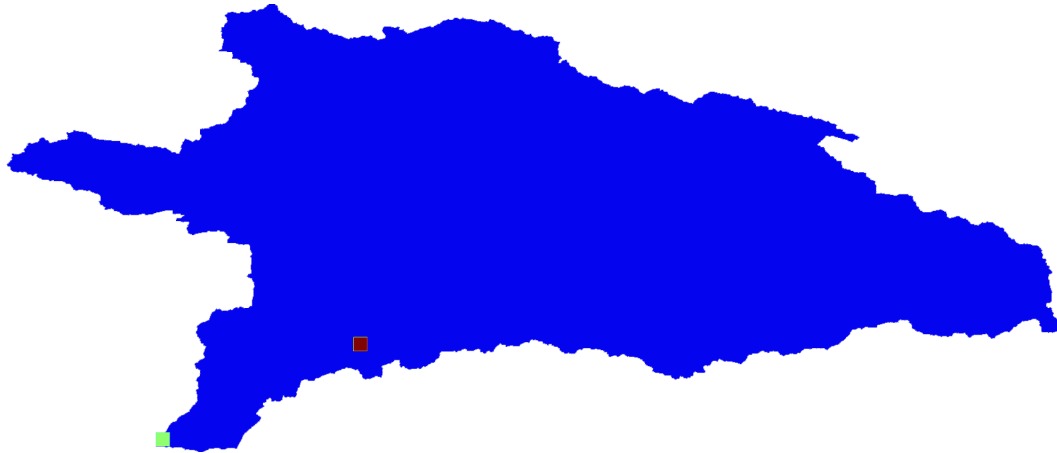


Figure 4.22: Oxnard Region Proposed Corridor Endpoints

4.2.6 PROPOSED OBJECTIVE LAYERS

In Figures 4.23 through 4.25 the three independent objective layers used as inputs to the MOGADOR problem specification for the Oxnard study site are shown. These three layers correspond to the categories of landuse disturbance, accessibility, and slope described previously for the Santa Barbara case study region and used for all of the other case studies in the analysis.

4.2.7 PROPOSED CORRIDOR SOLUTIONS

Figure 4.26 presents a figure panel containing the outputs of the three separate MOGADOR algorithm runs for the Oxnard study site problem specification using three different population sizes. As this figure panel illustrates, the first algorithm run, with a population size of 1, 000, delivered a set of 100 top output corridor solutions with aggregate objective score

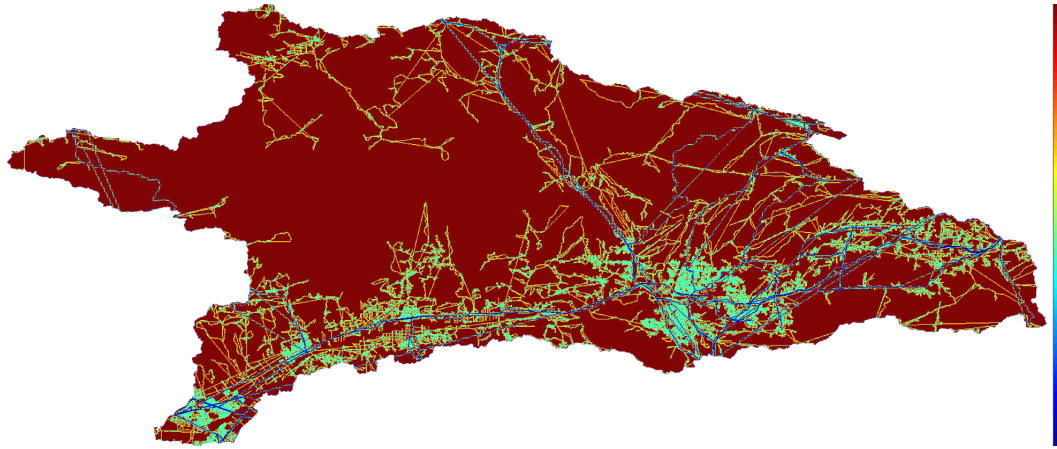


Figure 4.23: Oxnard Region Accessibility Based Objective Scores

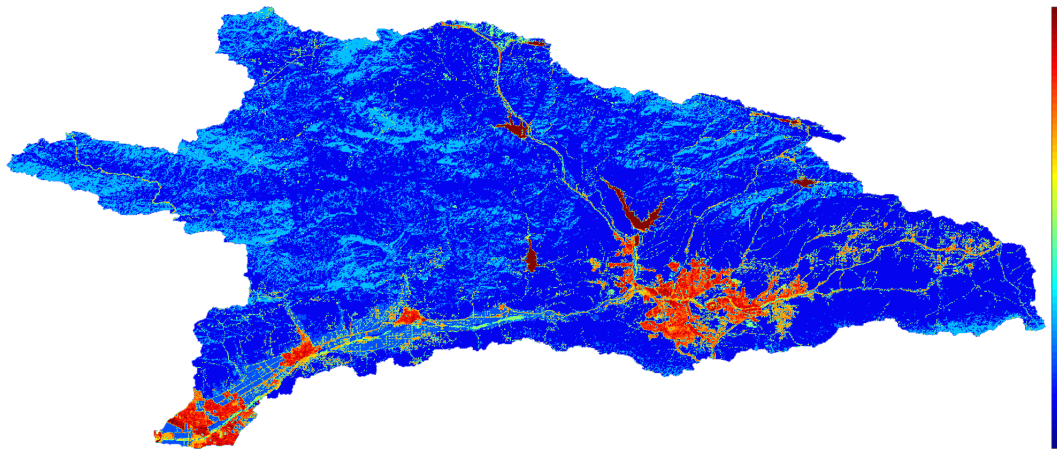


Figure 4.24: Oxnard Region Land Use Based Disturbance Objective Scores

values ranging from 3,585 to 3,615. With the second run of the algorithm, where the population size was increased to a 10,000, the top 100 output corridor solutions' aggregate objective scores can be observed to have improved markedly, covering a range from 2,910 to 2,935. The line plot in the center of the figure attests to the fact that this improvement came from reductions in both the accessibility and disturbance scores associated with the new output corridor set.

The final corridor solution set, generated from a MOGADOR model run where the in-

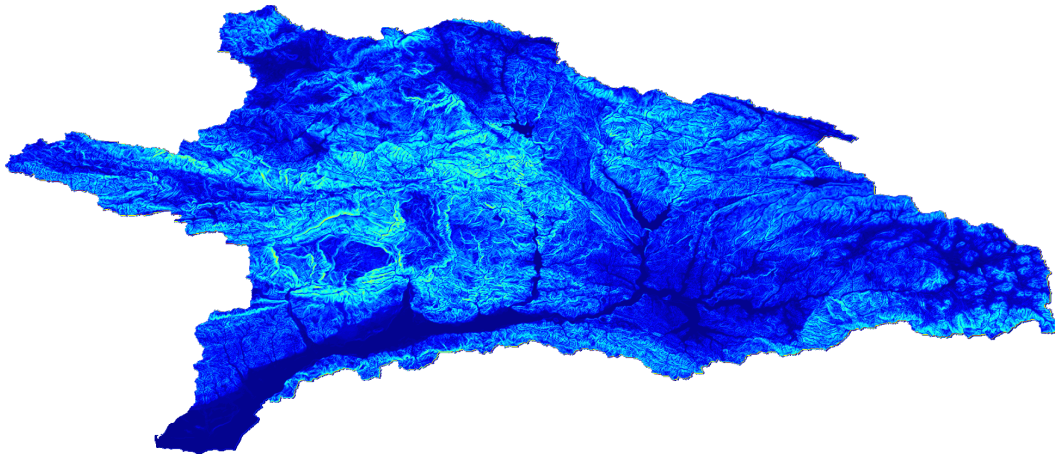


Figure 4.25: Oxnard Region Slope Based Objective Scores

put population size was fixed at a value of 100,000, produced an output set of top 100 solutions with an even lower range of composite objective scores: ranging from between 2, 740 to 2, 760. The improvement in this overall composite objective scores, as shown by the line plot at the lower center portion of the figure panel, can be observed as being attributable to marginal reductions in the accessibility and disturbance objective scores. This can be interpreted as the algorithm locating corridors which route around areas with high intensity land uses and routing along the more highly accessible transportation network.

Figure 4.27 provides a broad plan overview illustration of the final output corridors produced by the MOGADOR solution run where the population size was set to a value of 100,000.

The corresponding elevation profile for the solution illustrated in Figure 4.27 can be observed plotted in Figure 4.28. This elevation profile reveals that there is only a modest amount of elevation change along the length of the proposed corridor solution (roughly 130 meters). It also shows that this elevation gain is discontinuous along the length of the proposed corridor solution with there being two modest hills – each roughly 40 meters in height – that must be ascended and descended before the destination is reached.

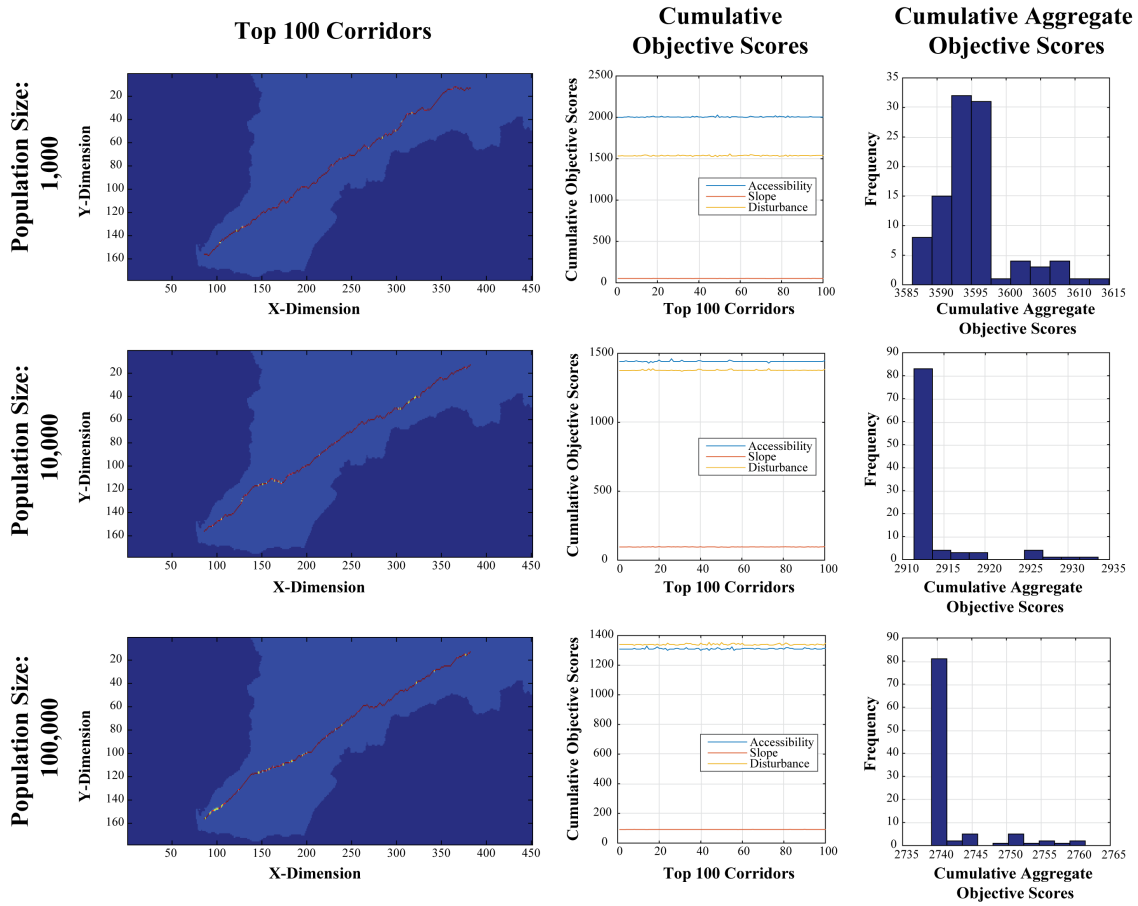


Figure 4.26: Oxnard Region Corridor Analysis Results



Figure 4.27: Oxnard Region Top 100 Corridors Basin Wide Overview

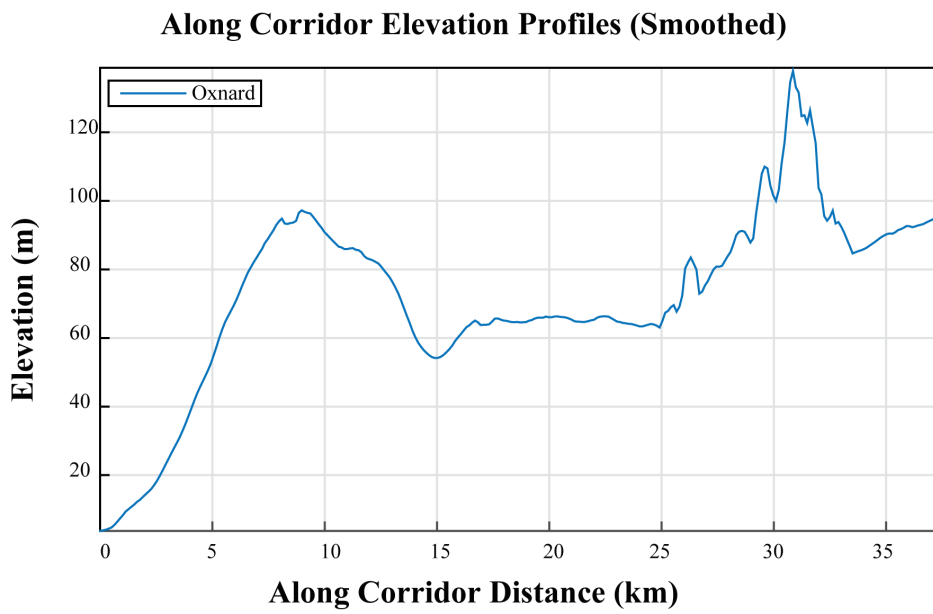


Figure 4.28: Oxnard Region Proposed Corridor Elevation Profile

4.3 SAN DIEGO REGION

The third case study region investigated as part of this dissertation consists of the HUC-8 basin comprising the city of San Diego and its adjacent metropolitan districts. This basin is situated at the southwestern most tip of the State of California and adjoins the international border between the United States and Mexico as shown by the black filled area plotted in Figure 4.29.

In terms of its water resource management history, San Diego has become world renowned as a leader in freshwater management for its innovative approaches to demand management policy and advanced technological solutions for providing alternatives supply. As is often the case, necessity has been the mother of this innovation, with the San Diego region experiencing explosive growth in population growth and associated freshwater demand over the past 50 years while at the same time being cutoff from major statewide inter-basin water transfer projects.

For example, from 2009 to 2013 the San Diego Municipal Water District embarked upon a large scale demonstration project to determine whether the advanced tertiary water treatment systems that would be necessary to facilitate large scale indirect, or possibly even direct, potable reuse could be implemented effectively and reliably at scale. In this project, purified water was blended with imported water supplies in the San Vicente Reservoir before going to the standard drinking water treatment plant. Due in large part to this success of the pilot program, the San Diego city council recently unanimously approved a three and a half billion dollar direct potable reuse project and plant that is to be constructed over the next decade. This facility is being planned in conjunction with another large scale desalination plant in a bid to build a portfolio of alternative freshwater supply and groundwater recharge capacity just as the state enters the fourth year of a crippling drought condition.

The San Diego case study region is unique in the context of the other case study regions

evaluated as part of this dissertation in that the destination location to be used for the corridor location problem specification has been designated as the location of the municipal drinking water treatment plant. As such, no destination search process was undertaken for this case study region.

4.3.1 REGIONAL CONTEXT

- HUC-8 Code: 18070304
- Total Area: 4, 338.1 *km*²
- Maximum Elevation: 1, 977 *m*
- Minimum Elevation: -0.7 *m*
- Mean Slope: 9.38 %
- Standard Deviation of Slope: 8.77 %
- Dominant Soil Composition: Hydrologic Soil Group - B: 10 – 20% clay, 50 – 90% sand, 35% rock fragments

4.3.2 SEARCH DOMAIN

The search domain comprising the San Diego study region is described in the statistics below and depicted graphically in the map panel contained within 4.30.

- Grid Dimensions: 798 *cells* x 898 *cells*
- Grid Cell Resolution: 100 *m* x 100 *m* (1 *ha*)
- Feasible Grid Cells: 433, 808 *cells*

4.3.3 PROPOSED CORRIDOR ENDPOINTS

The proposed endpoints to be used in the MOGADOR algorithm specification are shown in Figure 4.31. The source location was determined by the location of the largest NPDES



Figure 4.29: San Diego Region Overview

permitted WWTP in the basin while the destination location, in this case, was pre-determined as the location at which an artificial groundwater recharge basin has already been implemented.

- Start Location: (635, 42)
- End Destination: (453, 363)
- Shortest Euclidean Path Distance: 36, 901 *m* (36 *km*)

4.3.4 PROPOSED OBJECTIVE LAYERS

The three proposed objective layers which round out the MOGADOR algorithm problem specification and depicted in Figures 4.33 through 4.34, consist of the same accessibility, landuse disturbance, and slope based data layers as those described previously for Santa Barbara & Oxnard, and used for all of the case studies included in this analysis. In terms of the structure of these objectives in the San Diego region, the coastal areas tend to be very

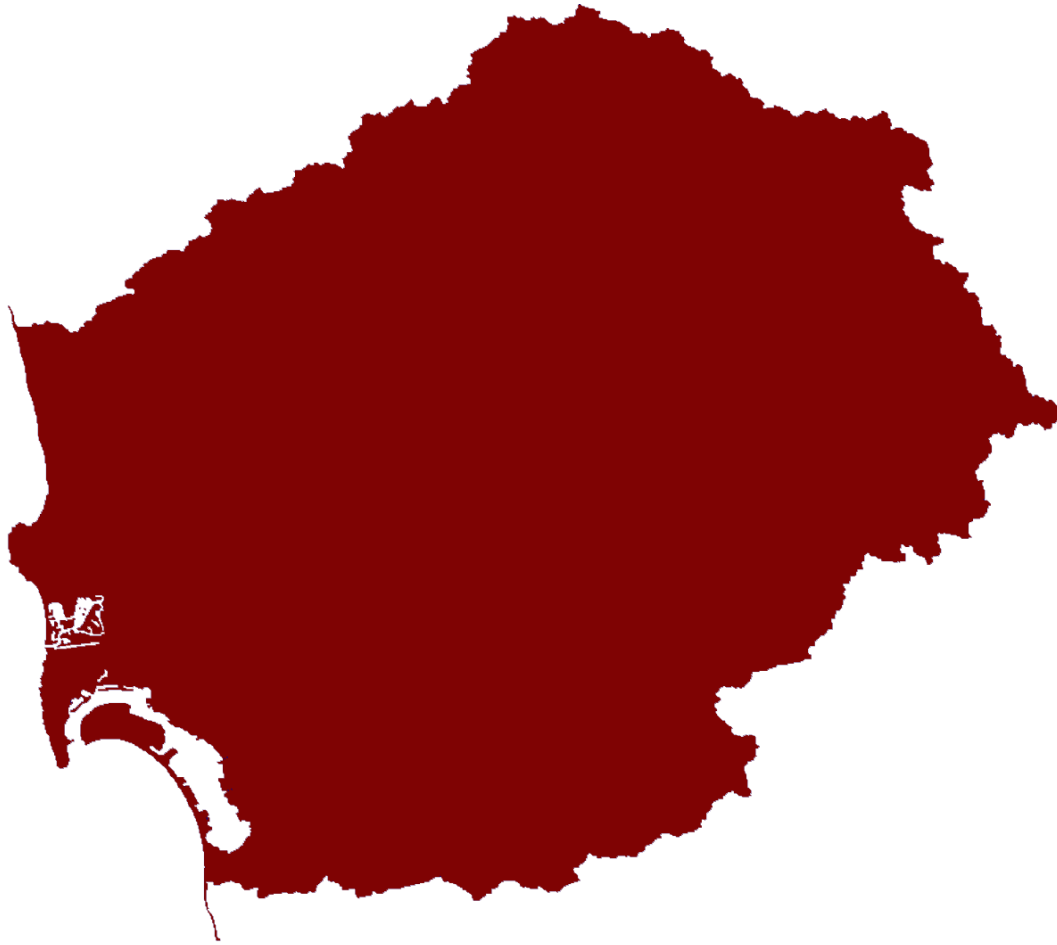


Figure 4.30: San Diego Region Search Domain

highly developed with large land use disturbance scores as well as a dense road network providing favorable accessibility values. The basin does not contain an extreme amount of topographic relief as evidenced by the fairly homogeneous distribution of slopes shown in Figure 4.34.

4.3.5 PROPOSED CORRIDOR SOLUTIONS

The results of the three runs of the MOGADOR algorithm for the San Diego region case study corridor location analysis are presented in Figure ?? and reflect the same three variations on the seed population size described for the previous case studies. Here again, the

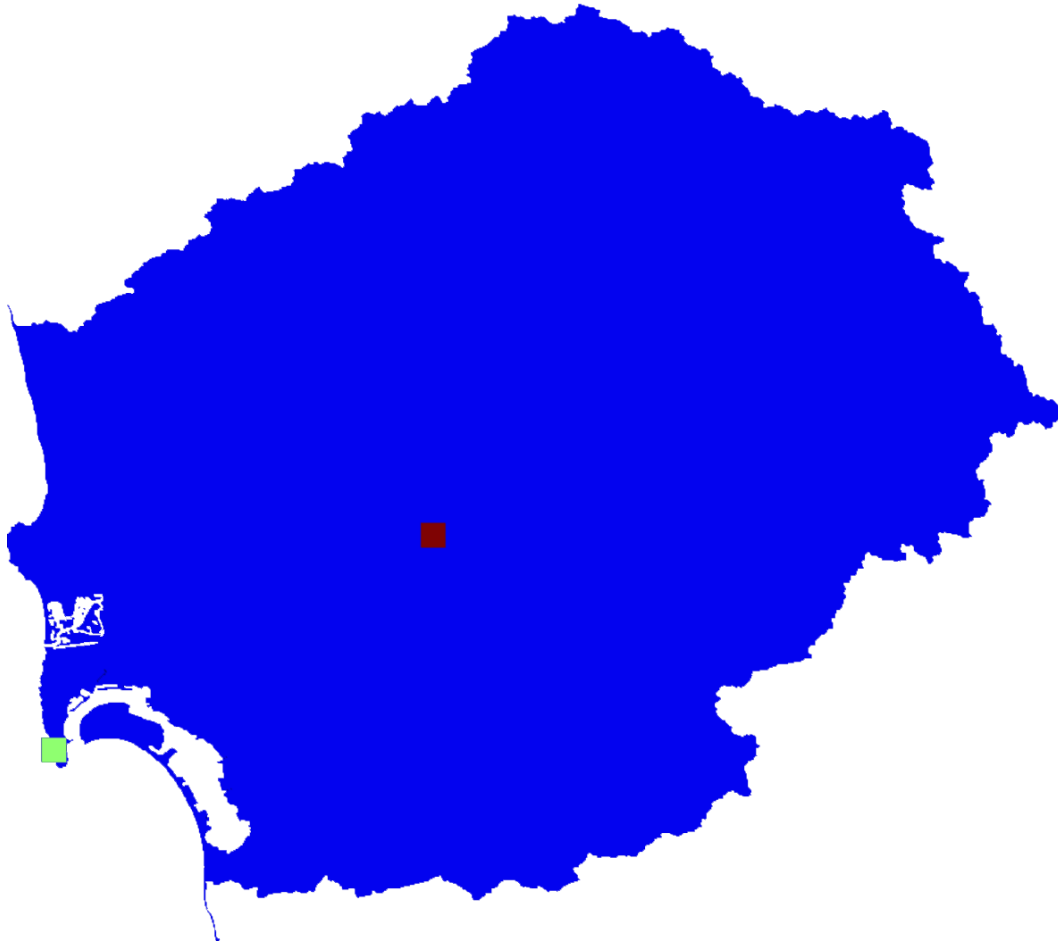


Figure 4.31: San Diego Region Proposed Corridor Endpoints

highest quality solution set was produced by the MOGADOR run using the largest population size with the minimum cumulative objective scores for the top 100 output solutions ranging from 3,840 to 3,865. Between the three algorithm runs, the majority of the aggregate objective score improvement came from reductions in the accessibility and disturbance scores; this, again, reflecting the algorithm's iterative discovery of those corridor sections running in and along road network sections while avoiding areas with higher intensity landuse.

The top output solution for the three runs is depicted in the context of the entire search domain in Figure 4.36. As this Figure shows the final corridor routes from the location of

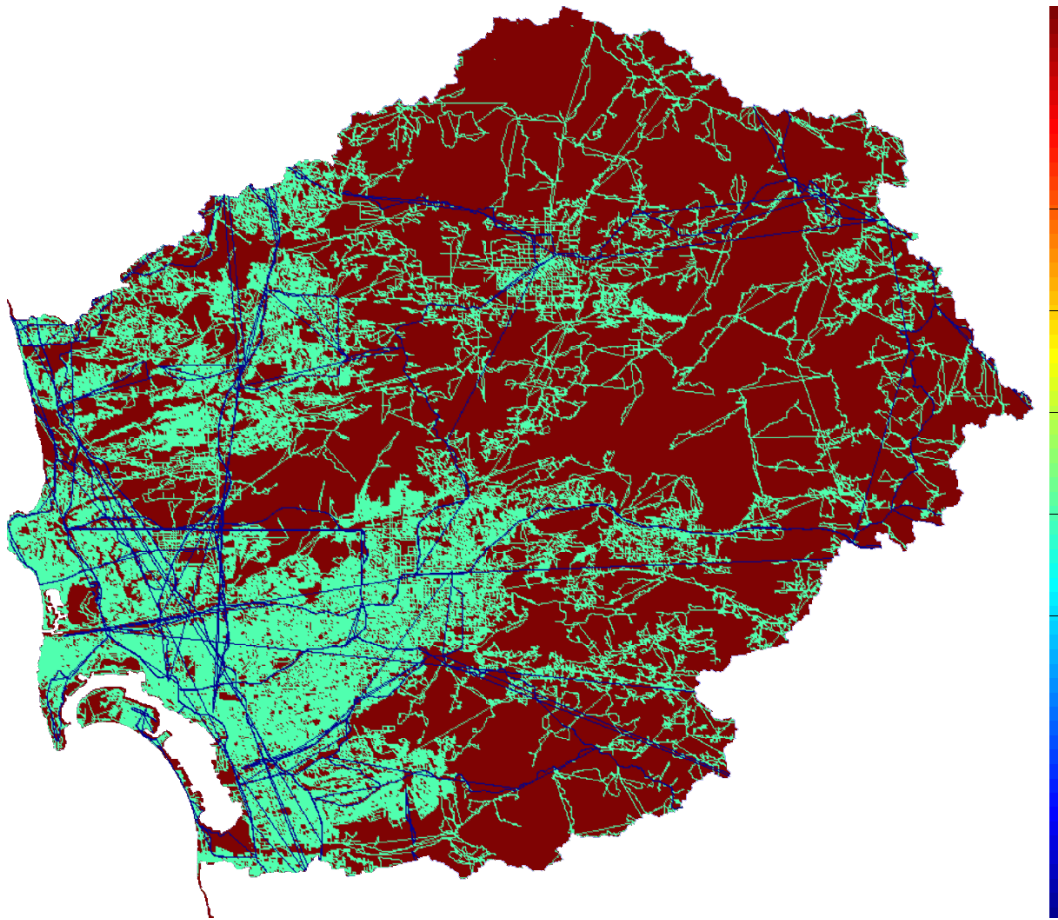


Figure 4.32: San Diego Region Accessibility Based Objective Scores

the coastal WWTP treatment plant, around the large harbor area at the Southwest portion of the search domain, and up towards the existing groundwater recharge facility located at the heart of the basin.

Figure 4.37 plots the elevation profile of the land surface along the length of the proposed corridor solution. The maximum elevation gain between the endpoints of the corridor is roughly 230 meters, however there is a considerable amount of ups and downs along the corridor's length. The jaggedness of the elevation profile reflects the extremely high density of the urban environment in the area immediately inland from the coastal WWTP. It reflects a necessary tradeoff between the accumulation of slope and the need to route

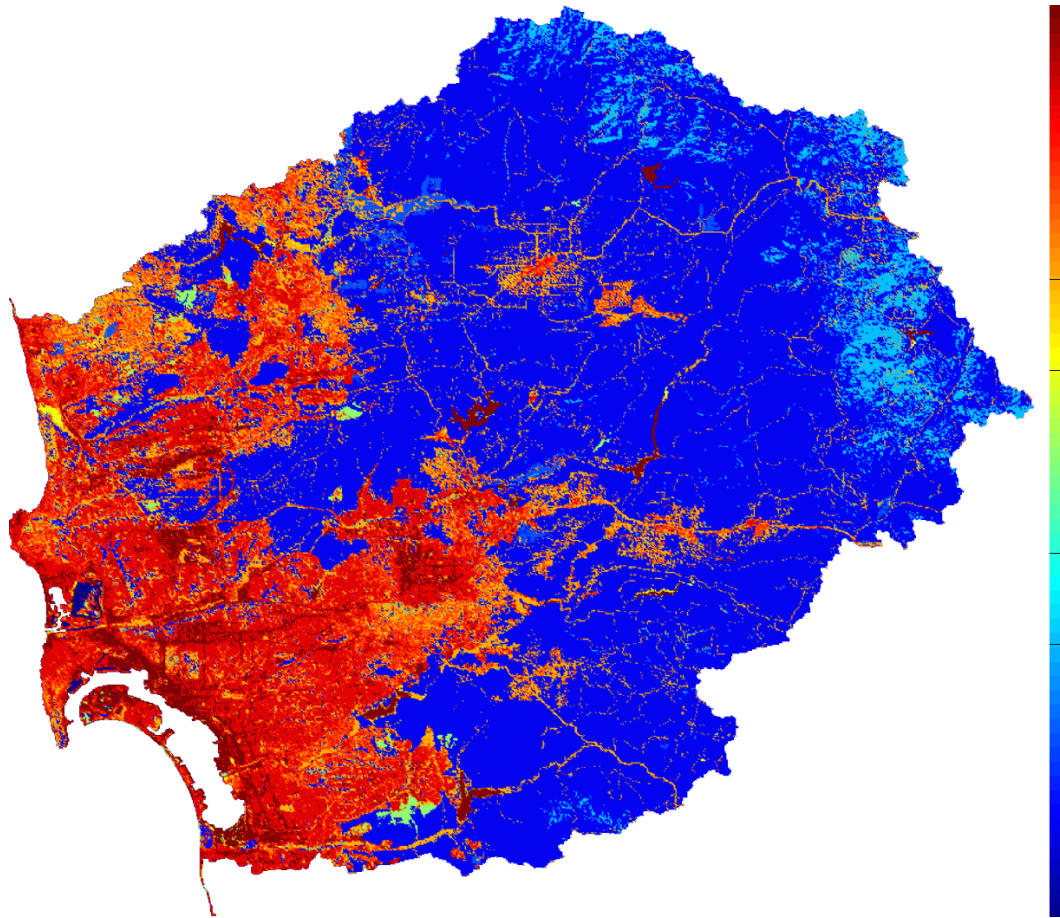


Figure 4.33: San Diego Region Land Use Disturbance Based Objective Scores

around areas with high intensity existing landuse.

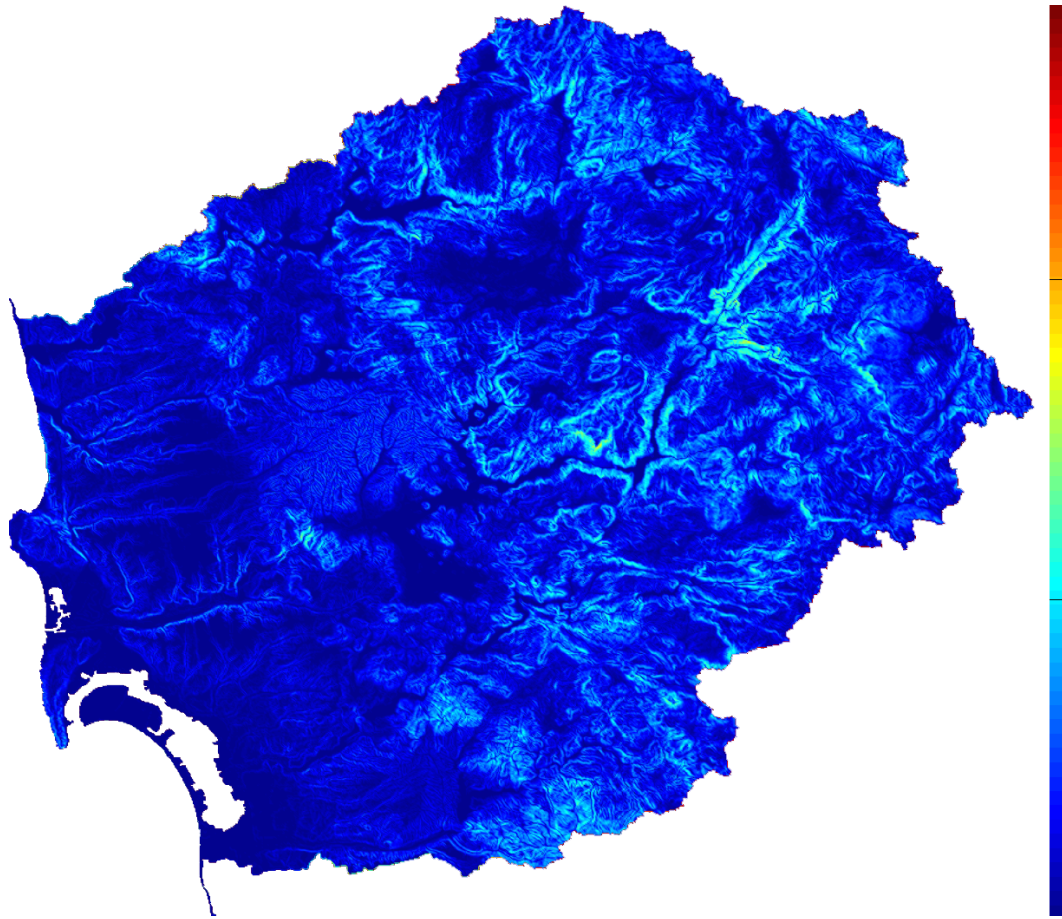


Figure 4.34: San Diego Region Slope Based Objective Scores

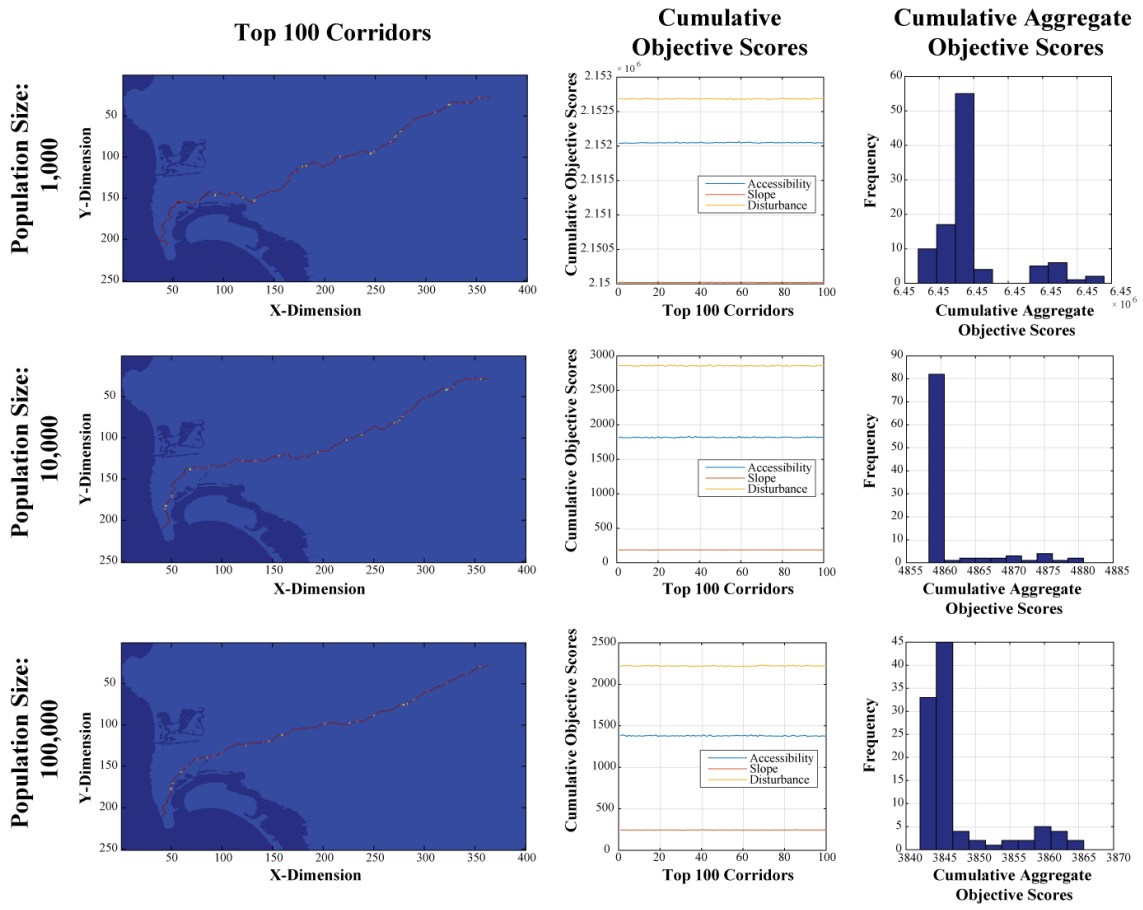


Figure 4.35: San Diego Region Corridor Analysis Results

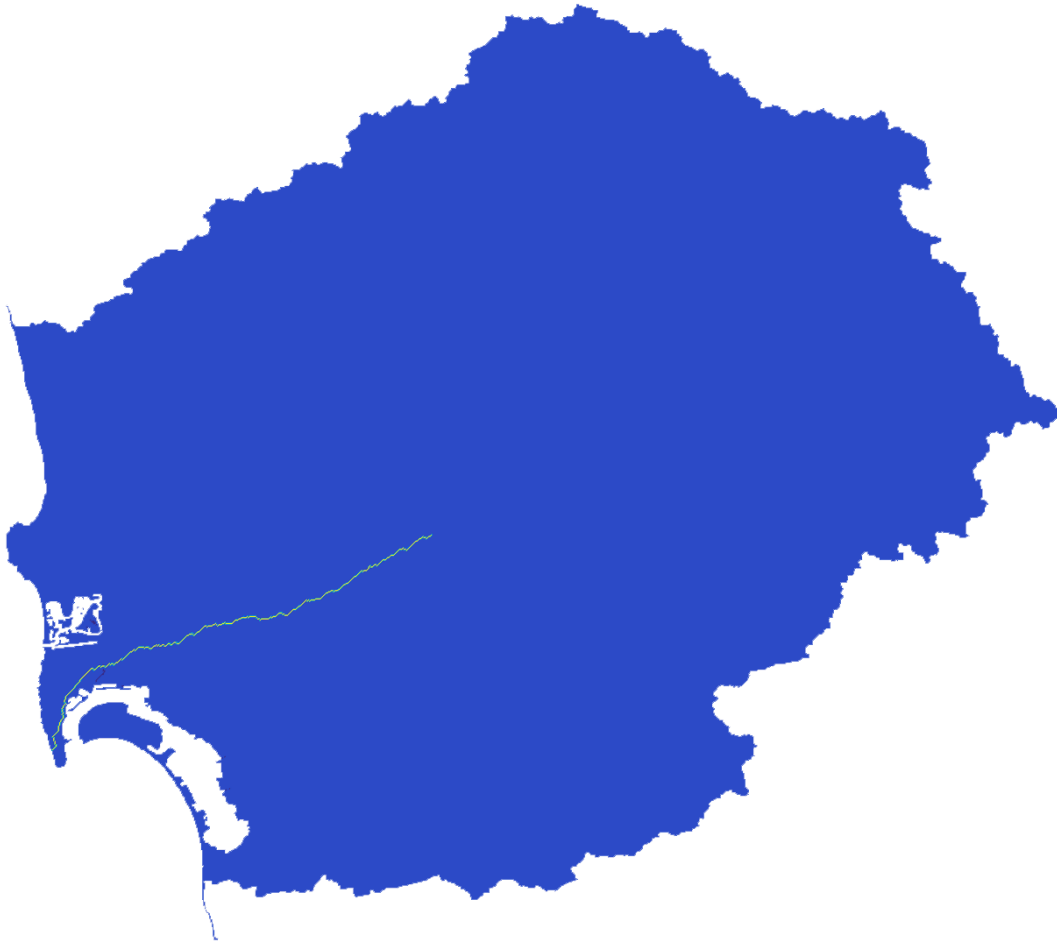


Figure 4.36: San Diego Region Top 100 Corridors Basin Wide Overview

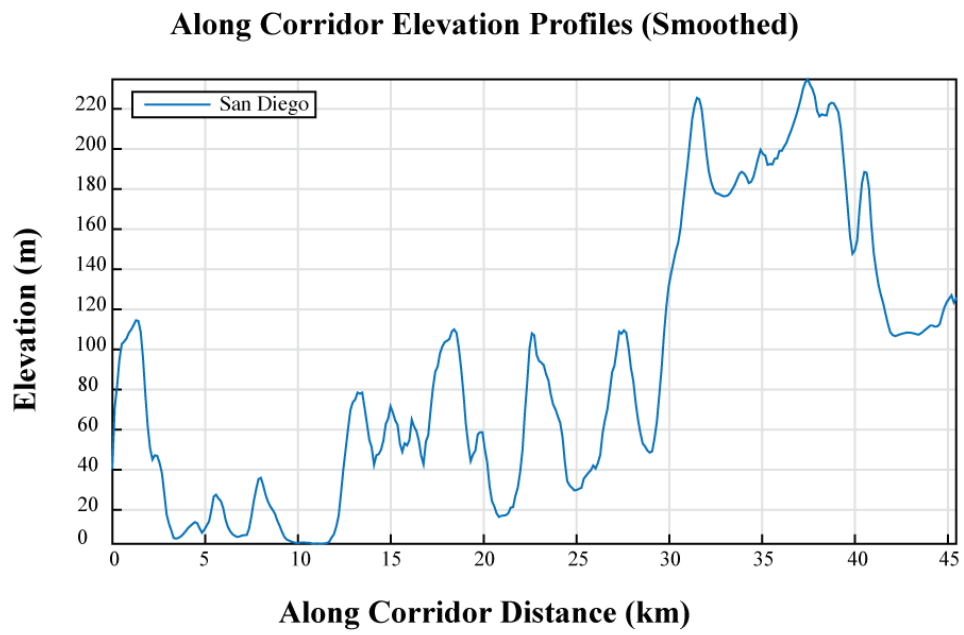


Figure 4.37: Santa Diego Region Proposed Corridor Elevation Profile

4.4 SANTA ANA – SAN BERNADINO REGION

The Santa Ana – San Bernadino case study region, filled in black in Figure 4.38, is comprised of another coastal HUC-8 basin that is situated north of San Diego and south of Oxnard. The majority of the basin's area is positioned inland with a small strip of land stretching westward towards the coast around the bed of the Santa Ana river. In terms of total area, the Santa Ana – San Bernadino is the second largest case study region being investigated as part of this dissertation analysis. It is almost four times the size of the Santa Barbara case study basin and is only marginally smaller in size than the largest of the five study sites: Fresno – Tulare.

The Santa Ana – San Bernadino region, which is positioned squarely within Orange County, shares a number of hydrologic similarities to the San Diego region and as a result, it too has been forced to adopt a whole suite of innovative water resource management policies and technological solutions. In fact, this region is home to the first large scale commercial municipal wastewater recycling and reuse installation in the United States; called Water Factory 21. This facility takes raw sewage as influent and uses a cutting edge treatment process chain to return that water to levels of purity that are of near potable standard. This reclaimed water is then pumped uphill to a series of interconnected recharge basins positioned along the bed of the Santa Ana river where it is allowed to infiltrate back into the subsurface aquifer, providing a crucial source of artificial recharge.

The Santa Ana – San Bernadino case study site provides a unique opportunity to benchmark the results of this modeling framework against an existing reuse facility that incorporates a significant component of artificial groundwater recharge. In this way, we can do things like compare the layout of this corridor solution proposed for this region to that implemented in the real world, as well as, hopefully in the future, evaluate the estimates for the water-energy usage efficiency associated with the proposed systems specification to that

experienced by the Water Factory 21 facility.

4.4.1 REGIONAL CONTEXT

- HUC-8 Code: 18070203
- Total Area: 5,375.9 km^2
- Maximum Elevation: 3,461.3 m
- Minimum Elevation: $-0.7 m$
- Mean Slope: 10.56 %
- Standard Deviation of Slope: 12.21 %
- Dominant Soil Composition: Hydrologic Soil Group - B: 10 – 20% clay, 50 – 90% sand, 35% rock fragments



Figure 4.38: Santa Ana – San Bernadino Region Overview

4.4.2 SEARCH DOMAIN

The search domain comprising the San Diego study region is described in the statistics below and depicted graphically in the map panel contained within 4.39.

- Grid Dimensions: 854 *cells* x 1463 *cells*
- Grid Cell Resolution: 100 *m* x 100 *m* (1 *ha*)
- Feasible Grid Cells: 537, 587 *cells*



Figure 4.39: Santa Ana - San Bernadino Region Search Domain

4.4.3 DESTINATION SEARCH INPUTS

In Figures 4.40 through 4.42 the three key inputs to the Santa Ana - San Bernadino region case study reuse destination search process are shown. Here again, a visual inspection of these three layers reveals that there is a large central plain of highly suitable areas in the left central portion of the basin. This area of high suitability is connected to the coast region,

where the WWTP is located by a thin strip of land area that is marginally suitable according to the three separated suitability layers which runs along the bed of the Santa Ana river.

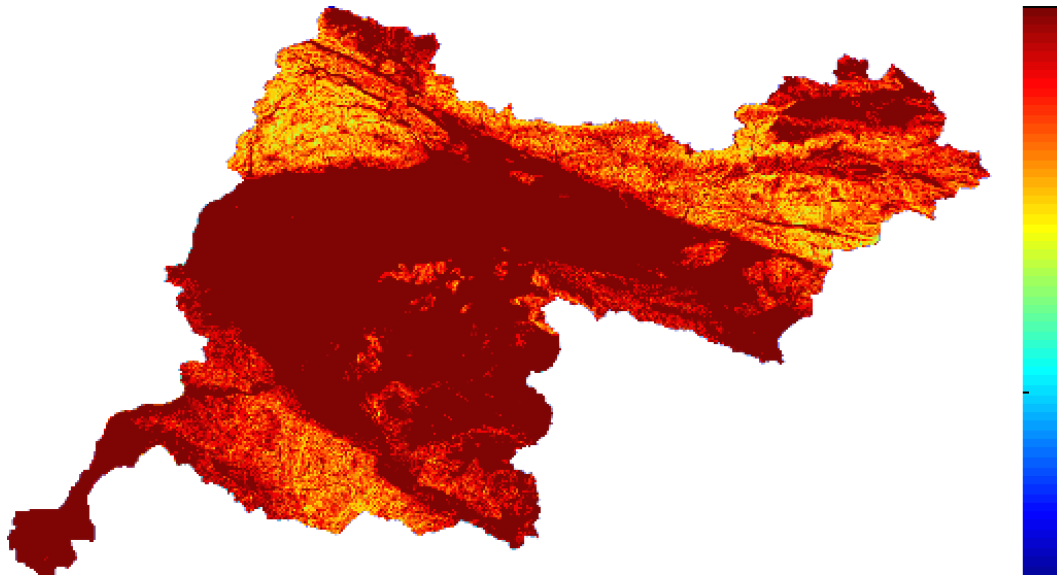


Figure 4.40: Santa Ana - San Bernadino Region Destination Search Inputs: Slope Scores

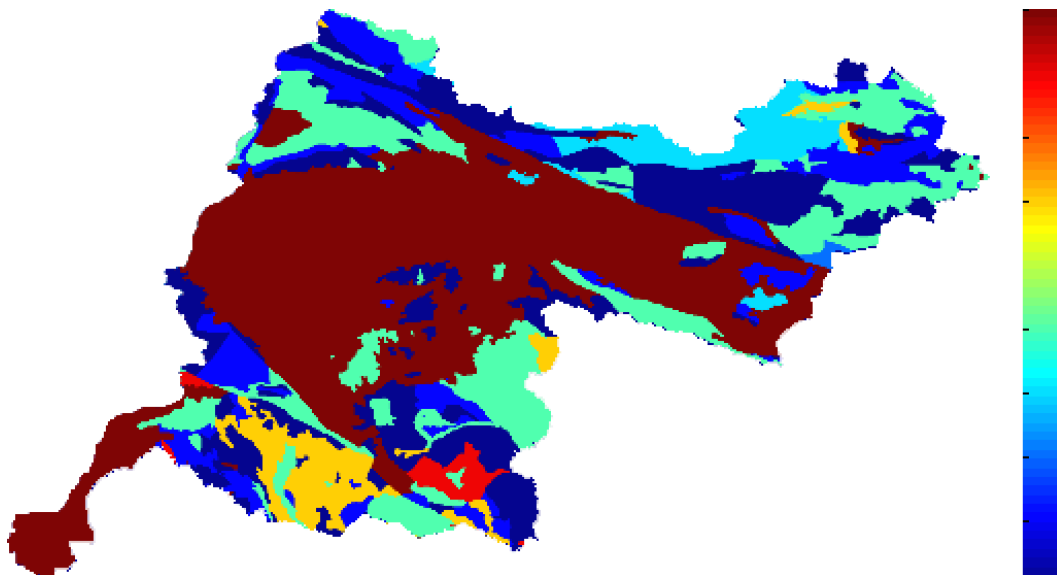


Figure 4.41: Santa Ana - San Bernadino Region Destination Search Inputs: Geology Scores

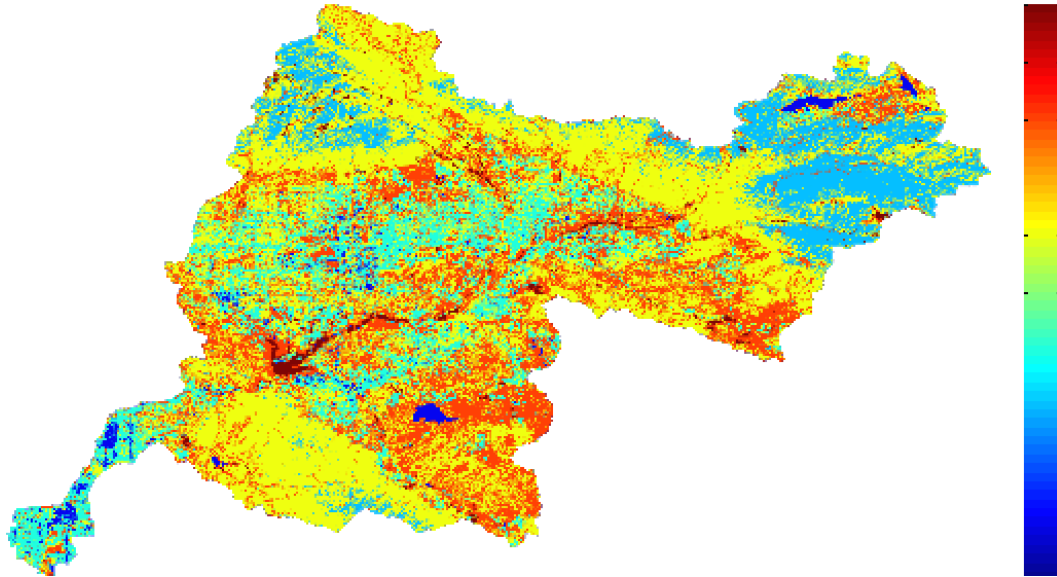


Figure 4.42: Santa Ana – San Bernadino Region Destination Search Inputs: Landuse Scores

4.4.4 DESTINATION SEARCH OUTPUTS

The output of the weighted overlay analysis used to engage in the search for suitable sites for the application of the artificial groundwater recharge surface infiltration basin are shown in the composite site suitability layer depicted in Figure ???. The largest patches of contiguous high suitability are highlighted in the red portions of Figure ??. The obvious best candidate for a recharge basin site within this search domain can be seen as the large red area positioned along the left center edge of the basin.

4.4.5 PROPOSED CORRIDOR ENDPOINTS

The proposed endpoints for the Santa Ana – San Bernadino corridor location problem specification to be delivered to the MOGADOR algorithm are plotted in Figure 4.45. The location of the destination site has been selected as the centroid of the large contiguous area of high suitability referenced in the previous section.

- Start Location: (840, 48)

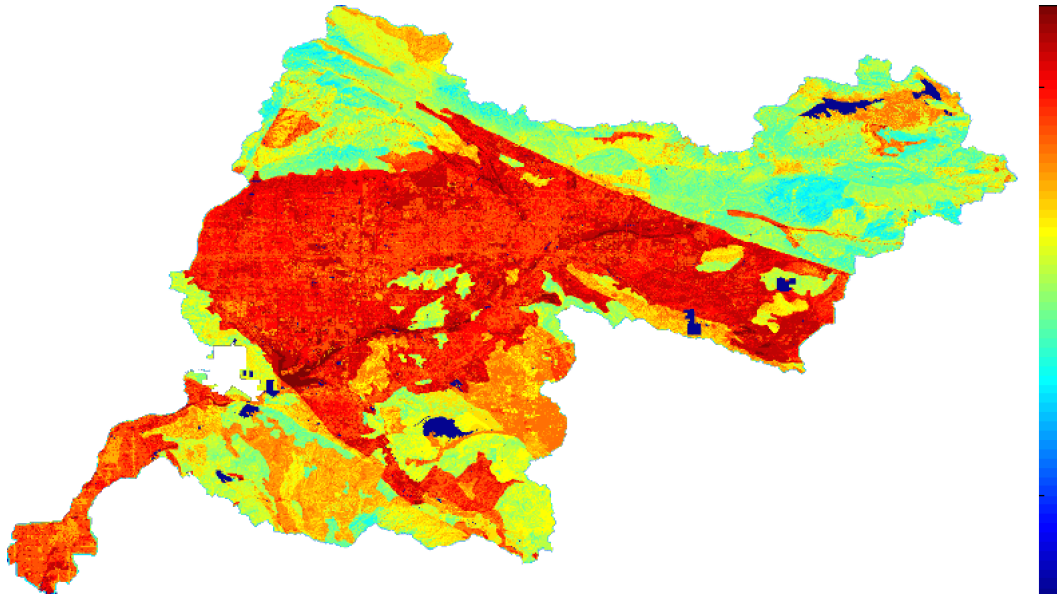


Figure 4.43: Santa Ana - San Bernardino Region Destination Search Outputs: Composite Scores

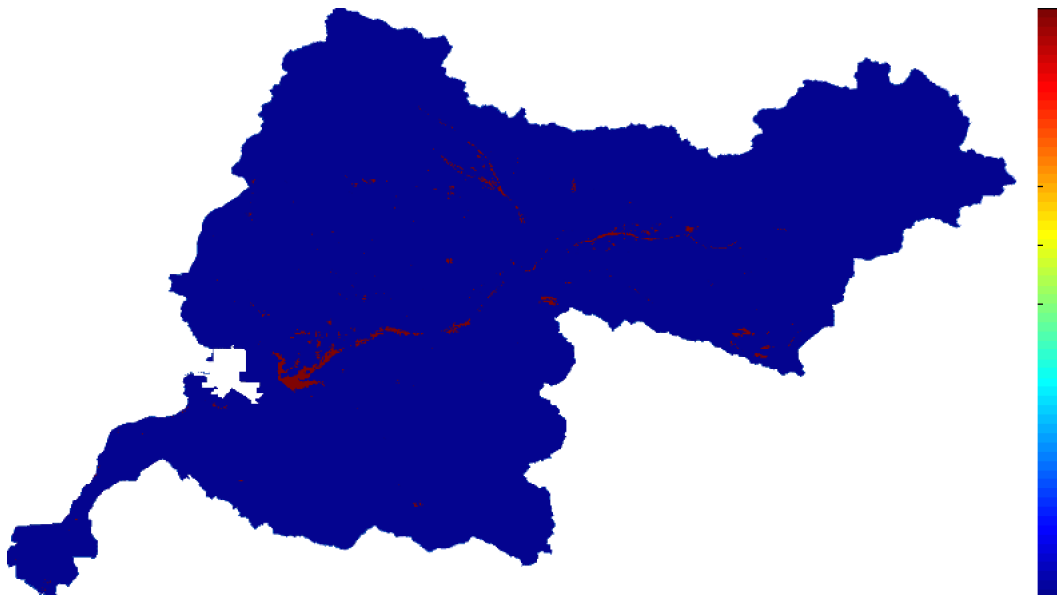


Figure 4.44: Santa Ana - San Bernardino Region Destination Search Outputs: Candidate Regions

- End Destination: (528, 430)
- Shortest Euclidean Path Distance: 49,322 m (49 km)

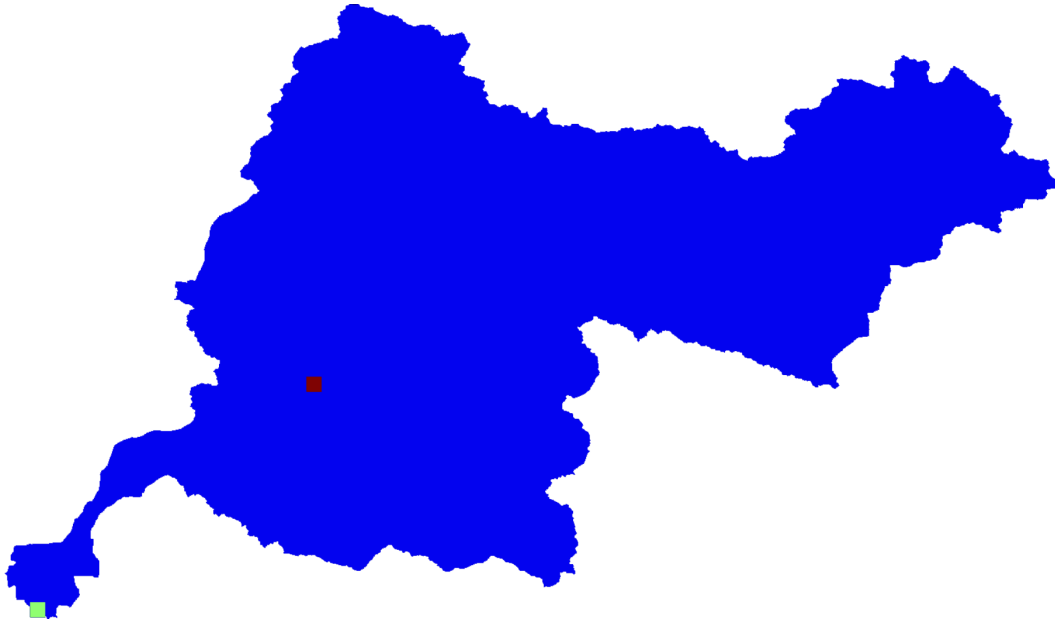


Figure 4.45: Santa Ana - San Bernadino Region Proposed Corridor Endpoints

4.4.6 PROPOSED OBJECTIVE LAYERS

The three proposed objective layers to be used as part of the MOGADOR algorithm corridor location problem specification are illustrated graphically in Figures ?? through 4.47. Structurally, these objective layers were generated according to the same procedures used to generate the corresponding objective layers for each one of the other five case study sites. As the figures show, the coastal area is a flat, low lying spit with a high average landuse intensity and a very dense road network. This coastal region is largely separated from other populated areas in the basin's interior by coastal mountain range with only a narrow passage having been cut by the Santa Ana River.

4.4.7 PROPOSED CORRIDOR SOLUTIONS

As illustrated in Figure 4.49 The proposed corridor solutions for the three MOGADOR model runs with initial population sizes of 1,000, 10,000, and 100,000 show some inter-

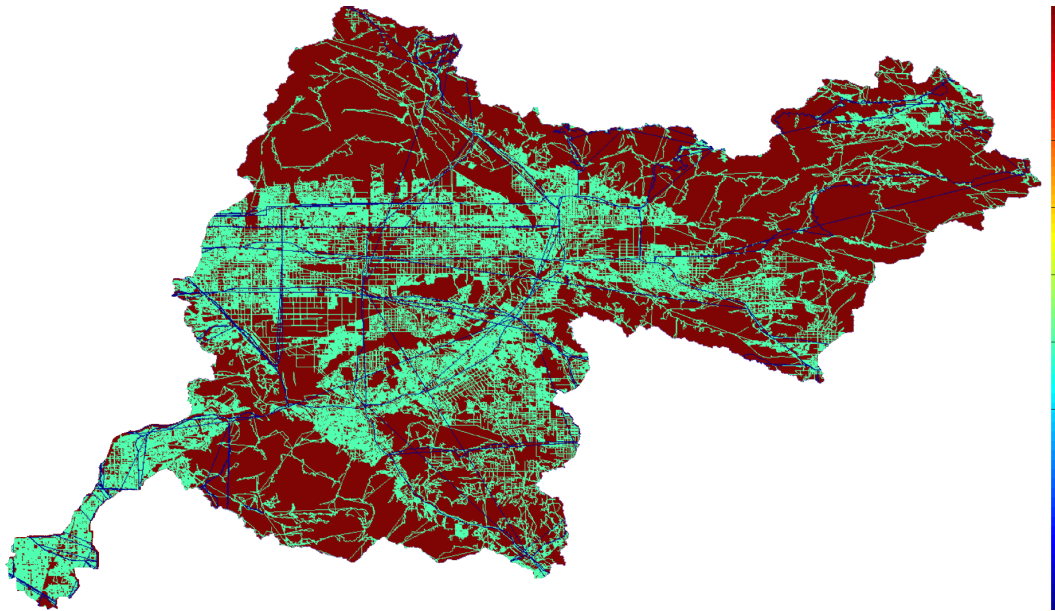


Figure 4.46: Santa Ana - San Bernadino Region Accessibility Based Objective Scores

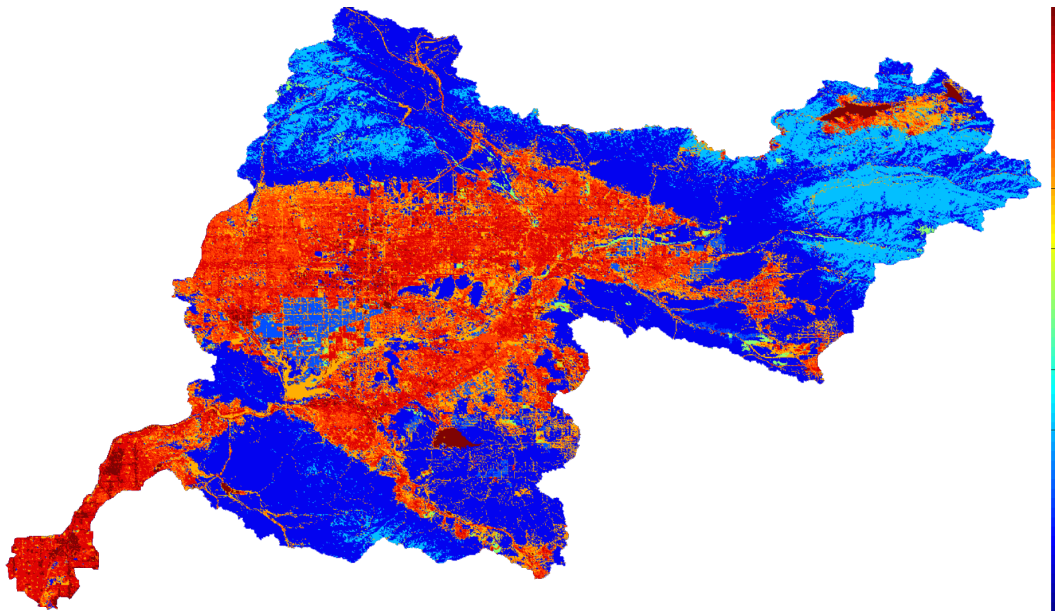


Figure 4.47: Santa Ana - San Bernadino Region Land Use Disturbance Based Objective Scores

esting results. For example, with a population size of 1,000, the algorithm is not able to explore enough of the decision space to produce an output solution set which does not exit

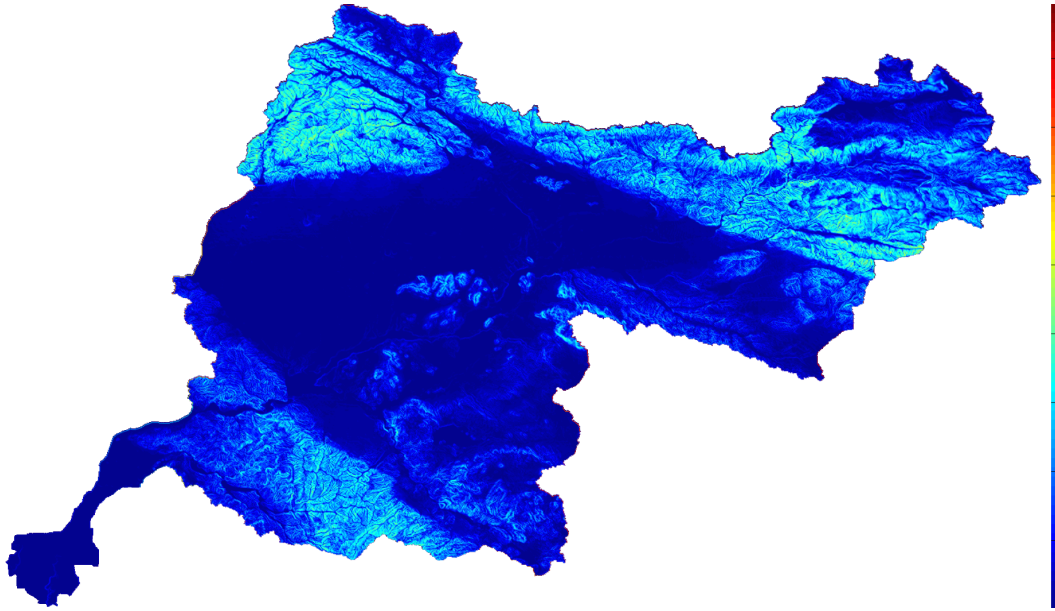


Figure 4.48: Santa Ana – San Bernadino Region Slope Based Objective Scores

the search domain boundary. As a result of this, the range of cumulative aggregate objective function values for the top 100 solutions produced by this run of the algorithm are enormous in size, reflecting the arbitrarily high objective scores assigned to all grid cells outside the feasible search domain for all of the objectives.

As the population size is increased however, we can see that the output solution sets begin to respect the search domain boundary and that the composite aggregate objective scores for the top 100 solutions in each set decrease dramatically. The top 100 solutions for the MOGADOR run with a population size of 100,000 can be seen to have relatively lower disturbance scores compared to the top 100 solutions generated by the algorithm run with a population size of 10,000. This difference reflects that ability of the run with the larger population size to route corridors that minimally disturb areas within the study site with intensive or otherwise sensitive existing landuse types.

The top 100 solutions generated by the MOGADOR algorithm run with a population of 100,000 are plotted relative to the entire study site's search domain in Figure 4.50.

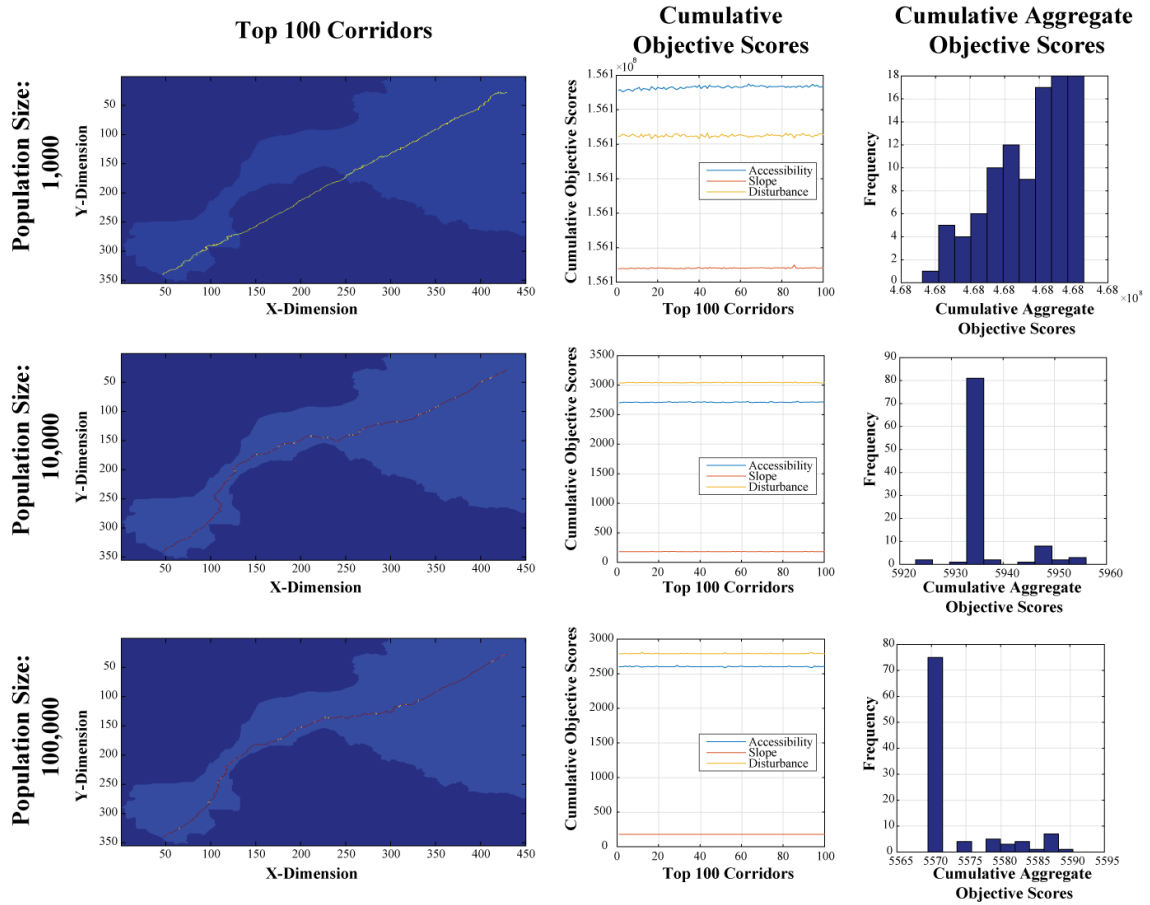


Figure 4.49: Santa Ana – San Bernadino Region Corridor Analysis Results

Figure 4.51 plots the along corridor elevation profile for the best corridor solution produced as an output of the MOGADOR algorithm. This elevation profile reveals that the Santa Ana – San Bernadino study site has the largest net elevation gradient of all of the case study regions: a total of 350 meters. It also shows that the accumulation of elevation along the length of the corridor is fairly continuous with two small declines which must be navigated at the very end section of the proposed corridor.

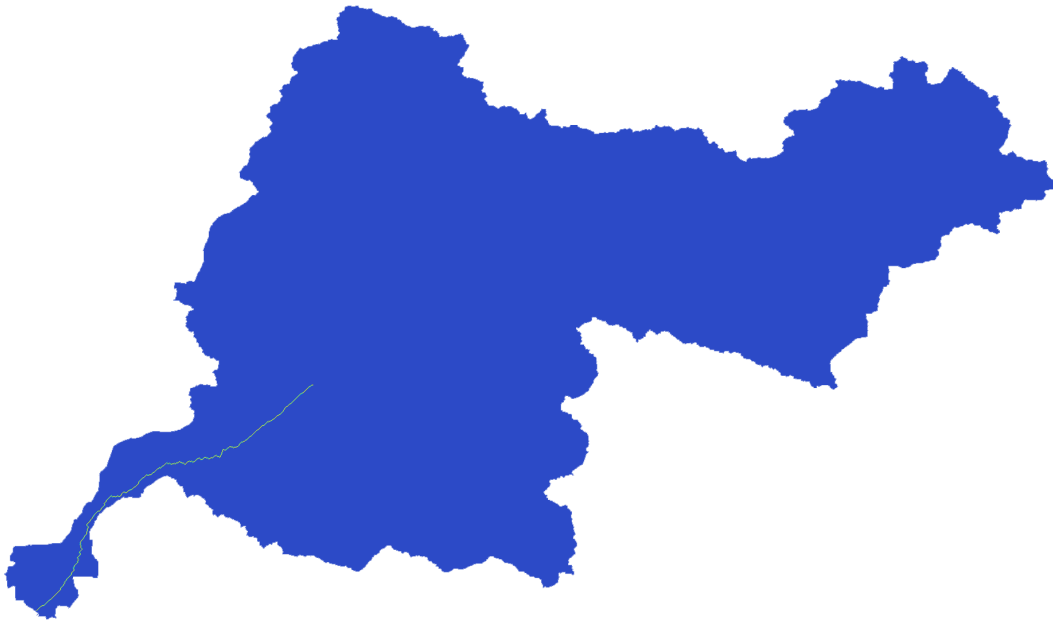


Figure 4.50: Santa Ana - San Bernadino Region Top 100 Corridors Basin Wide Overview

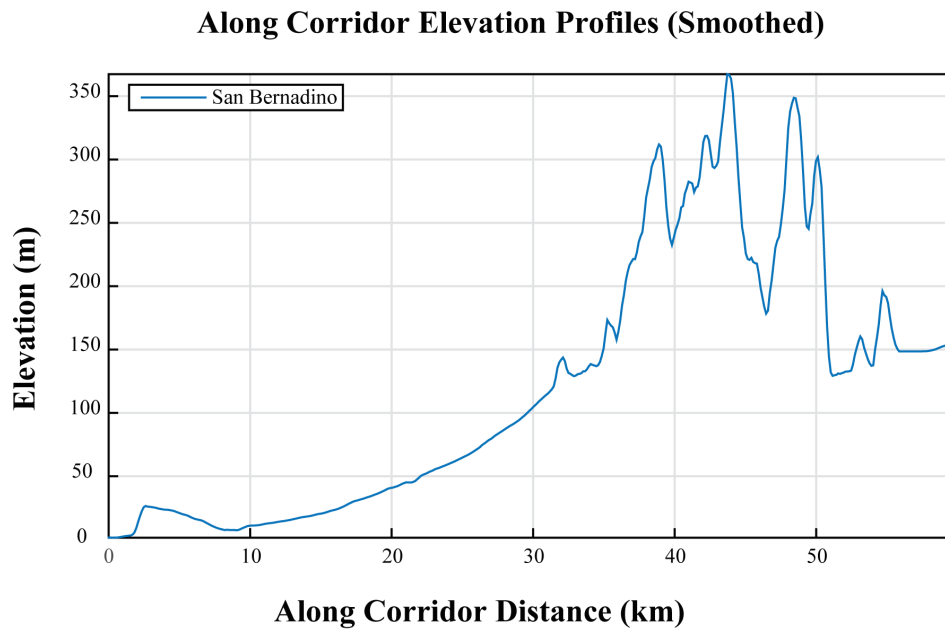


Figure 4.51: San Bernadino Region Proposed Corridor Elevation Profile

4.5 FRESNO – TULARE REGION

The fifth and final case study region is comprised of the HUC-8 basin containing the cities of Fresno and Tulare. This case study region is depicted graphically by the region filled in black in Figure 4.52. This basin differs from those included in the previous case studies in that it is internally drained – i.e. landlocked. This unique hydrologic feature is due to the fact that it is situated within California’s Central Valley. In terms of total area, Fresno is the largest of the five case study regions. However, its topography and landuse characteristics are significantly more homogeneous than those for the other case study regions. Fresno – Tulare, and indeed the majority of the southern portion of the California Central Valley are heavily agricultural. This is a result of the area’s high quality soils, evenly flat topography, and favorable climactic regime with a large number of annual growing days.

Due to the historic prominence of agricultural activity in this region, the local economy of the Fresno – Tulare region is heavily skewed towards agricultural activity. As a result, there has evolved a sort of lock-in effect where the region is relied upon to produce crop outputs for national and international export regardless of the local precipitation patterns. For decades now, this situation has caused farmers to turn to local groundwater resources to offset deficiencies in freshwater supply in periods of drought. This has led to unsustainable rates of subsurface aquifer withdrawals; on state of groundwater overdraft that in many places within the study site threaten the long term health and viability of the aquifers.

In an effort to fight harmful consequences of this overdraft condition such as groundwater contamination and land surface subsidence, regional freshwater managers have been exploring the use of treated wastewater to provide an artificial source of groundwater recharge. The need to better understand the energy-water usage efficiencies of these types of reuse systems in this area make it a prime candidate for assessment as part of this dissertation project.

4.5.1 REGIONAL CONTEXT

- HUC-8 Code: 18030009
- Total Area: 6,943.6 km^2
- Maximum Elevation: 1,536.6 m
- Minimum Elevation: 0 m
- Mean Slope: 2.16 %
- Standard Deviation of Slope: 6.24 %
- Dominant Soil Composition: Hydrologic Soil Group - B: 10 – 20% clay, 50 – 90% sand, 35% rock fragments



Figure 4.52: Fresno – Tulare Region Overview

4.5.2 SEARCH DOMAIN

The search domain comprising the Fresno – Tulare case study region is described in the statistics below and depicted graphically in the map panel contained within 4.53.

- Grid Dimensions: 1018 *cells* x 1459 *cells*
- Grid Cell Resolution: 100 *m* x 100 *m* (1 *ha*)
- Feasible Grid Cells: 694, 365 *cells*



Figure 4.53: Fresno – Tulare Region Search Domain

4.5.3 DESTINATION SEARCH INPUTS

The destination search inputs for the siting of the groundwater recharge basin are illustrated in Figures 4.54 through 4.56. Here again, as with the four other case study regions, these are comprised of the same slope, surface geology, and landuse based nominally standardized spatial data layers.



Figure 4.54: Fresno - Tulare Region Destination Search Inputs: Slope Scores

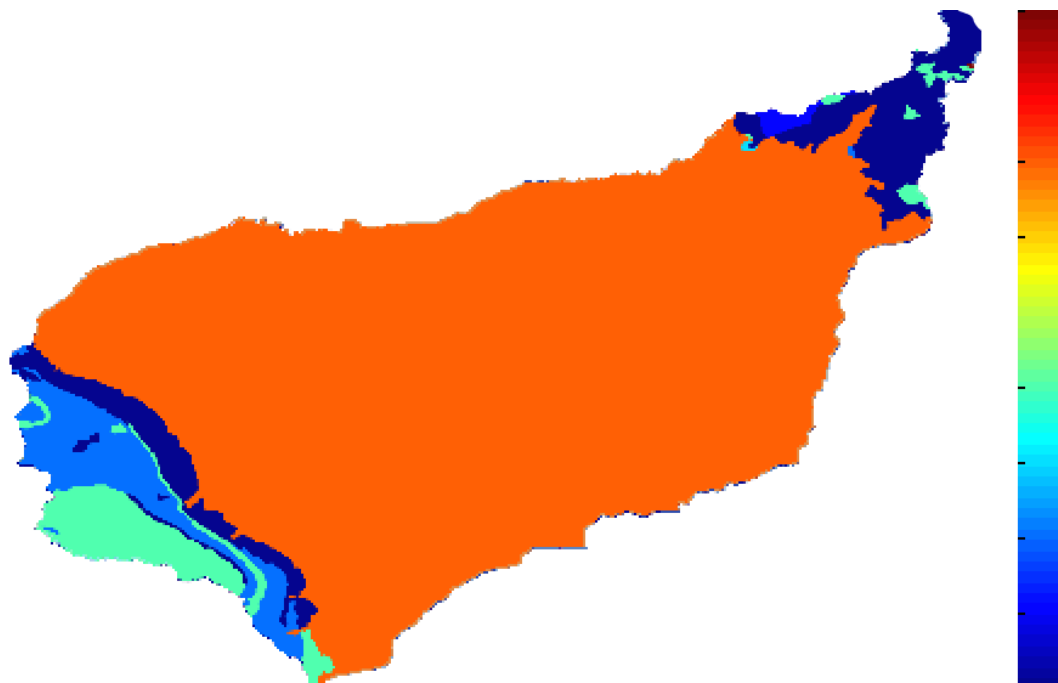


Figure 4.55: Fresno - Tulare Region Destination Search Inputs: Geology Scores

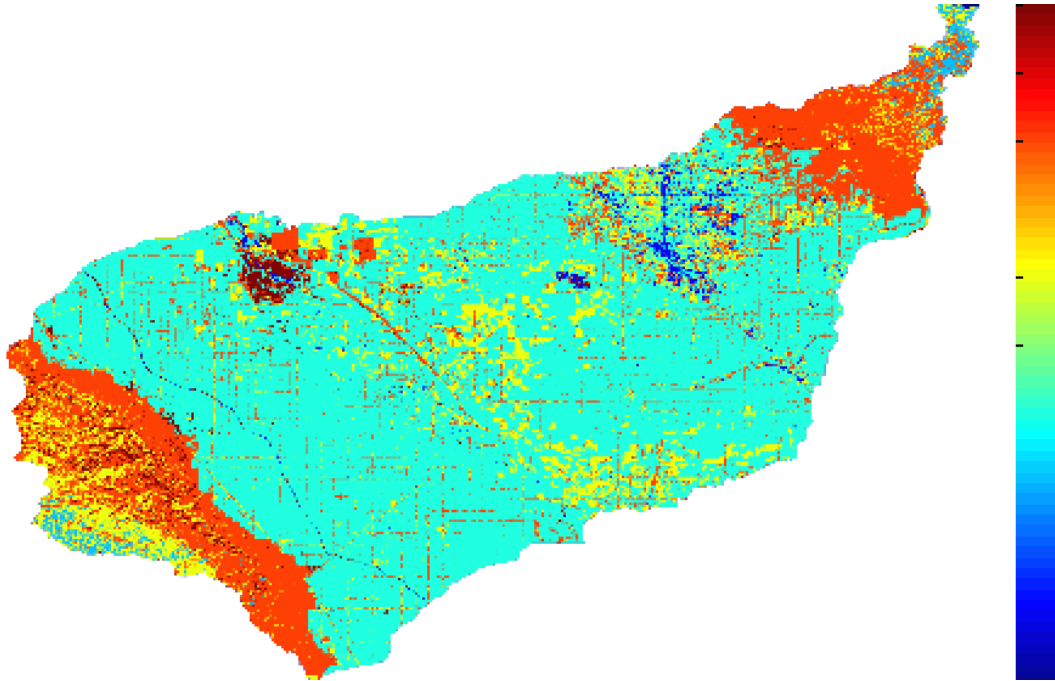


Figure 4.56: Fresno – Tulare Region Destination Search Inputs: Landuse Scores

4.5.4 DESTINATION SEARCH OUTPUTS

In absolute terms, the majority of the area contained within the Fresno – Tulare search domain is actually quite highly suitable for the implementation of a groundwater recharge basin. In terms of relative suitability however, the most favorable region was found to be located in the Northwestern portion of the search domain adjacent to an existing surface water feature and depicted graphically by the connected candidate regions plotted in Figure 4.58.

4.5.5 PROPOSED CORRIDOR ENDPOINTS

The proposed corridor endpoints for the MOGADOR algorithm problem specification are plotted in Figure 4.59. The spacing between the source and destination cells within the search domain is the largest of that for any of the case studies included in this entire analy-

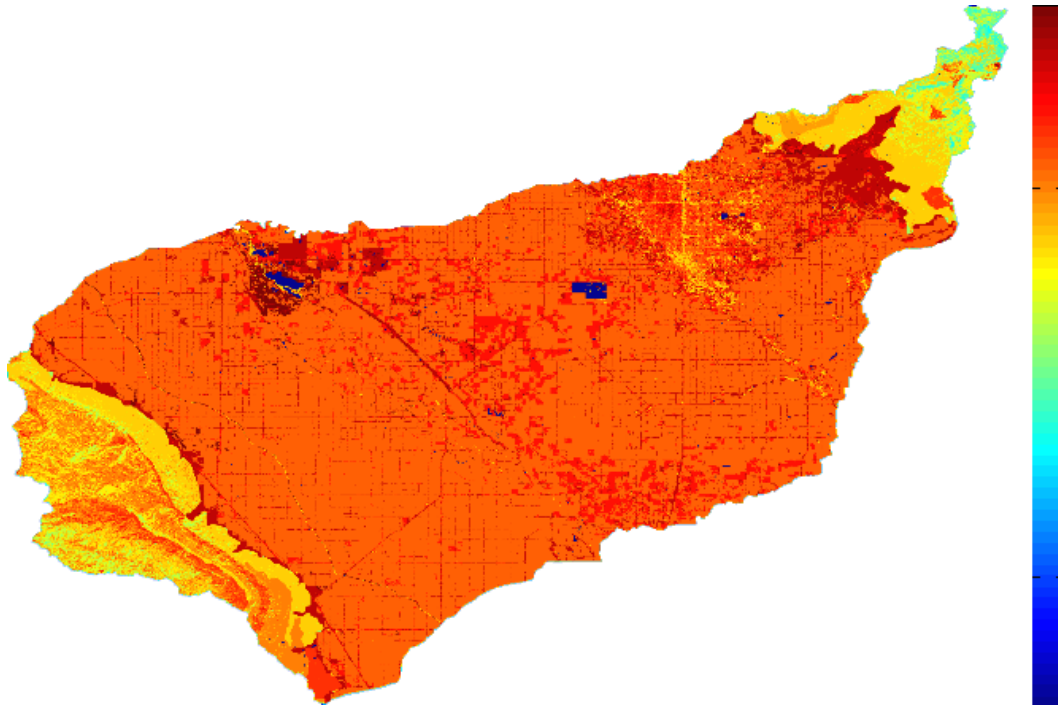


Figure 4.57: Fresno – Tulare Region Destination Search Outputs: Composite Scores

sis. This feature, combined with the sheer size of the Fresno – Tulare regions search domain makes it a challenging candidate candidate for the corridor location optimization procedure.

- Start Location: (435, 1037)
- End Destination: (421, 387)
- Shortest Euclidean Path Distance: 65, 015 *m* (65 *km*)

4.5.6 PROPOSED OBJECTIVE LAYERS

The proposed objective for the MOGADOR algorithm problem specification are plotted graphically in Figures 4.60 through 4.62. More so than for any other case study region investigated as part of this analysis, these layers are homogeneous in structure. This presents an additional challenge to the operation of the corridor location optimization procedure.



Figure 4.58: Fresno – Tulare Region Destination Search Outputs: Candidate Regions

4.5.7 PROPOSED CORRIDOR SOLUTIONS

The characteristics of the proposed corridor location solutions generated as outputs from the MOGADOR algorithm for three different population sizes are depicted in Figure 4.63. As this figure shows, and as might be expected, the best final solution set by the algorithm very closely approximates the euclidean shortest path between the input source and the input destination provided in the problem specification. The seeming simplicity of this final solution belies the significant computation effort required to search such a large decision space. For, as it shall be discussed in greater detail in subsequent sections, the runtime of the MOGADOR algorithm for the Fresno – Tulare case study region was far and away the longest among all of the case study sites.

Figure 4.65 plots the along corridor elevation profile for the best output corridor solution generated by the MOGADOR algorithm with an initial seed population of 100,000.

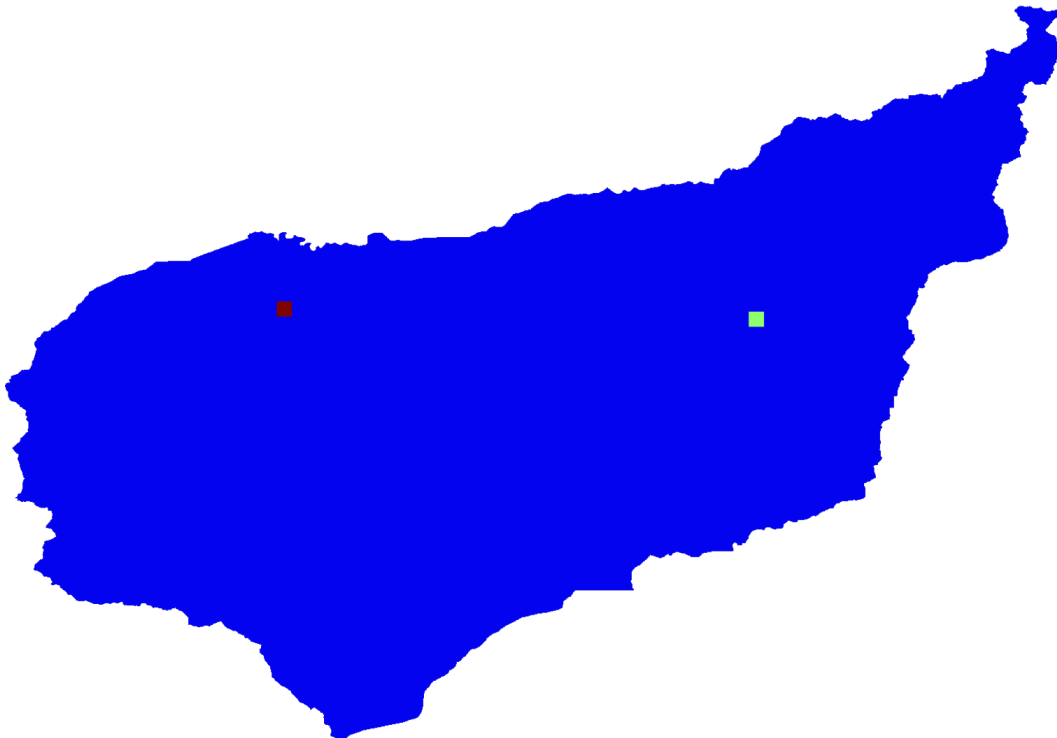


Figure 4.59: Fresno – Tulare Region Proposed Corridor Endpoints

As the profile plot reveals, for the Fresno – Tulare region, the corridor solution actually routes along a path of decreasing elevation from the source to the destination. This feature is unique among all of the case study regions, with all of the four others involving a route that moves progressively uphill to a higher elevation location.

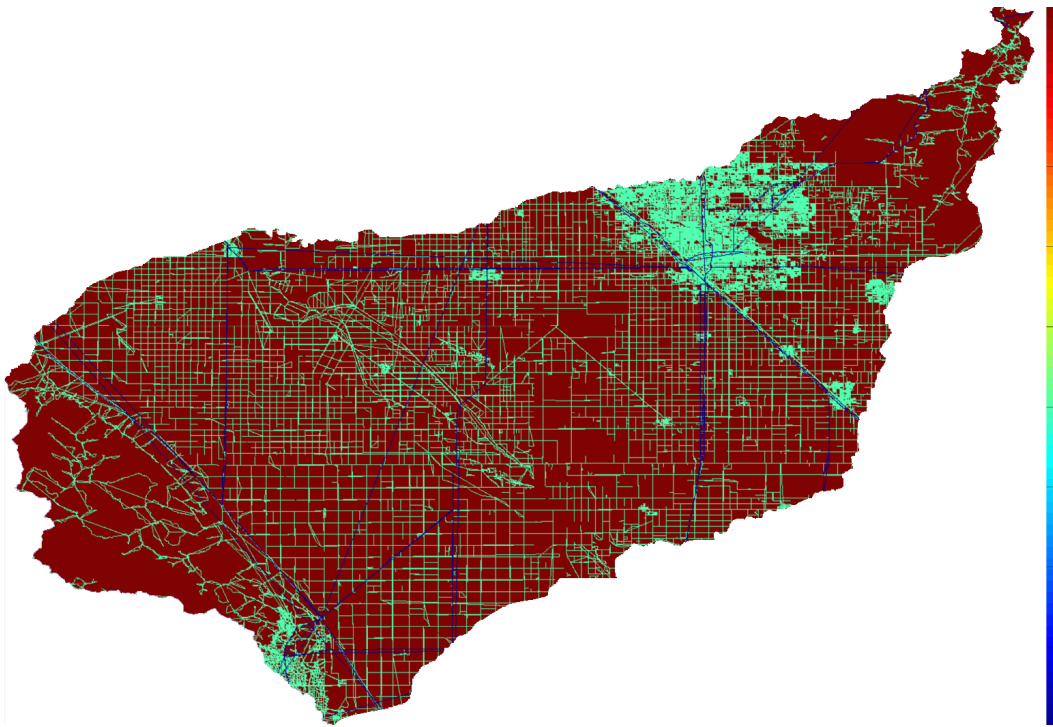


Figure 4.60: Fresno - Tulare Region Accessibility Based Objective Scores

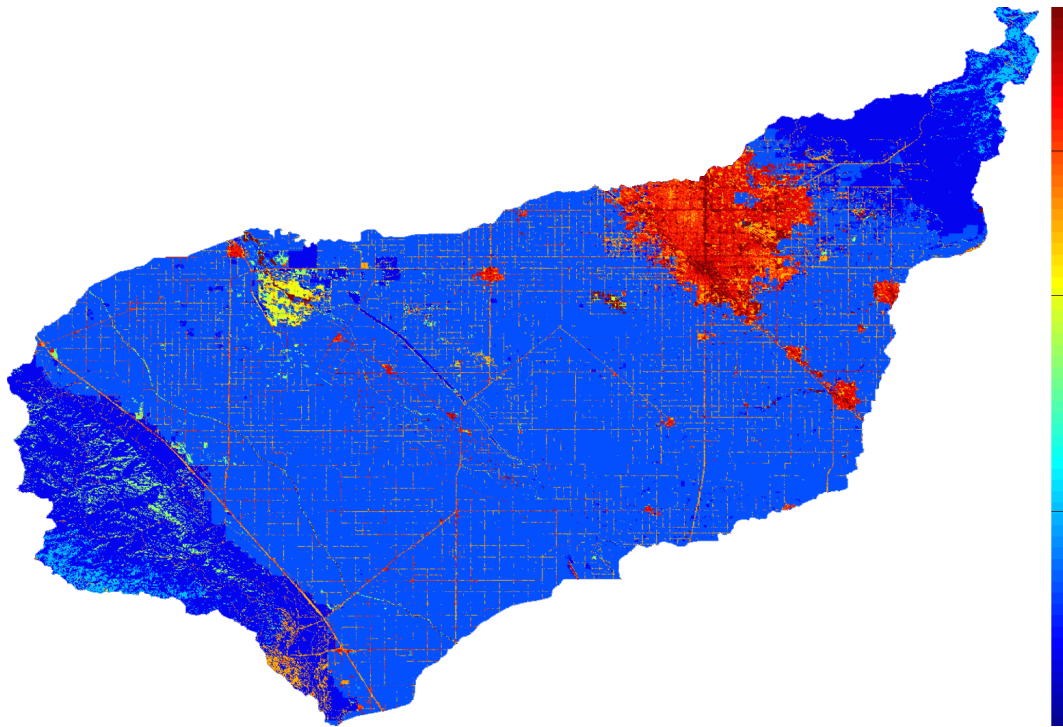


Figure 4.61: Fresno - Tulare Region Land Use Disturbance Based Objective Scores

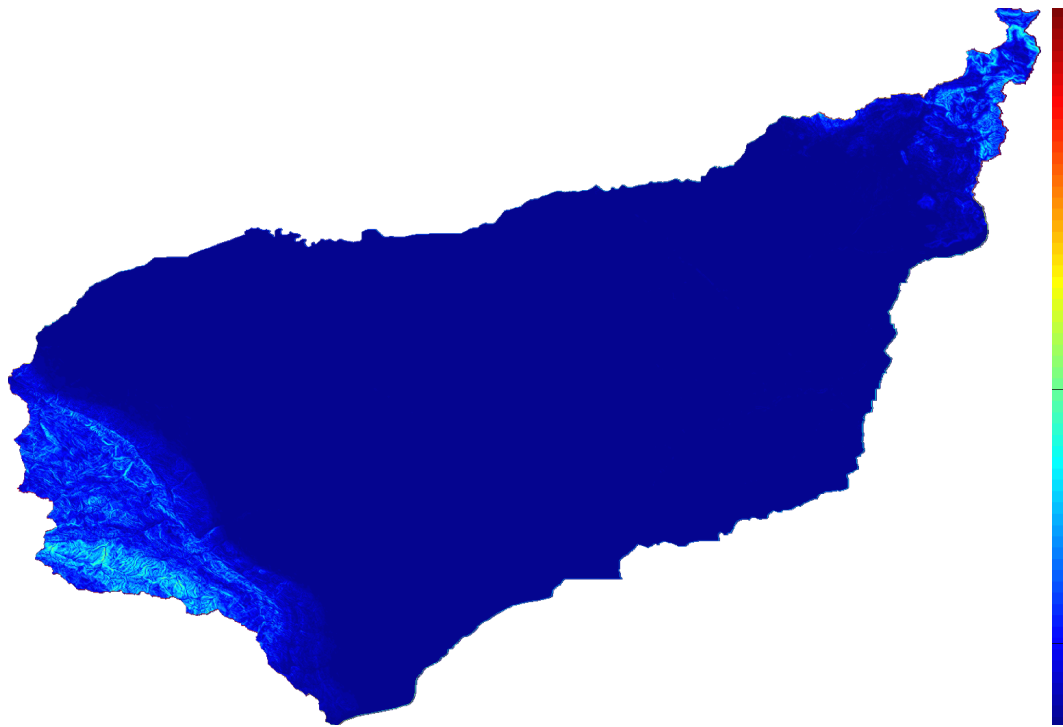


Figure 4.62: Fresno - Tulare Region Slope Based Objective Scores

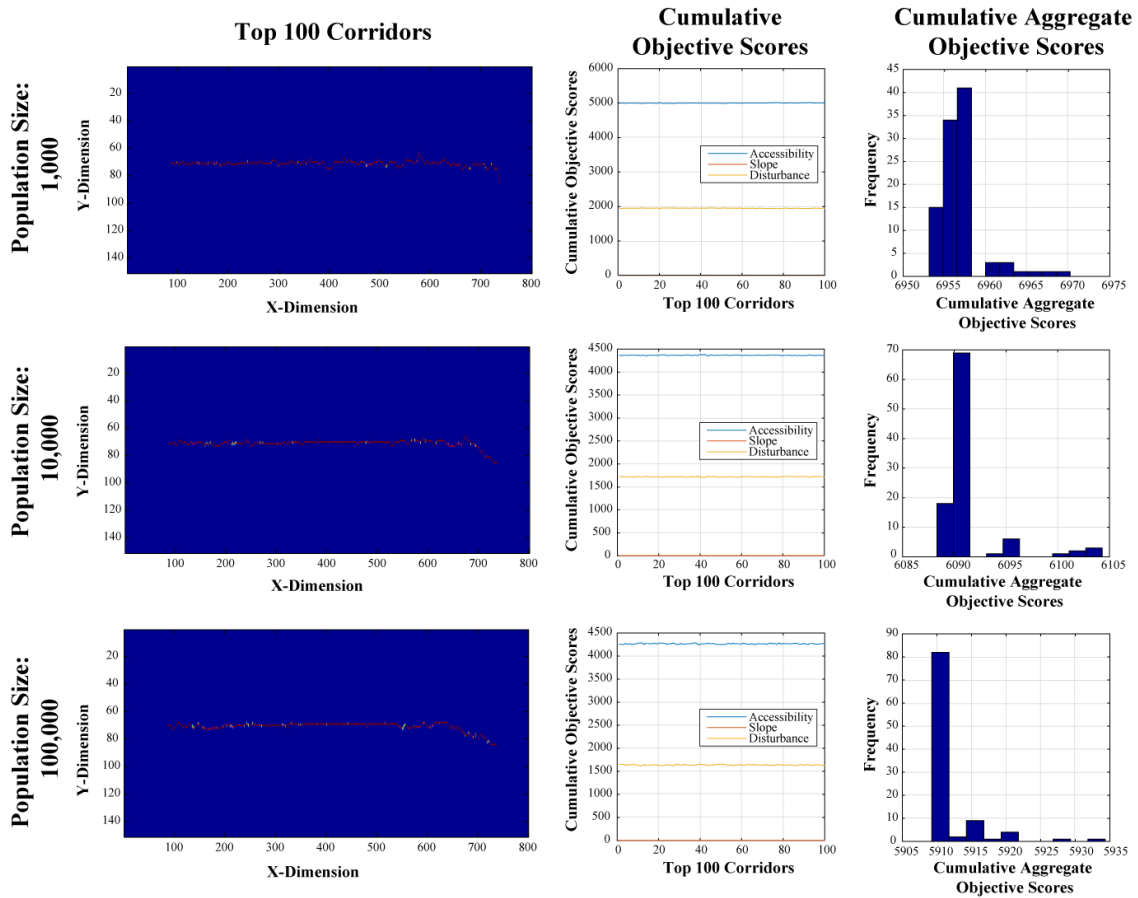


Figure 4.63: Fresno Region Corridor Analysis Results



Figure 4.64: Fresno Region Top 100 Corridors Basin Wide Overview

Along Corridor Elevation Profile (Smoothed)

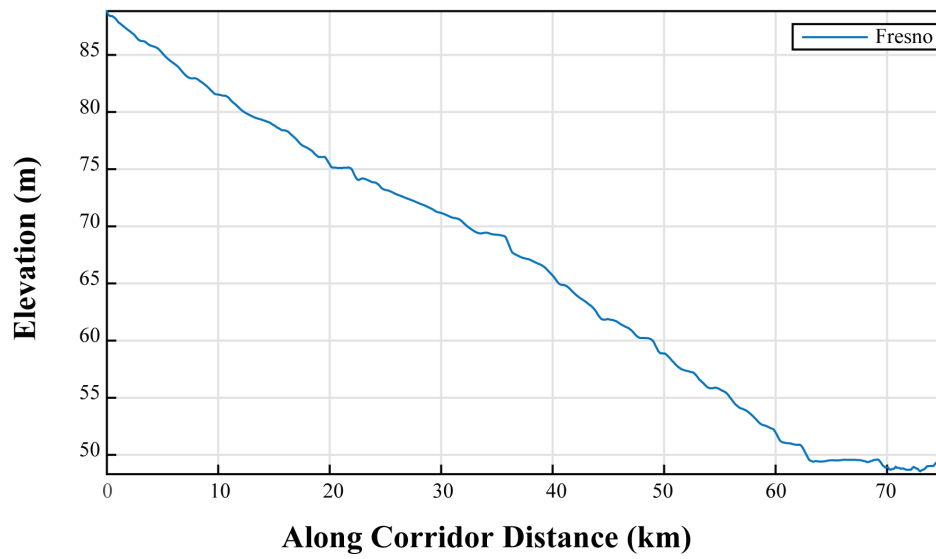


Figure 4.65: Fresno Region Proposed Corridor Elevation Profile

4.6 EVALUATING THE MOGADOR ALGORITHM'S RUNTIME PERFORMANCE

Figure 4.66 depicts the runtime performance of the MOGADOR algorithm for the five case study regions previously introduced with treatments per case study. As the figure shows, the performance of the algorithm scales roughly linearly with respect to problem size – as measured both in terms of the scale of the search domain and the breadth of the search effort. Due to the stochastic nature of the MOGADOR optimization routine and discrepancies between the source to destination separation distances as well as the morphological structure of the search domains for each of the case study regions, a more formal analysis of the runtime performance is discouraged so as not to generate misleading conclusions.

Figure 4.67 plots the number of evolutionary iterations required to achieve convergence for each run of the MOGADOR algorithm across the five different case study regions and the three population sizes evaluated per region. No trend was expected between either the identity of the case study region or the population size. And, as the figure illustrates, indeed no trend was observed.

4.7 EVALUATING THE MOGADOR ALGORITHM'S SOLUTION QUALITY

Figure 4.68 presents an analysis of the quality of the best output solutions generated by the MOGADOR algorithm for each of the case study regions compared relative to that of the euclidean shortest corridor linking the source location to the destination location. Two plot series are shown, the first, in red, described as the *Margin of Deviation*, is the percent increase in the along path distance of the output solution corridor relative to that of the Euclidean shortest corridor. The expectation for this series is that all the values greater than or equal to 0%. This expectation reflects the understanding that the optimal corridor solution must be at least as long as the Euclidean shortest corridor. As the Margin of Deviation plot

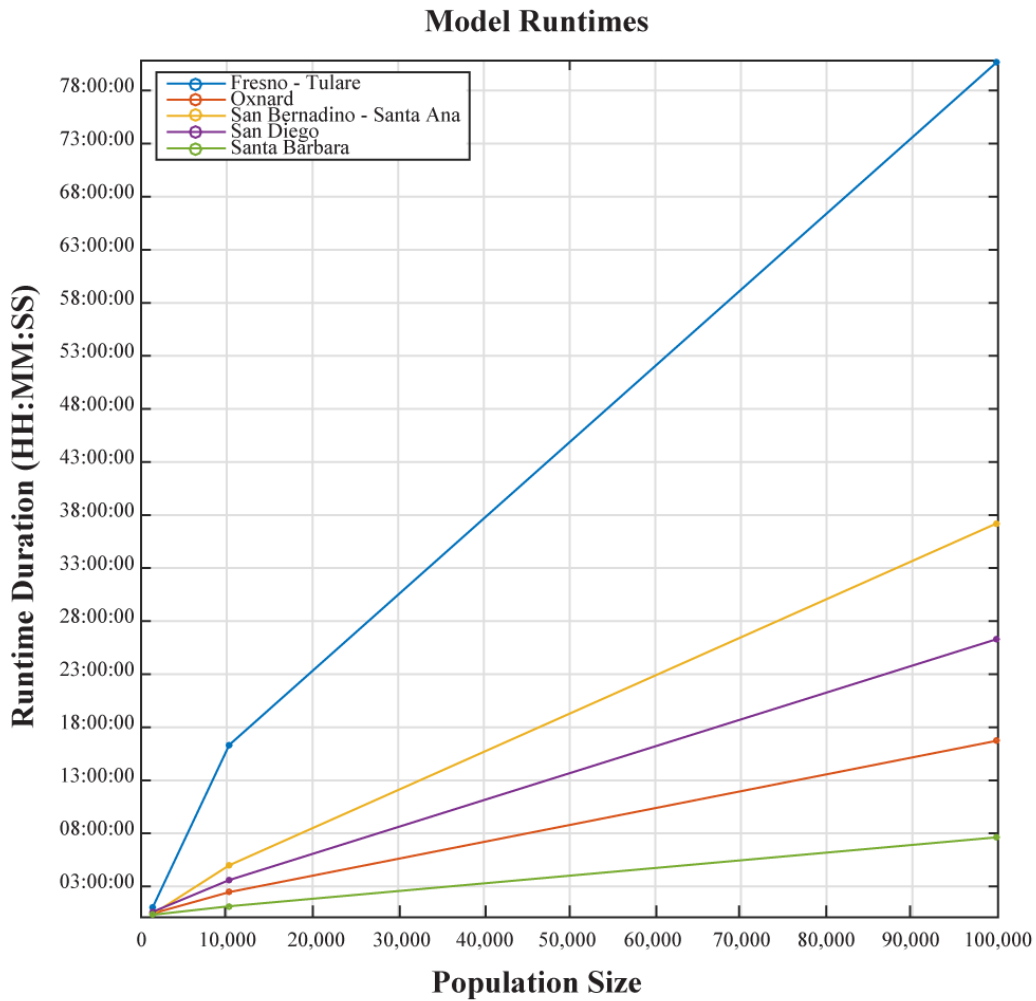


Figure 4.66: Algorithm Runtime Performance for Each of the Five Case Study Regions for Three Population Sizes

series illustrates, the output solutions generated by the MOGADOR algorithm are 18% to 22% longer than the Euclidean shortest path alternatives.

The second plot series, in blue, depicts what is termed as the *Margin of Improvement*. These values correspond to the percent decrease in the cumulative aggregate objective scores associated with the MOGADOR output corridor solution relative to that of the Euclidean shortest corridor. The initial expectation here is that these values should always be nega-

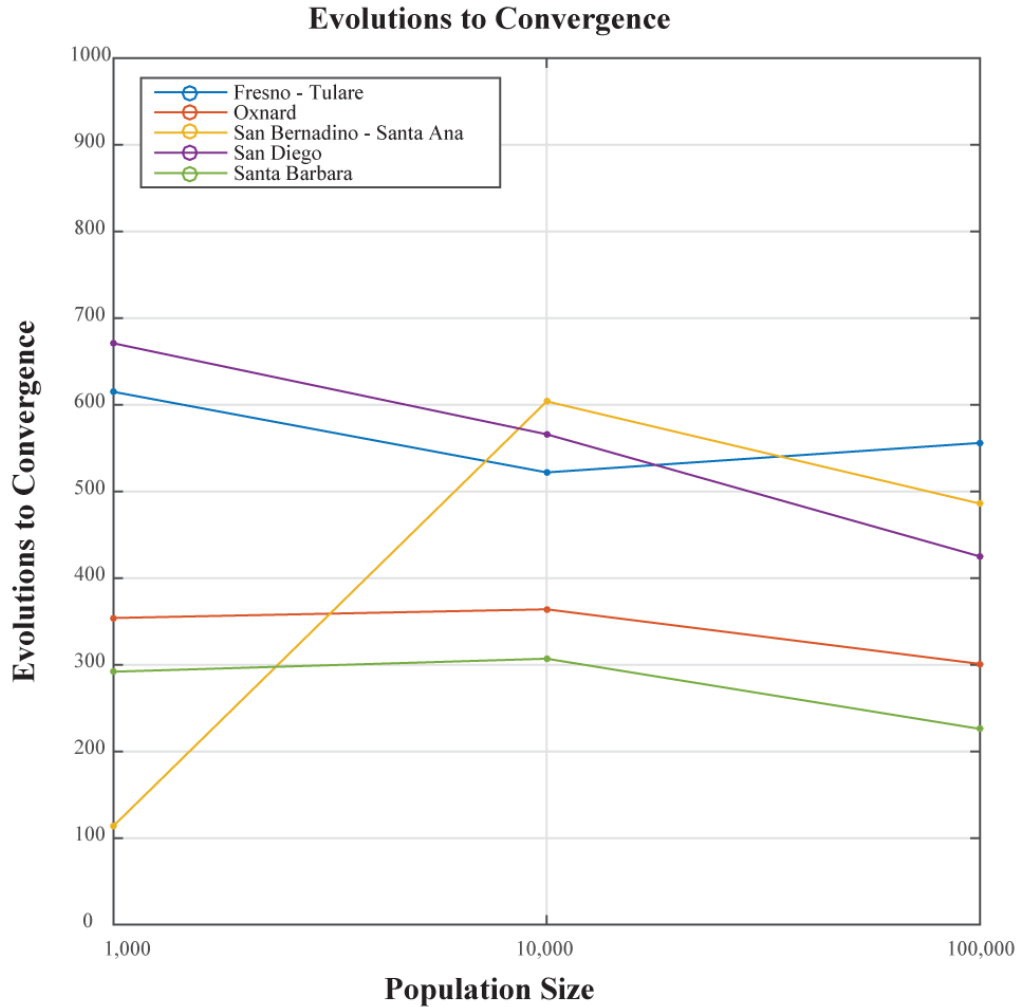


Figure 4.67: Algorithm Convergence Rates for Each of the Five Case Study Regions for Three Population Sizes

tive, or at least equal to zero, reflecting the degree to which the MOGADOR algorithm was able to deliver a solution that is improved, in terms of reduced along path cost, over the Euclidean shortest corridor. As the Margin of Improvement plot series illustrates, for Fresno – Tulare, Oxnard, and Santa Barbara, the MOGADOR algorithm’s best solutions achieved between a 37% to 46% reduction in cumulative aggregate objective scores over the Euclidean shortest corridor alternative. For the San-Bernadino and San-Diego regions

the Margin of Improvement appears to be 100%. This feature reflects the fact that the Euclidean shortest corridor for these two regions exits the search domain and thus results in an arbitrarily high cumulative aggregate objective score value.

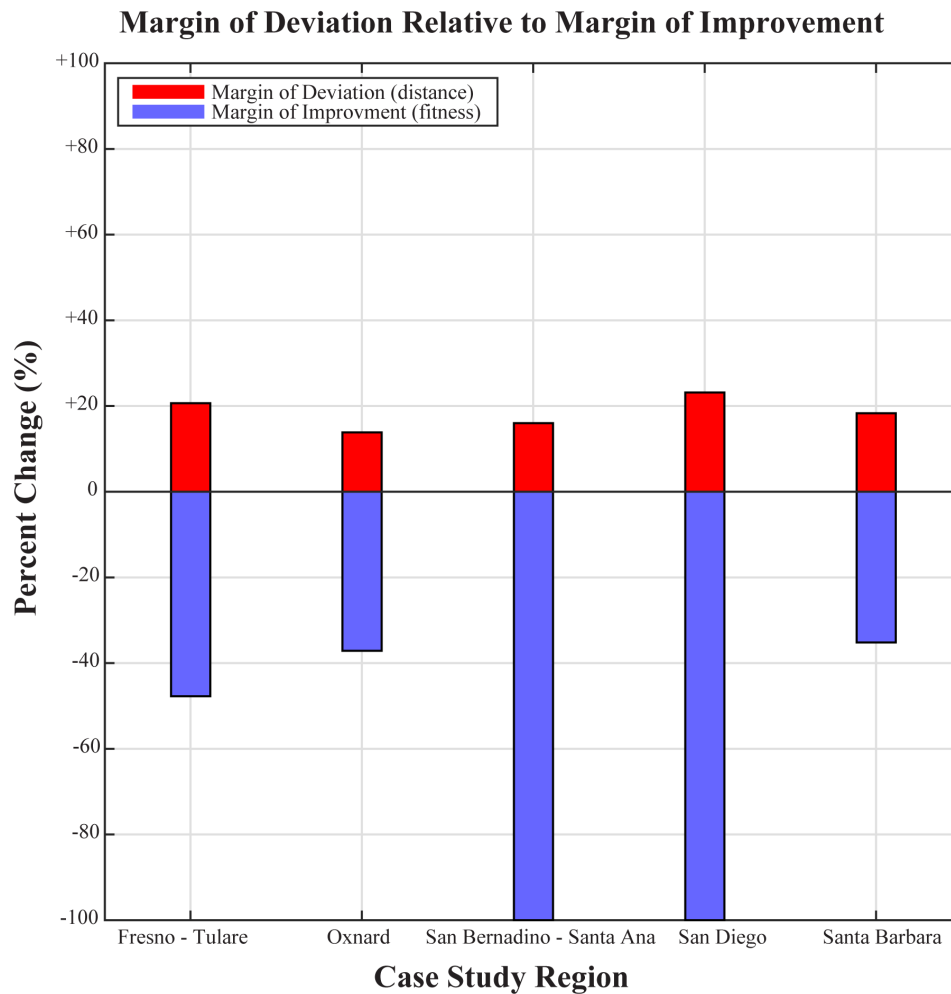


Figure 4.68: Comparison of the Along Path Distance and Cumulative Objective Scores between the Solution Corridors and the Euclidean Shortest Corridors

4.8 EVALUATING THE MOGADOR ALGORITHM'S SOLUTION ELEVATION PROFILES

Figure 4.69 plots the along path elevation profiles for each of the best MOGADOR algorithm output corridor solutions relative to one another. This figure is useful for gauging [1] the relative length of each corridor [2] the relative elevation gain of each corridor and [3] the degree to which each corridor is trading a smooth accumulation of slope for routing either away from high intensity landuse areas or towards highly accessible areas.

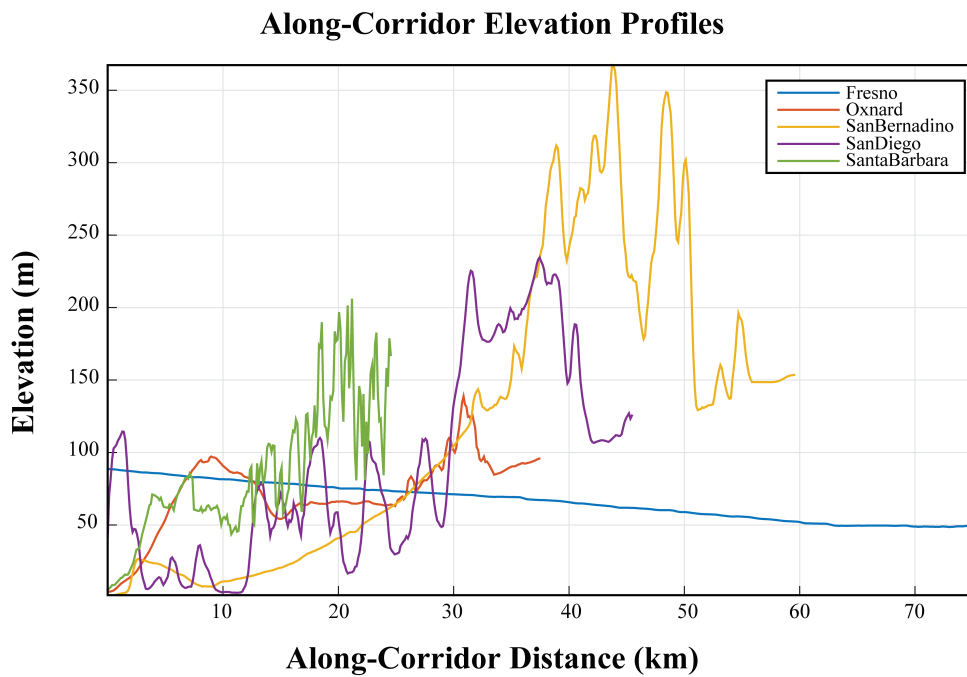


Figure 4.69: Comparison of the Along Corridor Elevation Profiles for each of the Solution Corridors

4.9 EVALUATING THE LIFE-CYCLE WATER-ENERGY USAGE EFFICIENCIES OF PROPOSED REUSE SYSTEMS

Figure 4.70 provides an information rich perspective on the final output results generated from the synthetic combination all three of the separate modeling components described in the previous Chapters of this dissertation. It depicts, the ratio of water withdrawals and water consumption relative to the volume of water recovered by reuse. This ratio assumes that the rate of reuse equals 100% of the permitted wastewater flows for each of the WWTPs in the five case study regions previously discussed.

The water withdrawal and consumption figures presented are generated by combining a calculated instantaneous flow rate with the the proposed proposed corridor specification for each case study region into an expected annual pump energy consumption figure. This pump energy consumption figure is then translated into an expected water withdrawal figure through an interpretation of the fractional energy generation technology mix responsible for the production of electricity in each region.

The horizontal red line plotted on the figure shows the critical threshold at which the energy consumed in the operation of a reuse systems results in either the withdrawal or consumption of more water – at the point of electricity production – than is able to be reclaimed by the reuse process. The range of values depicted by the plot series bands reflects an assumed range of pump operational efficiencies of between 25% - 75%.

In only one of the case study regions, Fresno – Tulare, does there appear to be a net savings of water associated with the practice of reuse. This is largely due to the minimal pump energy requirements associated with the proposed reuse system in this region, which involves a corridor specification that routes downhill and is able to take advantage of gravity to overcome most of the total head associated with the water delivery effort. In all of the other case study regions, the range of consumption and withdrawals exceeds the critical

threshold. This can be interpreted a situation where the practice of reuse is tantamount to the importation of water – in the form of energy – from the region in which the requisite energy has been produced.

These findings suggest that the systemic benefits of the reuse of treated wastewater for the practice of artificial groundwater reuse are not so great as initially assumed to be. Furthermore, they demonstrate that the efficiency of a reuse project is highly dependent upon the local geographic context in which the system is to be implemented. An interesting question which remains, is how the energy-water usage efficiency characteristics of these types of reuse projects – involving significant artificial groundwater recharge components – will change over time as the energy grid mix evolves, presumably, towards a greater fraction of renewable energy supply technologies. For, as was mentioned in the introductory Chapter (o) these renewable technologies tend to have much lower water requirements relative to their heat-engine based, fossil fueled counterparts. As such, it is possible, that energy-water usage efficiencies of these systems may improve, not necessarily because of some significant new development in the actual system design, but rather solely due to a reduction in the water usage intensity of the overall electricity grid.

Ratio of Water Expenditures for Reuse to Water Recovered Via Reuse

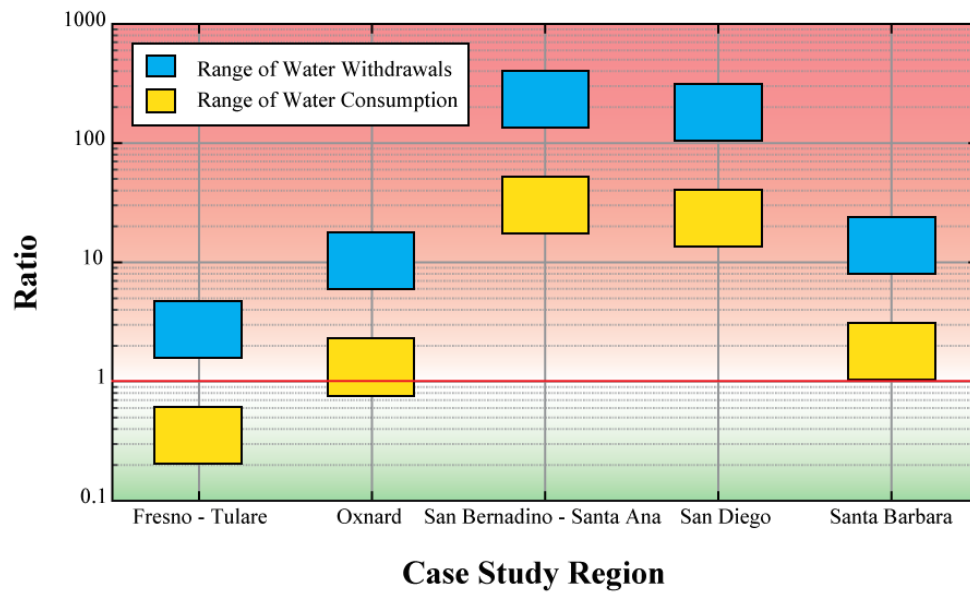
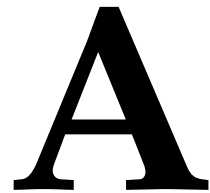


Figure 4.70: Comparison of the Net Water Usage Efficiencies of Reuse for each of the Case Study Regions Measured in Terms of Both the Withdrawals and Consumption of Water for the Production of Energy Required for Reuse



Go Language Source Code Repository for a Parallel + Concurrent Implementation of the
MOGADOR Algorithm for the Multi-Objective Corridor Location Problem

<https://github.com/ericdfournier/corridor>

<LICENSE>

Copyright ©2015, Eric Daniel Fournier

All rights reserved.

Redistribution and use in source and binary forms, with or without modification, are permitted provided that the following conditions are met:

* Redistributions of source code must retain the above copyright notice, this

list of conditions and the following disclaimer.

* Redistributions in binary form must reproduce the above copyright notice, this list of conditions and the following disclaimer in the documentation and/or other materials provided with the distribution.

* Neither the name of corridor nor the names of its contributors may be used to endorse or promote products derived from this software without specific prior written permission.

THIS SOFTWARE IS PROVIDED BY THE COPYRIGHT HOLDERS AND CONTRIBUTORS "AS IS" AND ANY EXPRESS OR IMPLIED WARRANTIES, INCLUDING, BUT NOT LIMITED TO, THE IMPLIED WARRANTIES OF MERCHANTABILITY AND FITNESS

FOR A PARTICULAR PURPOSE ARE DISCLAIMED. IN NO EVENT SHALL THE COPYRIGHT HOLDER OR CONTRIBUTORS BE LIABLE FOR ANY DIRECT, INDIRECT, INCIDENTAL, SPECIAL, EXEMPLARY, OR CONSEQUENTIAL DAMAGES (INCLUDING, BUT NOT LIMITED TO, PROCUREMENT OF SUBSTITUTE GOODS OR SERVICES; LOSS OF USE, DATA, OR PROFITS; OR BUSINESS INTERRUPTION) HOWEVER CAUSED AND ON ANY THEORY OF LIABILITY, WHETHER IN CONTRACT, STRICT LIABILITY, OR TORT (INCLUDING NEGLIGENCE OR OTHERWISE) ARISING IN ANY WAY OUT OF THE USE OF THIS SOFTWARE, EVEN IF ADVISED OF THE POSSIBILITY OF SUCH DAMAGE.

<initialize.go>

```
/*
Copyright ©2015 The corridor Authors. All rights
reserved. Use of this source code is governed by a
BSD-style license that can be found in the LICENSE
file.
*/

package corridor

import (
    "errors"
    "fmt"
    "math"
    "runtime"
    "sort"

    "github.com/gonum/diff/fd"
    "github.com/gonum/matrix/mat64"
    "github.com/satori/go.uuid"
)

// new problem parameters function
func NewParameters(sourceSubscripts,
    destinationSubscripts []int, populationSize,
    evolutionSize int, randomnessCoefficient float64)
```

```

*Parameters {

    // set default mutation count
    mutationCount := 1

    // set default mutation fraction
    mutationFraction := 0.2

    // set selection fraction
    selectionFraction := 0.5

    // set selection probability
    selectionProbability := 0.8

    // get concurrency size
    maxConcurrency := runtime.NumCPU()

    // return output
    return &Parameters{
        SrcSubs: sourceSubscripts ,
        DstSubs: destinationSubscripts ,
        RndCoef: randomnessCoefficient ,
        PopSize: populationSize ,
        SelFrac: selectionFraction ,
        SelProb: selectionProbability ,
        MutaCnt: mutationCount ,
        MutaFrc: mutationFraction ,
    }
}

```

```

        EvoSize: evolutionSize ,
        ConSize: maxConcurrency ,
    }
}

// new domain initialization function
func NewDomain(domainMatrix *mat64.Dense) *Domain {

    // get domain size
    rows, cols := domainMatrix.Dims()

    // compute band count
    bandCount := 2 +
        (int(math.Floor(math.Sqrt(math.Pow(float64(rows),
            2.0)+math.Pow(float64(cols), 2.0)))) / 142)

    //return output
    return &Domain{
        Rows:    rows ,
        Cols:    cols ,
        Matrix:  domainMatrix ,
        BndCnt:  bandCount ,
    }
}

// new objective initialization function
func NewObjective(identifier int, fitnessMatrix

```

```

*mat64.Dense) *Objective {

    // return output
    return &Objective{
        Id:    identifier ,
        Matrix: fitnessMatrix ,
    }
}

// new basis solution initialization function
func NewBasis(sourceSubs , destinationSubs []int ,
searchDomain *Domain) *Basis {

    // compute all minimum euclidean distances for
    // search domain
    allMinimumDistances := AllMinDistance(sourceSubs ,
destinationSubs , searchDomain.Matrix)

    // generate subscripts from bresenham's algorithm
    subs := Bresenham(sourceSubs , destinationSubs)

    // compute maximum permitted chromosome length
    maxLength := len(subs) * 10

    // return output
    return &Basis{
        Matrix: allMinimumDistances ,

```

```

        Subs:    subs ,
        MaxLen:  maxLength ,
    }
}

// new chromosome initialization function
func NewChromosome(searchDomain *Domain,
searchParameters *Parameters, searchObjectives
*MultiObjective) *Chromosome {

    // generate node subscripts
    nodeSubs := NewNodeSubs(searchDomain ,
searchParameters)

    // generate subscripts from directed walk
    procedure
    subs := MultiPartDirectedWalk(nodeSubs ,
searchDomain , searchParameters)

    // initialize empty fitness place holders
    fitVal := make([][]float64 ,
searchObjectives.ObjectiveCount)
    for i := 0; i < searchObjectives.ObjectiveCount;
i++ {
        fitVal[i] = make([]float64 , len(subs))
    }
    totFit := make([]float64 ,

```

```

searchObjectives.ObjectiveCount)
var aggFit float64 = 0.0

// generate placeholder variables
uuid := uuid.NewV4()

// return output
return &Chromosome{
    Id:          uuid,
    Subs:       subs,
    Fitness:    fitVal,
    TotalFitness: totFit,
    AggregateFitness: aggFit,
}
}

// new empty chromosome initialization function
func NewEmptyChromosome(searchDomain *Domain,
searchObjectives *MultiObjective) *Chromosome {

    // initialize subscripts
    subs := make([][]int, 0)

    // generate placeholder id
    uuid := uuid.NewV4()

    // initialize empty fitness place holders

```

```

fitVal := make([][] float64 ,
searchObjectives . ObjectiveCount)
for i := 0; i < searchObjectives . ObjectiveCount ;
i++ {
    fitVal [ i ] = make ( [] float64 , len ( subs ))
}
totFit := make ( [] float64 ,
searchObjectives . ObjectiveCount)
var aggFit float64 = 0.0

// return output
return &Chromosome {
    Id:          uuid ,
    Subs:       subs ,
    Fitness:    fitVal ,
    TotalFitness: totFit ,
    AggregateFitness: aggFit ,
}
}

// new population initialization function
func NewPopulation ( identifier int , searchDomain
*Domain , searchParameters *Parameters ,
searchObjectives *MultiObjective ) *Population {

// initialize communication channel
chr := make ( chan *Chromosome ,

```

```

searchParameters.PopSize)

// initialize new empty chromosome before
// entering loop
newChrom := NewEmptyChromosome(searchDomain,
searchObjectives)

// initialize concurrency limit channel
conc := make(chan bool, searchParameters.ConSize)

// generate chromosomes via go routines
for i := 0; i < searchParameters.PopSize; i++ {

    // write to control channel
    conc <- true

    // launch chromosome initialization go
    // routines
    go func(searchDomain *Domain, searchParameters
*Parameters, searchObjectives *MultiObjective)
    {
        defer func() { <-conc }()
        newChrom = NewChromosome(searchDomain,
searchParameters, searchObjectives)
        chr <- ChromosomeFitness(newChrom,
searchObjectives)
    }(searchDomain, searchParameters,

```



```

        searchObjectives)
    }

    // cap parallelism at concurrency limit
    for j := 0; j < cap(conc); j++ {
        conc <- true
    }

    // initialize fitness placeholder
    meanFit := make([]float64,
        searchObjectives.ObjectiveCount)
    var aggMeanFit float64 = 0.0

    // return output
    return &Population{
        Id:                identifier,
        Chromosomes:       chr,
        MeanFitness:       meanFit,
        AggregateMeanFitness: aggMeanFit,
    }
}

// new empty population initialization function
func NewEmptyPopulation(identifier int,
    searchObjectives *MultiObjective) *Population {

```

```

// initialize empty chromosomes channel
chr := make(chan *Chromosome)

// initialize fitness placeholder
meanFit := make([]float64 ,
searchObjectives.ObjectiveCount)
var aggMeanFit float64 = 0.0

// return output
return &Population{
    Id: identifier ,
    Chromosomes: chr ,
    MeanFitness: meanFit ,
    AggregateMeanFitness: aggMeanFit ,
}
}

// new empty evolution initialization function
func NewEmptyEvolution(searchParameters *Parameters)
*Evolution {

// initialize empty population channel
popChan := make(chan *Population ,
searchParameters.EvoSize)

// initialize empty fitness gradient
gradFit := make([]float64 ,

```

```

searchParameters.EvoSize)

// return output
return &Evolution{
    Populations:    popChan,
    FitnessGradient: gradFit,
}
}

// new evolution initialization function
func NewEvolution(searchParameters *Parameters ,
searchDomain *Domain, searchObjectives
*MultiObjective) *Evolution {

    // initialize seed population identifier
    var popID int = 0

    // initialize population channel
    popChan := make(chan *Population, 1)

    // print initialization status message
    fmt.Println("Initializing Seed Population...")

    // initialize seed population
    seedPop := NewPopulation(popID, searchDomain,
searchParameters, searchObjectives)
    popChan <- PopulationFitness(seedPop,

```

```

searchParameters , searchObjectives)

// initialize raw fitness data slice
rawAggMeanFit := make([]float64 ,
searchParameters.EvoSize)

// initialize fitness gradient variable
gradFit := make([]float64 ,
searchParameters.EvoSize)

// enter loop
for i := 0; i < searchParameters.EvoSize; i++ {

    // perform population evolution
    newPop := PopulationEvolution(<-popChan ,
searchDomain , searchParameters ,
searchObjectives)

    // compute population fitness
    newPop = PopulationFitness(newPop ,
searchParameters , searchObjectives)

    // write aggregate mean fitness value to
// vector
    rawAggMeanFit[i] = newPop.AggregateMeanFitness

    // generate inline fitness gradient function

```

```

var fitnessGradFnc = func(n float64) float64
{ return rawAggMeanFit[int(n)] }

// compute fitness gradient
gradFit[i] = fd.Derivative(fitnessGradFnc,
float64(i), nil)

// skip gradient check on first iteration
if i < 1 {

    // return new population to channel
    popChan <- newPop

    // increment progress bar
    fmt.Println(" Evolution: ", i+1)

} else if i >= 1 && i <
(searchParameters.EvoSize - 1) {

    if gradFit[i] > 0 {

        // return current population
        // to channel
        popChan <- newPop

        // close population channel
        close(popChan)
    }
}

```

```

        // print success message
        fmt.Println("Convergence Achieved ,
Evolution Complete!")

        // break loop
        break
    } else if gradFit[i] <= 0 {

        // return new population to channel
        popChan <- newPop

        // increment progress bar
        fmt.Println("Evolution: ", i+1)

    }

} else if i == searchParameters.EvoSize -1 {

    // return new population to channel
    popChan <- newPop

    // close population channel
    close(popChan)

    // print termination message

```

```

        fmt.Println("Convergence Not Achieved ,
Maximum Number of Evolutions Reached...")

        // break loop
        break
    }
}

// return output
return &Evolution{
    Populations:    popChan,
    FitnessGradient: gradFit,
}
}

/*
function to return copies of a user specified
fraction of the individual chromosomes within a
population ranked in terms of individual aggregate
fitness
*/
func NewEliteFraction(inputFraction float64 ,
inputPopulation *Population) (outputChromosomes
[]*Chromosome) {

    // count input chromosomes
    chromCount := cap(inputPopulation.Chromosomes)

```

```

// initialize aggregate score slice
chromFrac := int(math.Ceil(inputFraction *
float64(chromCount)))

// initialize chromosome map
chromMap := make(map[float64]*Chromosome)

// initialize chromosome map key slice
chromKey := make([]float64, chromCount)

// initialize output slice
output := make([]*Chromosome, chromFrac)

// loop through channel to populate slice
for i := 0; i < chromCount; i++ {
    curChrom := <-inputPopulation.Chromosomes
    chromMap[curChrom.AggregateFitness] = curChrom
    chromKey[i] = curChrom.AggregateFitness
}

// sort on aggregate fitness keys
sort.Float64s(chromKey)

// loop through and generate output slice fraction
for j := 0; j < chromFrac; j++ {
    output[j] = chromMap[chromKey[j]]
}

```



```

    }

    // return output
    return output
}

/*
function to return copies of a user specified
number of unique individual chromosomes from within a
population with each chromosome being ranked in terms
of its individual aggregate fitness
*/
func NewEliteSet(inputCount int, inputPopulation
*Population, inputParameters *Parameters)
(outputChromosomes []*Chromosome) {

    // check band count against population size
    if inputCount >= int(math.Floor((0.5 *
float64(inputParameters.PopSize)))) {
        err := errors.New("Input elite set count must
be less than 1/2 the input population size
\n")
        panic(err)
    }

    // count input chromosomes
    chromCount := cap(inputPopulation.Chromosomes)

```

```

// initialize chromosome map
chromMap := make(map[float64]*Chromosome)

// initialize chromosome map key slice
chromKey := make([]float64, chromCount)

// initialize output slice
output := make([]*Chromosome, inputCount)

// loop through channel to populate slice from
// channel
for i := 0; i < chromCount; i++ {
    curChrom := <-inputPopulation.Chromosomes
    chromMap[curChrom.AggregateFitness] = curChrom
    chromKey[i] = curChrom.AggregateFitness
    inputPopulation.Chromosomes <- curChrom
}

// sort on aggregate fitness keys
sort.Float64s(chromKey)

// initialize iteration counter
var iter int = 0

// loop through and generate output slice set
for j := 0; j < chromCount; j++ {

```

```

// deal with initial state
if j == 0 {
    output[iter] = chromMap[chromKey[j]]
    iter += 1
    continue
}

// get uuids
prevUuid :=
chromMap[chromKey[j-1]].Id.String()
curUuid := chromMap[chromKey[j]].Id.String()

// impose uniqueness constraint
if prevUuid != curUuid {
    output[iter] = chromMap[chromKey[j]]
    iter += 1
} else {
    continue
}

// stop if inputCount reached
if iter == inputCount {
    break
}
}

```

```
    // return output  
    return output  
}
```

```

<io.go>

/*
Copyright ©2015 The corridor Authors. All rights
reserved. Use of this source code is governed by a
BSD-style license that can be found in the LICENSE
file.
*/

package corridor

import (
    "encoding/csv"
    "fmt"
    "os"
    "strconv"
    "time"

    "github.com/gonum/matrix/mat64"
)

// function to write an input comma separated value
// file's contents to an output domain structure
func CsvToSubs(inputFilepath string) (outputSubs
[]int) {

    // open file

```

```

data, err := os.Open(inputFilepath)

// parse error if file not found
if err != nil {
    fmt.Println(err)
    return
}

// close file on completion
defer data.Close()

// generate new reader from open file
reader := csv.NewReader(data)

// set reader structure field
reader.FieldsPerRecord = -1

// use reader to read raw csv data
rawCSVdata, err := reader.ReadAll()

// parse csv file formatting errors
if err != nil {
    fmt.Println(err)
    os.Exit(1)
}

// initialize empty row and column counts

```

```

rows := len(rawCSVdata)
cols := len(rawCSVdata[0])

// initialize output
output := make([]int, 2)

// loop through and extract values
for i := 0; i < rows; i++ {
    for j := 0; j < cols; j++ {

        // get string value and convert
        // to integer
        strVal := rawCSVdata[i][j]
        intVal, err := strconv.Atoi(strVal)

        // shift value by one to account for
        // buffer boundaries
        output[j] = intVal + 1

        // parse error
        if err != nil {
            fmt.Println(err)
            os.Exit(1)
        }
    }
}

```

```

        // return output
        return output
    }

// function to write an input comma separated value
// file 's contents to an output domain structure
func CsvToDomain(inputFilepath string) (outputDomain
*Domain) {

    // open file
    data, err := os.Open(inputFilepath)

    // parse error if file not found
    if err != nil {
        fmt.Println(err)
        return
    }

    // close file on completion
    defer data.Close()

    // generate new reader from open file
    reader := csv.NewReader(data)

    // set reader structure field
    reader.FieldsPerRecord = -1

```



```

// use reader to read raw csv data
rawCSVdata, err := reader.ReadAll()

// parse csv file formatting errors
if err != nil {
    fmt.Println(err)
    os.Exit(1)
}

// initialize empty row and column counts
rows := len(rawCSVdata)
cols := len(rawCSVdata[0])

// initialize domain matrix
domMat := mat64.NewDense(rows+2, cols+2, nil)

// write values from rawCSVdata to domain matrix
for i := 0; i < rows+2; i++ {
    for j := 0; j < cols+2; j++ {
        // create a 1 pixel boundary buffer of
        zeros
        if i == 0 {
            domMat.Set(i, j, 0.0)
        } else if i == rows+1 {
            domMat.Set(i, j, 0.0)
        } else if j == 0 {
            domMat.Set(i, j, 0.0)
        }
    }
}

```

```

    } else if j == cols+1 {
        domMat.Set(i, j, o.o)
    } else {

        // get string value and
        // convert to integer
        strVal := rawCSVdata[i-1][j-1]
        fltVal, err :=
            strconv.ParseFloat(strVal, 64)

        // parse error
        if err != nil {
            fmt.Println(err)
            os.Exit(1)
        }

        // write value to matrix
        domMat.Set(i, j, fltVal)
    }
}

// initialize new domain
output := NewDomain(domMat)

// return output
return output

```

```

}

// function to write an input comma separated value
// file 's contents to an output objective structure
func CsvToObjective(identifier int, inputFilepath
string) (outputObjective *Objective) {

    // open file
    dataFile, err := os.Open(inputFilepath)

    // parse error if file not found
    if err != nil {
        fmt.Println(err)
        return
    }

    // close file on completion
    defer dataFile.Close()

    // generate new reader from open file
    reader := csv.NewReader(dataFile)

    // set reader structure field
    reader.FieldsPerRecord = -1

    // use reader to read raw csv data
    rawCSVdata, err := reader.ReadAll()

```

```

// parse csv file formatting errors
if err != nil {
    fmt.Println(err)
    os.Exit(1)
}

// initialize empty row and column counts
rows := len(rowCSVdata)
cols := len(rowCSVdata[0])

// initialize domain matrix
objMat := mat64.NewDense(rows+2, cols+2, nil)

// write values from rowCSVdata to domain matrix
for i := 0; i < rows+2; i++ {
    for j := 0; j < cols+2; j++ {

        // create a 1 pixel boundary
        // buffer of zeros
        if i == 0 {
            objMat.Set(i, j, 0.0)
        } else if i == rows+1 {
            objMat.Set(i, j, 0.0)
        } else if j == 0 {
            objMat.Set(i, j, 0.0)
        } else if j == cols+1 {

```

```

        objMat.Set(i, j, o.o)
    } else {

        // get string value and
        // convert to float
        strVal := rawCSVdata[i-1][j-1]
        fltVal, err :=
            strconv.ParseFloat(strVal, 64)

        // parse error
        if err != nil {
            fmt.Println(err)
            os.Exit(1)
        }

        // write matrix value
        objMat.Set(i, j, fltVal)
    }
}

// initialize new domain
output := NewObjective(identifier, objMat)

// return output
return output
}

```

```

/*
function to write a set of input comma separated
value files ' contents to an output multiobjective
structure
*/
func CsvToMultiObjective(inputFilePaths ... string)
(outputMultiObjective *MultiObjective) {

    // get variadic input length
    objectiveCount := len(inputFilePaths)

    // initialize objective slice
    objectiveSlice := make([]* Objective ,
objectiveCount)

    // initialize objectives identifier
    var objectiveID int = 0

    // loop through and extract objectives
    for i := 0; i < objectiveCount; i++ {

        // read CSV data to objective
        objectiveSlice[i] =
        CsvToObjective(objectiveID , inputFilePaths[i])

        // increment objective identifier

```

```

        objectiveID += 1
    }

    // return multiObjective output
    return &MultiObjective{
        ObjectiveCount: objectiveCount,
        Objectives:     objectiveSlice,
    }
}

// function to write the values from an input
// chromosome structure to an output csv file
func ChromosomeToString(inputChromosome *Chromosome)
(outputRawString [][] string) {

    // get input chromosome length
    chromLen := len(inputChromosome.Subs)

    // count input chromosome objectives
    objCount := len(inputChromosome.TotalFitness)

    // initialize raw output string slice
    rawCSVdata := make([][] string, objCount+2)

    // loop through and format values as strings for
    // output encoding

```

```

for j := 0; j < objCount+2; j++ {

    // allocate inner slice
    rawCSVdata[j] = make([]string, chromLen)

    for i := 0; i < chromLen; i++ {

        // transpose subs by one to account for
        // boundary buffer
        if j == 0 {
            rawCSVdata[j][i] =
                strconv.Itoa(
                    inputChromosome.Subs[i][0] - 1)
        } else if j == 1 {
            rawCSVdata[j][i] =
                strconv.Itoa(
                    inputChromosome.Subs[i][1] - 1)
        } else {
            rawCSVdata[j][i] =
                strconv.FormatFloat(
                    inputChromosome.Fitness[j-2][i],
                    'f', 2, 64)
        }
    }
}

// return output

```



```

        return rawCSVdata
    }

    /*
    function to write the values from an input elite set
    to an output csv file
    */
    func EliteSetToCsv(inputEliteSet []*Chromosome,
        outputFilepath string) {

        // open file
        csvfile, err := os.Create(outputFilepath)

        // parse file opening errors
        if err != nil {
            fmt.Println("Error:", err)
            return
        }

        // close file on completion
        defer csvfile.Close()

        // get chromosome count
        chromCount := len(inputEliteSet)

        // initialize rawCSVdata and chromosome string
        // structures

```

```

var chromString, rawCSVdata [][] string

// loop through chromosomes and generate composite
// string structure
for i := 0; i < chromCount; i++ {
    chromString =
        ChromosomeToString(inputEliteSet[i])
    rawCSVdata = append(rawCSVdata,
        chromString...)
}

// initialize writer object
writer := csv.NewWriter(csvfile)

// write data or get error
err = writer.WriteAll(rawCSVdata)

// parse errors
if err != nil {
    fmt.Println("Error:", err)
    return
}

// flush writer object
writer.Flush()
}

```

```

/*
function to write the runtime parameters from an
evolution to an output csv file
*/
func RuntimeLogToCsv(inputEvolution *Evolution ,
inputRuntime time.Duration , outputPath string) {

    // open file
    csvfile , err := os.Create(outputFilePath)

    // parse file opening errors
    if err != nil {
        fmt.Println("Error:" , err)
        return
    }

    // close file on completion
    defer csvfile.Close()

    // initialize rawCSVdata structure
    var rawCSVdata []string

    // populate string slice
    rawCSVdata = append(rawCSVdata ,
inputRuntime.String())

    // initialize evolutionary counter

```

```

var evo int = 0

// count required evolutions
for i := 0; i <
len(inputEvolution.FitnessGradient); i++ {
    if inputEvolution.FitnessGradient[i] != 0 {
        evo += 1
    } else {
        continue
    }
}

// convert to string
rawCSVdata = append(rawCSVdata,
strconv.Itoa(evo))

// initialize writer object
writer := csv.NewWriter(csvfile)

// write data or get error
err = writer.Write(rawCSVdata)

// parse errors
if err != nil {
    fmt.Println("Error:", err)
    return
}

```

```
        // flush writer object
        writer.Flush()
    }
```

<lib.go>

```
/*
Copyright ©2015 The corridor Authors. All rights
reserved. Use of this source code is governed by a
BSD-style license that can be found in the LICENSE
file.package main
*/

package corridor

import (
    "errors"
    "math"

    "github.com/gonum/matrix/mat64"
)

// compute euclidean distance for a pair of subscript
// indices
func Distance(aSubs, bSubs []int) (dist float64) {

    // initialize variables
    var xo float64 = float64(aSubs[0])
    var xi float64 = float64(bSubs[0])
    var yo float64 = float64(aSubs[1])
    var yi float64 = float64(bSubs[1])
```

```

var pow float64 = 2.0
var dx float64 = x1 - x0
var dy float64 = y1 - y0

// compute distance
var output float64 = math.Sqrt(math.Pow(dx, pow)
+ math.Pow(dy, pow))

// return final output
return output
}

/*
alldistance computes the distance from each
location with the input search domain and a given
point defined by an input pair of row column
subscripts
*/
func AllDistance(aSubs []int, searchDomainMatrix
*mat64.Dense) (allDistMatrix *mat64.Dense) {

// get matrix dimensions
rows, cols := searchDomainMatrix.Dims()

// initialize new output matrix
output := mat64.NewDense(rows, cols, nil)

```

```

// initialize destination point subscript slice
bSubs := make([]int, 2)

// loop through all values and compute minimum
// distances
for i := 0; i < rows; i++ {
    for j := 0; j < cols; j++ {
        bSubs[0] = i
        bSubs[1] = j
        output.Set(bSubs[0], bSubs[1],
            Distance(aSubs, bSubs))
    }
}

// return output
return output
}

/*
compute the minimum distance between a given input
point and the subscripts comprised of a line
segment joining two other input points
*/
func MinDistance(pSubs, aSubs, bSubs []int)
(minDist float64) {

```



```

// initialize variables
var x float64 = float64(pSubs[0])
var y float64 = float64(pSubs[1])
var xo float64 = float64(aSubs[0])
var yo float64 = float64(aSubs[1])
var x1 float64 = float64(bSubs[0])
var y1 float64 = float64(bSubs[1])

// compute difference components
a := x - xo
b := y - yo
c := x1 - xo
d := y1 - yo

// compute dot product of difference components
dot := a*c + b*d
lenSq := c*c + d*d

// initialize parameter
var param float64 = -1.0

// if zero length condition
if lenSq != 0 {
    param = dot / lenSq
}

// initialize transform variables

```

```

var xx, yy float64

// switch transform mechanism on orientation
if param < 0 {
    xx = x0
    yy = y0
} else if param > 1 {
    xx = x1
    yy = y1
} else {
    xx = x0 + param*c
    yy = y0 + param*d
}

// execute transform
var dx float64 = x - xx
var dy float64 = y - yy

// generate output
output := math.Sqrt(dx*dx + dy*dy)

// return final output
return output
}

```

/*

allmindistance computes the distance from each

```

location within the input search domain and to the
nearest subscript located along the line formed by
the two input subscripts
*/
func AllMinDistance(aSubs, bSubs []int,
searchDomainMatrix *mat64.Dense) (allMinDistMatrix
*mat64.Dense) {

    // get matrix dimensions
    rows, cols := searchDomainMatrix.Dims()

    // initialize new output matrix
    output := mat64.NewDense(rows, cols, nil)

    // initialize slice
    pSubs := make([]int, 2)

    // loop through all values and compute minimum
    // distances
    for i := 0; i < rows; i++ {
        for j := 0; j < cols; j++ {
            pSubs[0] = i
            pSubs[1] = j
            curMinDist := MinDistance(
                pSubs, aSubs, bSubs)
            output.Set(pSubs[0], pSubs[1],
                curMinDist)
        }
    }
}

```

```

        }
    }

    // return final output
    return output
}

/*
distancebands recodes a distance matrix computed from
a single source location to ordinal set of bands of
increasing distance
*/
func DistanceBands(bandCount int, distanceMatrix
*mat64.Dense) (bandMatrix *mat64.Dense) {

    // get matrix dimensions
    rows, cols := distanceMatrix.Dims()

    // check band count against input distance matrix
    // size
    if bandCount > rows || bandCount > cols {
        err := errors.New("Input band count too large
for input distance matrix \n")
        panic(err)
    }

    // initialize output

```

```

output := mat64.NewDense(rows, cols, nil)

// generate band range
minDist := distanceMatrix.Min()
maxDist := distanceMatrix.Max()

// initialize band interval unit and slice
bandUnit := (maxDist - minDist) /
float64(bandCount+1)
bandInt := make([]float64, bandCount+1)

// generate band intervals
for i := 0; i < bandCount+1; i++ {
    if i == 0 {
        bandInt[i] = 0
    } else {
        bandInt[i] = bandInt[i-1] + bandUnit
    }
}

// perform conversion to the appropriate band
// interval
for i := 0; i < len(bandInt)-1; i++ {
    for j := 0; j < rows; j++ {
        for k := 0; k < rows; k++ {
            if
                distanceMatrix.At(j, k) >=

```

```

        bandInt[i] &&
        distanceMatrix.At(j, k)
        < bandInt[i+1] {
            output.Set(j, k,
                float64(i))
        } else if
        distanceMatrix.At(j, k) >=
        bandInt[i+1] {
            output.Set(j, k,
                float64(i+1))
        }
    }
}

// return output
return output
}

/*
bandmask selects the elements in a distance band
matrix corresponding to a specified input band
identification number and outputs a binary matrix of
the same dimensions as the distance band matrix with
the values at those locations encoded as ones and all
other locations encoded as zeros
*/

```

```

func BandMask(bandValue float64, bandMatrix
*mat64.Dense) (binaryBandMat *mat64.Dense) {

    // get row column dimensions of band matrix
    rows, cols := bandMatrix.Dims()

    // initialize output
    output := mat64.NewDense(rows, cols, nil)

    // loop through matrix values and perform binary
    encoding
    for i := 0; i < rows; i++ {
        for j := 0; j < cols; j++ {

            // perform elementwise equality test
            if i == 0 ||
            i == rows-1 ||
            j == 0 ||
            j == cols-1 {
                output.Set(i, j, 0.0)
            } else {
                if bandValue ==
                bandMatrix.At(i, j) {
                    output.Set(i, j, 1.0)
                } else {
                    output.Set(i, j, 0.0)
                }
            }
        }
    }
}

```

```

        }
    }
}

// return output
return output
}

/*
nonzerosubs returns a 2-D slice containing the row
column indices of all nonzero elements contained
within a given input matrix
*/
func NonZeroSubs(inputMatrix *mat64.Dense)
(nonZeroSubs [][]int) {

    // get matrix dimensions
    rows, cols := inputMatrix.Dims()

    // initialize output
    output := make([][]int, 1)
    output[0] = make([]int, 2)

    // initialize iterator and current subscript
    // slice
    var iter int = 0

```



```

// loop through and check values
for i := 0; i < rows; i++ {
    for j := 0; j < cols; j++ {

        // test for non-zero values
        if inputMatrix.At(i, j) != 0.0 {
            if iter == 0 {
                output[iter] =
                    []int{i, j}
                iter += 1
            } else if iter > 0 {
                output =
                    append(output, []int{i, j})
                iter += 1
            }
        }
    }
}

// return output
return output
}

```

/*
findsubs returns a 2-D slice containing the row
column indices of all of the elements contained
within a given input matrix that are equal in value

```

to some provided input value
*/
func FindSubs(inputValue float64 , inputMatrix
*mat64.Dense) (foundSubs [][]int) {

    // get matrix dimensions
    rows, cols := inputMatrix.Dims()

    // initialize output
    output := make([][]int , 1)
    output[0] = make([]int , 2)

    // initialize iterator and current subscript
    // slice
    var iter int = 0

    // loop through and check values
    for i := 0; i < rows; i++ {
        for j := 0; j < cols; j++ {

            // test for equality
            if inputMatrix.At(i, j) ==
            inputValue {
                if iter == 0 {
                    output[iter] =
                    []int{i, j}
                    iter += 1
                }
            }
        }
    }
}

```

```

        } else if iter > 0 {
            output =
                append(output, []int{i, j})
            iter += 1
        }
    }
}

// return output
return output
}

```

```

/*
orientation accepts as inputs a pair of point
subscripts and returns a binary vector indicating the
relative orientation of the first point to the second
in binary terms
*/
func Orientation(aSubs, bSubs []int)
(orientationVector []int) {

```

```

    // initialize output
    output := make([]int, 2)

    // generate reference orientation row parameter
    if aSubs[0]-bSubs[0] < 0 {

```

```

        output[o] = 1
    } else if aSubs[o]-bSubs[o] == 0 {
        output[o] = 0
    } else if aSubs[o]-bSubs[o] > 0 {
        output[o] = -1
    }

    // generate reference orientation column
    // parameter
    if aSubs[1]-bSubs[1] < 0 {
        output[1] = 1
    } else if aSubs[1]-bSubs[1] == 0 {
        output[1] = 0
    } else if aSubs[1]-bSubs[1] > 0 {
        output[1] = -1
    }

    // return output
    return output
}

```

```

/*
orientation mask returns a binary encoded matrix for
a given point where all points orientated towards
a given second point are encoded as 1 and all points
orientated away from the given second point as 0
*/

```

```

func OrientationMask(aSubs, bSubs []int,
searchDomainMatrix *mat64.Dense) (orientationMask
*mat64.Dense) {

    // generate matrix dimensions
    rows, cols := searchDomainMatrix.Dims()

    // initialize output matrix
    output := mat64.NewDense(rows, cols, nil)

    // generate reference orientation vectors
    sRefOrientVec := Orientation(aSubs, bSubs)
    dRefOrientVec := Orientation(bSubs, aSubs)

    // initialize current subs and orientation
    // vectors
    curSubs := make([]int, 2)
    sOrientVec := make([]int, 2)
    dOrientVec := make([]int, 2)

    // loop through domain matrix and generate
    // orientation matrix values
    for i := 0; i < rows; i++ {
        for j := 0; j < cols; j++ {

            // compute current orientation
            curSubs[0] = i

```

```

curSubs [1] = j
sOrientVec = Orientation(curSubs, bSubs)
dOrientVec = Orientation(curSubs, aSubs)

// check for match and assign values
if sOrientVec[o] ==
sRefOrientVec[o] &&
sOrientVec [1] ==
sRefOrientVec [1] {
    if dOrientVec[o] ==
dRefOrientVec[o] &&
dOrientVec [1] ==
dRefOrientVec [1] {
        output.Set(i, j, 1.0)
    }
}
}
}

// return output
return output
}

```

```

/*
bresenham generates the list of subscript indices
corresponding to the euclidean shortest paths
connecting two subscript pairs in discrete space

```

```

*/
func Bresenham(aSubs, bSubs []int) (lineSubs [][]int)
{

    // initialize variables
    var xo int = aSubs[0]
    var x1 int = bSubs[0]
    var yo int = aSubs[1]
    var y1 int = bSubs[1]

    // check row differential
    dx := x1 - xo
    if dx < 0 {
        dx = -dx
    }

    // check column differential
    dy := y1 - yo

    // if differential is negative flip
    if dy < 0 {
        dy = -dy
    }

    // initialize stride variables
    var sx, sy int

```

```

// set row stride direction
if xo < x1 {
    sx = 1
} else {
    sx = -1
}

// set column stride direction
if yo < y1 {
    sy = 1
} else {
    sy = -1
}

// calculate error component
err := dx - dy

// initialize output 2D slice vector
dist := math.Ceil(Distance(aSubs, bSubs))
maxLen := int(dist)
output := make([][]int, 0, maxLen)

// loop through and generate subscripts
for {
    var val = []int{xo, yo}
    output = append(output, val)
    if xo == x1 && yo == y1 {

```



```

                break
            }
            e2 := 2 * err
            if e2 > -dy {
                err -= dy
                xo += sx
            }
            if e2 < dx {
                err += dx
                yo += sy
            }
        }

        // return final output
        return output
    }

    /*
    function to return the subscript indices of the cells
    corresponding to the queens neighborhood for a given
    subscript pair
    */
    func NeighborhoodSubs(aSubs []int)
    (neighSubs [][]int) {

        // initialize output slice
        output := make([][]int, 0)

```

```

// write neighborhood subscript values
output = append(output, []int{aSubs[o] - 1,
aSubs[o] + 1})
output = append(output, []int{aSubs[o] - 1,
aSubs[o]})
output = append(output, []int{aSubs[o] - 1,
aSubs[o] + 1})
output = append(output, []int{aSubs[o],
aSubs[o] - 1})
output = append(output, []int{aSubs[o],
aSubs[o]})
output = append(output, []int{aSubs[o],
aSubs[o] + 1})
output = append(output, []int{aSubs[o] + 1,
aSubs[o] - 1})
output = append(output, []int{aSubs[o] + 1,
aSubs[o]})
output = append(output, []int{aSubs[o] + 1,
aSubs[o] + 1})

// return output
return output
}

```

/*

function to validate an input sub domain for use in

```

generating a chromosomal mutation via the random walk
procedure
*/
func ValidateMutationSubDomain(subSource, subDestin
[]int, subMat *mat64.Dense) bool {

    // initialize output
    var output bool

    // generate sub source neighborhood
    sNeigh := NeighborhoodSubs(subSource)

    // generate sub destination neighborhood
    dNeigh := NeighborhoodSubs(subDestin)

    // generate center row
    centerRow := subMat.RowView(2)

    // generate center column
    centerCol := subMat.ColView(2)

    // initialize summation variables
    var sSum float64 = 0.0
    var dSum float64 = 0.0
    var rSum float64 = 0.0
    var cSum float64 = 0.0

```

```

// enter for loop for start and destination sums
for i := 0; i < 9; i++ {
    sSum = sSum + subMat.At(sNeigh[i][0],
    sNeigh[i][1])
    dSum = dSum + subMat.At(dNeigh[i][0],
    dNeigh[i][1])
}

// enter for loop for row column sums
for j := 0; j < 5; j++ {
    rSum = rSum + centerRow.At(j, 0)
    cSum = cSum + centerCol.At(j, 0)
}

// check conditions to validate neighborhood
if sSum <= 1.0 || dSum <= 1.0 || rSum == 0.0 ||
cSum == 0.0 {
    output = false
} else {
    output = true
}

//return final output
return output
}

/*

```

```

function validate the tabu neighborhood of an input
pair of row column subscripts
*/
func ValidateTabu(currentSubs []int, tabuMatrix
*mat64.Dense) bool {

    // initialize output
    var output bool

    // initialize tabu neighborhood sum
    var tSum int = 0

    // generate neighborhood subscripts
    tNeigh := NeighborhoodSubs(currentSubs)

    // loop through and compute sum
    for i := 0; i < 9; i++ {
        if i != 4 {
            tSum +=
                int(tabuMatrix.At(tNeigh[i][0],
                    tNeigh[i][1]))
        }
    }

    // write output boolean
    if tSum == 0 {
        output = false
    }
}

```

```

    } else {
        output = true
    }

    // return output
    return output
}

/*
function to count the number of digits in an input
integer as its base ten logarithm
*/
func DigitCount(input int) (digits int) {

    // compute digits as the log of the input
    output :=
    int(math.Floor(math.Log10(float64(input))))

    // return output
    return output
}

```

```

<operators.go>

/*
Copyright ©2015 The corridor Authors. All rights
reserved. Use of this source code is governed by a
BSD-style license that can be found in the LICENSE
file.package main
*/

package corridor

import (
    "math"
    "math/rand"
    "time"

    "github.com/gonum/matrix/mat64"
)

/* fitness function to generate the total fitness and
chromosome fitness values for a given input
chromosome
*/
func ChromosomeFitness(inputChromosome *Chromosome,
inputObjectives *MultiObjective) (outputChromosome
*Chromosome) {

```

```

// get chromosome length
chromLen := len(inputChromosome.Subs)

// clear current chromosome fitness values
inputChromosome.Fitness = make([][]float64,
inputObjectives.ObjectiveCount)
for i := 0; i < inputObjectives.ObjectiveCount; i
++ {
    inputChromosome.Fitness[i] = make([]float64,
len(inputChromosome.Subs))
}

// initialize current & aggregate fitness
var aggFit float64 = 0.0
var curFit float64 = 0.0

// evaluate chromosome length and objectives to
// compute fitnesses
for i := 0; i < inputObjectives.ObjectiveCount; i
++ {
    for j := 0; j < chromLen; j++ {
        curFit =
            inputObjectives.Objectives[i].
            Matrix.At(
                inputChromosome.Subs[j][0],
                inputChromosome.Subs[j][1])
            inputChromosome.Fitness[i][j] =

```



```

        curFit
        inputChromosome.TotalFitness[i] =
        inputChromosome.TotalFitness[i] +
        curFit
    }

    // compute aggregate fitness
    aggFit = aggFit +
    inputChromosome.TotalFitness[i]
}

// calculate aggregate fitness
inputChromosome.AggregateFitness = aggFit

// return outputs
return inputChromosome
}

/*
fitness function generate the mean fitness values for
all of the chromosomes in a given population
*/
func PopulationFitness(inputPopulation *Population ,
inputParameters *Parameters , inputObjectives
*MultiObjective) (outputPopulation *Population) {

    // initialize output

```

```

var cumFit float64 = 0.0
var aggMeanFit float64 = 0.0

// iterate over the different objectives and
// drain channel to compute fitness
for i := 0; i < inputObjectives.ObjectiveCount; i
++ {
    for j := 0; j < inputParameters.PopSize; j++ {

        // read current chromosome from channel
        curChrom := <-inputPopulation.Chromosomes

        // compute cumulative fitness
        cumFit = cumFit + curChrom.TotalFitness[i]

        // receive from channel
        inputPopulation.Chromosomes <- curChrom
    }

    // compute mean from cumulative
    inputPopulation.MeanFitness[i] = cumFit /
float64(inputParameters.PopSize)

    // compute aggregate mean fitness
    aggMeanFit = aggMeanFit +
inputPopulation.MeanFitness[i]
}

```

```

        // write aggregate mean fitness to output
        inputPopulation.AggregateMeanFitness = aggMeanFit

        // return output
        return inputPopulation
    }

    /*
    selection operator selects between two chromosomes
    with a probability of the most fit chromosome being
    selected determined by the input selection
    probability ratio
    */
    func ChromosomeSelection(chrom1, chrom2 *Chromosome,
        selectionProb float64) (selectedChrom *Chromosome) {

        // initialize output
        output := chrom1

        // get current time for random number seed
        rand.Seed(time.Now().UnixNano())

        // generate random number to determine selection
        // result
        dec := rand.Float64()

```

```

// perform conditional selection
if dec > selectionProb { // normal
    if chrom1.AggregateFitness >
        chrom2.AggregateFitness {
        output = chrom1
    } else {
        output = chrom2
    }
} else { // inverted
    if chrom1.AggregateFitness >
        chrom2.AggregateFitness {
        output = chrom2
    } else {
        output = chrom1
    }
}

// return output
return output
}

```

```

/*
population selection operator selects half of the
input population for reproduction based upon
comparative fitness and some randomized input
selection fraction
*/

```

```

func PopulationSelection(inputPopulation *Population,
inputParameters *Parameters) (selection chan
*Chromosome) {

    // initialize selection channel size
    selSize := int(math.Floor(float64(cap(
inputPopulation.Chromosomes)) *
inputParameters.SelFrac))

    // initialize selection channel
    output := make(chan *Chromosome, selSize)

    // initialize selection probability
    selProb := inputParameters.SelProb

    // initialize selection loop
    for i := 0; i < selSize; i++ {
        chrom1 := <-inputPopulation.Chromosomes
        chrom2 := <-inputPopulation.Chromosomes

        go func(chrom1, chrom2 *Chromosome) {
            // write selection to output channel
            output <- ChromosomeSelection(chrom1,
chrom2, selProb)
        }(chrom1, chrom2)
    }
}

```

```

    // return selection channel
    return output
}

/*
intersection determines whether or not the subscripts
associated with two input chromosomes share any in
values in common and reports their relative indices
*/
func ChromosomeIntersection(subs1, subs2 [][]int)
(subs1Indices, subs2Indices []int) {

    // initialize output index slice
    output1 := make([]int, 0)
    output2 := make([]int, 0)

    // initialize subscript lengths
    len1 := len(subs1)
    len2 := len(subs2)

    // enter intersection loop
    for i := 0; i < len1; i++ {
        for j := 0; j < len2; j++ {
            if subs1[i][0] == subs2[j][0] &&
                subs1[i][1] == subs2[j][1] {
                output1 = append(output1, i)
                output2 = append(output2, j)
            }
        }
    }
}

```

```

        }
    }
}

// return intersection output
return output1, output2

}

/*
crossover operator performs the single point
crossover operation for two input chromosomes that
have previously been selected from a source
population
*/
func ChromosomeCrossover(chrom1Ind, chrom2Ind []int,
chrom1Subs, chrom2Subs [][]int) (crossoverChrom []
[]int) {

    // initialize maximum length
    maxLen := len(chrom1Subs) + len(chrom2Subs)

    // initialize output
    output := make([][]int, 0, maxLen)

    // get current time for random number seed
    rand.Seed(time.Now().UnixNano())

```

```

var r int

// generate random number to determine selection
// result while screening out initial source
// index match
for {
    r = rand.Intn(len(chrom1Ind) - 1)
    if r == 0 {
        continue
    } else {
        break
    }
}

// generate subscript slice 1
for i := 0; i < (chrom1Ind[r] + 1); i++ {
    output = append(output, chrom1Subs[i])
}

// generate subscript slice 2
for j := (chrom2Ind[r] + 1); j < len(chrom2Subs);
j++ {
    output = append(output, chrom2Subs[j])
}

// return output

```



```

        return output
    }

/*
selection crossover operator performs a single part
crossover on each of the individuals provided in an
input selection channel of chromosomes
*/
func SelectionCrossover(inputSelection chan
*Chromosome, inputParameters *Parameters,
inputObjectives *MultiObjective, inputDomain *Domain)
(crossover chan *Chromosome) {

    // initialize crossover channel
    output := make(chan *Chromosome,
inputParameters.PopSize)

    // initialize crossover loop
    for i := 0; i < inputParameters.PopSize; i++ {
        for {

            // extract chromosomes
            chrom1 := <-inputSelection
            chrom2 := <-inputSelection

            // initialize empty index slices
            var chrom1Ind []int

```

```

var chrom2Ind []int

// initialize empty chromosome
empChrom :=
NewEmptyChromosome(inputDomain ,
inputObjectives)

// check for valid crossover point
chrom1Ind , chrom2Ind =
ChromosomeIntersection(chrom1.Subs ,
chrom2.Subs)

// resample chromosomes if no intersection
if len(chrom1Ind) > 2 {
    empChrom.Subs =
    ChromosomeCrossover(chrom1Ind ,
    chrom2Ind , chrom1.Subs ,
    chrom2.Subs)
    empChrom = ChromosomeFitness(
    empChrom , inputObjectives)
    output <- empChrom
    inputSelection <- chrom1
    inputSelection <- chrom2
    break
} else {
    inputSelection <- chrom2
    inputSelection <- chrom1

```

```

                                continue
                                }
                                }
                                }

// return output
return output
}

/*
mutationLocus to randomly select a mutation locus and
return the adjacent loci along the length of the
chromosome
*/
func MutationLoci(inputChromosome *Chromosome)
(previousLocus, mutationLocus, nextLocus []int,
mutationIndex int) {

    // compute chromosome length
    lenChrom := len(inputChromosome.Subs)

    // seed random number generator
    rand.Seed(time.Now().UnixNano())

    // randomly select mutation index
    mutIndex := rand.Intn(lenChrom-4) + 2

```

```

// get mutation loci subscripts from mutIndex
mutLocus := inputChromosome.Subs[mutIndex]
prvLocus := inputChromosome.Subs[mutIndex-1]
nxtLocus := inputChromosome.Subs[mutIndex+1]

// return output
return prvLocus, mutLocus, nxtLocus, mutIndex
}

/*
mutation sub domain returns the subdomain to be used
for the mutation specific directed walk procedure
*/
func MutationSubDomain(previousLocus, mutationLocus,
nextLocus []int, inputDomain *mat64.Dense)
(outputSubDomain *mat64.Dense) {

// generate mutation locus neighborhood indices
nInd := NeighborhoodSubs(mutationLocus)

// initialize iterator
var n int = 0

// initialize sub domain matrix
subMat := mat64.NewDense(5, 5, nil)

// clean sub domain

```

```

for i := 0; i < 5; i++ {
    for j := 0; j < 5; j++ {
        if i == 0 {
            subMat.Set(i, j, 0.0)
        } else if i == 4 {
            subMat.Set(i, j, 0.0)
        } else if j == 0 {
            subMat.Set(i, j, 0.0)
        } else if j == 4 {
            subMat.Set(i, j, 0.0)
        } else if nInd[n][0] == previousLocus[0]
&& nInd[n][1] == previousLocus[1] {
            subMat.Set(i, j, 1.0)
            // iterate counter
            n += 1
        } else if nInd[n][0] == nextLocus[0] &&
nInd[n][1] == nextLocus[1] {
            subMat.Set(i, j, 1.0)
            // iterate counter
            n += 1
        } else {
            subMat.Set(i, j,
inputDomain.At(nInd[n]
[0], nInd[n][1]))
            // iterate counter
            n += 1
        }
    }
}

```

```

        }
    }

    // return output
    return subMat
}

/*
function to generate a generic subDomain for an
arbitrary set of node subscripts contained within a
given input search domain
*/
func SubDomain(sourceLocus , destinationLocus []int ,
inputDomain *mat64.Dense) (subDomain *Domain ,
subSourceLocus , subDestinationLocus []int) {

    // compute row index value ranges
    minRow := math.Min(float64(sourceLocus[0]),
float64(destinationLocus[0]))
    maxRow := math.Max(float64(sourceLocus[0]),
float64(destinationLocus[0]))

    // compute column index value ranges
    minCol := math.Min(float64(sourceLocus[1]),
float64(destinationLocus[1]))
    maxCol := math.Max(float64(sourceLocus[1]),
float64(destinationLocus[1]))

```

```

// generate ranges
rowRng := []int{int(minRow - 1.0), int(maxRow +
1.0)}
colRng := []int{int(minCol - 1.0), int(maxCol +
1.0)}

// extract raw domain values
rowSpread := rowRng[1] - rowRng[0]
colSpread := colRng[1] - colRng[0]

// initialize subdomain values
rawDomMat :=
mat64.DenseCopyOf(inputDomain.View(rowRng[0],
colRng[0], rowSpread, colSpread))

// overwrite matrix if singleton dimension
if rowSpread == 2 {
    rawDomMat =
    mat64.DenseCopyOf(inputDomain.View(rowRng[0],
colRng[0], rowSpread+1, colSpread))
}
if colSpread == 2 {
    rawDomMat =
    mat64.DenseCopyOf(inputDomain.View(rowRng[0],
colRng[0], rowSpread, colSpread+1))
}

```

```

// get subdomain matrix dimensions
rows, cols := rawDomMat.Dims()

// mask edge values
rawDomMat.SetRow(0, make([]float64, rows+cols))
rawDomMat.SetRow(rows-1, make([]float64, rows
+cols))
rawDomMat.SetCol(0, make([]float64, rows+cols))
rawDomMat.SetCol(cols-1, make([]float64, rows
+cols))

// generate sub domain structure
subDom := NewDomain(rawDomMat)

// compute sub source and sub destination
// subscript indexes
orient := Orientation(sourceLocus,
destinationLocus)

// allocate output variables
subSrc := make([]int, 2)
subDst := make([]int, 2)

// pivot output subscript values on orientation
// vector
if orient[0] == -1 && orient[1] == -1 {

```



```

        subSrc[o] = int(rows - 2.0)
        subSrc[1] = int(cols - 2.0)
        subDst[o] = int(1.0)
        subDst[1] = int(1.0)
    } else if orient[o] == -1 && orient[1] == 0 {
        subSrc[o] = int(rows - 2.0)
        subSrc[1] = int(cols - 2.0)
        subDst[o] = int(1.0)
        subDst[1] = int(1.0)
    } else if orient[o] == -1 && orient[1] == 1 {
        subSrc[o] = int(rows - 2.0)
        subSrc[1] = int(1.0)
        subDst[o] = int(1.0)
        subDst[1] = int(cols - 2.0)
    } else if orient[o] == 0 && orient[1] == -1 {
        subSrc[o] = int(rows - 2.0)
        subSrc[1] = int(cols - 2.0)
        subDst[o] = int(1.0)
        subDst[1] = int(1.0)
    } else if orient[o] == 0 && orient[1] == 1 {
        subSrc[o] = int(1.0)
        subSrc[1] = int(1.0)
        subDst[o] = int(rows - 2.0)
        subDst[1] = int(cols - 2.0)
    } else if orient[o] == 1 && orient[1] == -1 {
        subSrc[o] = int(1.0)
        subSrc[1] = int(cols - 2.0)

```

```

        subDst[o] = int(rows - 2.o)
        subDst[1] = int(1.o)
    } else if orient[o] == 1 && orient[1] == 0 {
        subSrc[o] = int(1.o)
        subSrc[1] = int(cols - 2.o)
        subDst[o] = int(rows - 2.o)
        subDst[1] = int(1.o)
    } else if orient[o] == 1 && orient[1] == 1 {
        subSrc[o] = int(1.o)
        subSrc[1] = int(1.o)
        subDst[o] = int(rows - 2.o)
        subDst[1] = int(cols - 2.o)
    }

    // return output
    return subDom, subSrc, subDst
}

```

```

/*
function to translate the subscript index values for
a given slice of input loci relative to a given
offset vector
*/
func TranslateWalkSubs(sourceSubs []int,
inputWalkSubs [][]int) (outputWalkSubs [][]int) {

```

```

    // initialize output

```

```

    wlkLen := len(inputWalkSubs)
    outWlkSubs := make([][]int, wlkLen)
    outWlkSubs[0] = make([]int, 2)
    outWlkSubs[0] = sourceSubs

    // loop through and translate subscript values
    for i := 1; i < wlkLen; i++ {
        nSubs := make([]int, 2)
        nSubs[0] = outWlkSubs[i-1][0] +
            (inputWalkSubs[i][0] - inputWalkSubs[i-1][0])
        nSubs[1] = outWlkSubs[i-1][1] +
            (inputWalkSubs[i][1] - inputWalkSubs[i-1][1])
        outWlkSubs[i] = nSubs
    }

    // return output
    return outWlkSubs
}

/*
function to generate a mutation within a given
chromosome at a specified number of mutation loci
*/
func ChromosomeMutation(inputChromosome *Chromosome,
inputDomain *Domain, inputParameters *Parameters,
inputObjectives *MultiObjective) (outputChromosome
*Chromosome) {

```

```

// compute chromosome length
lenChrom := len(inputChromosome.Subs)

// initialize output chromosome
output := inputChromosome

// initialize reference domain matrix
refDomain := mat64.NewDense(inputDomain.Rows,
inputDomain.Cols, nil)

// clone input domain matrix
refDomain.Clone(inputDomain.Matrix)

// block out cells on current chromosome
for k := 0; k < lenChrom; k++ {
    refDomain.Set(inputChromosome.Subs[k][0],
inputChromosome.Subs[k][1], 0.0)
}

// enter unbounded mutation search loop
for {
    // generate mutation loci
    prvLocus, mutLocus, nxtLocus, mutIndex :=
MutationLoci(inputChromosome)

    // first check if deletion is valid, else

```

```

// perform mutation
if Distance(prvLocus , nxtLocus) < 1.5 {

    // perform simple deletion of mutation
    // index
    output.Subs =
    append(output.Subs [: mutIndex],
    output.Subs [(mutIndex + 1):]...)

    // loop over objective and remove fitness
    // values
    for r := 0; r <
    inputObjectives.ObjectiveCount; r++ {
        output.Fitness[r] =
        append(
        output.Fitness[r][: mutIndex],
        output.Fitness[r][(mutIndex + 1):]
        ...)
    }
    break
} else {

    // generate mutation subdomain
    subMat := MutationSubDomain(prvLocus ,
    mutLocus , nxtLocus , refDomain)

    // generate sub source and sub destination

```

```

subSource := make([]int, 2)
subDestin := make([]int, 2)
subSource[0] = prvLocus[0] -
mutLocus[0] + 2
subSource[1] = prvLocus[1] -
mutLocus[1] + 2
subDestin[0] = nxtLocus[0] -
mutLocus[0] + 2
subDestin[1] = nxtLocus[1] -
mutLocus[1] + 2

// generate subdomain from sub matrix and
// generate sub basis
subDomain := NewDomain(subMat)
subParams := NewParameters(subSource,
subDestin, 1, 1, inputParameters.RndCoef)
subBasis := NewBasis(subSource, subDestin,
subDomain)

// check validity of sub domain
subDomainTest :=
ValidateMutationSubDomain(subSource,
subDestin, subMat)

// resample if subdomain is invalid
if subDomainTest == false {
    continue
}

```

```

} else {

    // generate directed walk based
    // mutation
    subWlk, tabuTest :=
MutationWalk(subParams.SrcSubs,
subParams.DstSubs, subDomain,
subParams, subBasis)

    // if tabu test fails abort mutation
    // and restart
    if tabuTest == false {
        subWlk = make([][]int, 1)
        continue
    } else {

        subLen := len(subWlk)
        subFit := make([][]float64,
inputObjectives.
ObjectiveCount)

        // translate subscripts
        // and evaluate
        // fitnesses
        for i := 0; i <
inputObjectives.
ObjectiveCount; i++

```

```

{

// initialize
// subfit
// section
subFit[i] =
make([]float64,
subLen)

// translate
// subscripts
// and
// compute sub
// walk fitness
for j := 0;
j < subLen;
j++ {
    if i == 0 {
        subWlk[j][0]
        = subWlk[j]
        [0] - 2 +
        mutLocus[0]
        subWlk[j][1]
        = subWlk[j]
        [1] - 2 +
        mutLocus[1]
    }
}

```



```

subFit[i][j] =
inputObjectives.
Objectives[i].
Matrix.At(
subWlk[j][0],
subWlk[j][1])
}

```

```

// delete mutation locus from
// fitnesses
output.
Fitness[i] =
append(
output.Fitness[i]
[:mutIndex],
output.Fitness[i]
[(mutIndex+1):]...)

// insert sub
// walk section
// into original
// chromosome
// fitnesses
output.
Fitness[i] =
append(output.

```

```

        Fitness [ i ]
        [: mutIndex -1],
        append( subFit [ i ],
        output .
        Fitness [ i ] [ mutIndex +1:]
        ...)...)
    }

// delete mutation
// locus from subs
output . Subs =
append(
output . Subs [: mutIndex ],
output . Subs [( mutIndex +1):]
...)

// insert new sub walk
// subscripts into subs
output . Subs =
append( output .
Subs [: mutIndex -1],
append( subWlk ,
output . Subs [ mutIndex +1:]
...)...)

break
}

```

```

        }
    }

}

// return output
return output
}

/*
function to generate multiple mutations on multiple
separate loci on the same input chromosome
*/
func ChromosomeMultiMutation(inputChromosome
*Chromosome, inputDomain *Domain, inputParameters
*Parameters, inputObjectives *MultiObjective)
(outputChromosome *Chromosome) {

    // loop through mutation count
    for i := 0; i < inputParameters.MutaCnt; i++ {
        inputChromosome =
            ChromosomeMutation(inputChromosome,
            inputDomain, inputParameters, inputObjectives)
    }

    // return output
    return inputChromosome
}

```

```

}

/*
function to generate mutations within a specified
fraction of an input population with those
chromosomes being selected at random
*/
func PopulationMutation(inputChromosomes chan
*Chromosome, inputParameters *Parameters,
inputObjectives *MultiObjective, inputDomain *Domain)
(outputChromosomes chan *Chromosome) {

    // calculate the total number of chromosomes that
    // are to receive mutations
    mutations :=
    int(math.Floor(float64(inputParameters.PopSize) *
    float64(inputParameters.MutaFrc)))

    // seed random number generator
    rand.Seed(time.Now().UnixNano())

    // initialize mutation selection test variable
    // and iteration counter variable
    var iter int
    var mutTest int

    // initialize throttle size

```

```

conc := make(chan bool, inputParameters.ConSize)

// initialize selection loop
for j := 0; j < inputParameters.PopSize; j++ {

    // get current chromosome from channel
    curChrom := <-inputChromosomes

    // generate random mutation selection binary
    integer
    mutTest = rand.Intn(2)

    // screen on mutation indices
    if mutTest == 1 {

        // write to control channel
        conc <- true

        // launch go routines
        go func(curChrom *Chromosome, inputDomain
        *Domain, inputParameters *Parameters,
        inputObjectives *MultiObjective) {
            defer func() { <-conc }()
            curChrom =
            ChromosomeMultiMutation(curChrom,
            inputDomain, inputParameters,
            inputObjectives)
        }()
    }
}

```

```

    }(curChrom, inputDomain, inputParameters,
    inputObjectives)

    // update iterator
    iter += 1

    // return current chromosome back to
    // channel
    inputChromosomes <- curChrom

} else {

    // return current chromosome back to
    // channel
    inputChromosomes <- curChrom
}

// break once the desired number of mutants
// has been generated
if iter == mutations {
    break
}

}

// cap parallelism at concurrency limit
for j := 0; j < cap(conc); j++ {
    conc <- true

```

```

    }

    // return selection channel
    return inputChromosomes
}

/*
population evolution operator generates a new
population from an input population using the
selection and crossover operators
*/
func PopulationEvolution(inputPopulation *Population ,
inputDomain *Domain, inputParameters *Parameters ,
inputObjectives *MultiObjective) (outputPopulation
*Population) {

    // initialize new empty population
    output := NewEmptyPopulation(inputPopulation.Id
+1, inputObjectives)

    // perform population selection
    popSel := PopulationSelection(inputPopulation ,
inputParameters)

    // perform selection crossover
    selCrs := SelectionCrossover(popSel ,
inputParameters , inputObjectives , inputDomain)

```

```
// fill empty population
popMut := PopulationMutation(selCrs ,
inputParameters , inputObjectives , inputDomain)

// assign channel to output population
output.Chromosomes = popMut

// return output
return output
}
```



```

<random.go>

/*
Copyright ©2015 The corridor Authors. All rights
reserved. Use of this source code is governed by a
BSD-style license that can be found in the LICENSE
file.
*/

package corridor

import (
    "math"
    "math/rand"
    "time"

    "github.com/gonum/matrix/mat64"
)

/*
multivariatenormalrandom generates pairs of
bivariate normally distributed random numbers given
an input mean vector and covariance matrix
func MultiVariateNormalRandom(mu *mat64.Dense, sigma
*mat64.SymDense) (rndsmp *mat64.Dense) {

    // initialize vector slices

```

```

o := make([] float64 , 2)
n := make([] float64 , 2)

// generate random numbers from normal
// distribution , prohibit [0,0]
// combinations
rand.Seed(time.Now().UnixNano())

// enter loop
for i := 0; i < 2; i++ {
    n[i] = rand.NormFloat64()
}

// convert to matrix type
rnd := mat64.NewDense(2 , 1, n)
output := mat64.NewDense(2 , 1, o)

// perform cholesky decomposition on covariance
// matrix
lower := mat64.NewTriDense(2 , false , nil)
lower.Cholesky(sigma , true)

// compute output
output.Mul(lower , rnd)
output.Add(output , mu)

//return final output

```

```

    return output
}

/*
fixmultivariatenormalrandom converts an input vector
of bivariate normally distributed random numbers into
a version where the values have been fixed to a [-1,
0,1] range
*/
func FixMultiVariateNormalRandom(rndsmpl *mat64.Dense)
(fixsmpl *mat64.Dense) {

    // initialize vector slice
    o := make([]float64, 2)

    // write up down movement direction
    if rndsmpl.At(0, 0) > 1.0 {
        o[0] = 1
    } else if rndsmpl.At(0, 0) >= -1.0 && rndsmpl.At(0,
0) <= 1.0 {
        o[0] = 0
    } else if rndsmpl.At(0, 0) < -1.0 {
        o[0] = -1
    }

    // write left right movement direction
    if rndsmpl.At(1, 0) > 1.0 {

```

```

        o[i] = i
    } else if rndsmp.At(i, o) >= -1.0 && rndsmp.At(i,
o) <= 1.0 {
        o[i] = o
    } else if rndsmp.At(i, o) < -1.0 {
        o[i] = -i
    }

    // convert to matrix type
    output := mat64.NewDense(i, 2, o)

    // return final output
    return output
}

/*
newrandom repeatedly generates a new random sample
from mvrnd and then fixes it using fixrandom until
the sample is comprised of a non [0, 0] case
*/
func NewRandom(mu *mat64.Dense, sigma
*mat64.SymDense) (newRand []int) {

    // initialize rndsmp and fixsmp and output
    // variables
    rndsmp := mat64.NewDense(2, 1, nil)
    fixsmp := mat64.NewDense(1, 2, nil)

```

```

// generate random vectors prohibiting zero-zero
// cases
for {
    rndsmp = MultiVariateNormalRandom(mu, sigma)
    fixsmp = FixMultiVariateNormalRandom(rndsmp)
    if fixsmp.At(o, o) == o && fixsmp.At(o, 1) ==
    o {
        continue
    } else {
        break
    }
}

// initialize output
output := make([]int, 2)

// write output values
output[o] = int(fixsmp.At(o, o))
output[1] = int(fixsmp.At(o, 1))

// return final output
return output
}

/*
newmu generates a matrix representation of mu that

```

```

reflects the spatial orientation between the input
current subscript and the destination subscript
*/
func NewMu(curSubs , dstSubs []int) (mu *mat64.Dense){
    // compute mu as the orientation vector
    orientVec := Orientation(curSubs , dstSubs)

    // convert mu to float
    var muVec = []float64{float64(orientVec[0]),
float64(orientVec[1])}

    // initialize matrix output
    output := mat64.NewDense(2 , 1, muVec)

    // return final output
    return output
}

/*
newsigma generates a matrix representation of sigma
that reflects the number of iterations in the
sampling process as well as the distance from the
basis euclidean solution
*/
func NewSigma(iterations int , randomness , distance
float64) (sigma *mat64.SymDense) {

```

```

// impose lower bound on distance
if distance < 1 {
    distance = 1.0
}

// set numerator
var num float64 = 1.0

// initialize covariance
var cov float64

// compute covariance
if distance == 1.0 {
    cov = 1.0
} else {
    cov = math.Pow(distance, (num/randomness)) /
    math.Pow(float64(iterations), (num/
    randomness))
}

// initialize matrix output
output := mat64.NewSymDense(2, nil)

// set values
output.SetSym(0, 0, cov)
output.SetSym(0, 1, 0.0)
output.SetSym(1, 0, 0.0)

```

```

output.SetSym(1, 1, cov)

// return final output
return output
}

/*
newsubs generates a feasible new subscript value set
within the input search domain
*/
func NewSubs(curSubs, destinationSubs []int, curDist
float64, searchParameters *Parameters, searchDomain
*Domain) (subs []int) {

    // initialize iteration counter
    var iterations int = 1

    // initialize output
    output := make([]int, 2)

    /*
generate and fix a bivariate normally
distributed random vector prohibit all zero cases
and validate using the search domain
*/
    for {

```



```

// generate mu and sigma values
mu := NewMu(curSubs, destinationSubs)
sigma := NewSigma(iterations,
searchParameters.RndCoef, curDist)

// generate fixed random bivariate normally
// distributed numbers
try := NewRandom(mu, sigma)

// write output
output[o] = curSubs[o] + try[o]
output[i] = curSubs[i] + try[i]

// DEBUG
// test if currentIndex is forbidden
if searchDomain.Matrix.At(output[o],
output[i]) == 0.0 {
    iterations += 1
    continue
}

// test if currentIndex inside search domain
if output[o] > searchDomain.Rows-1 ||
output[i] > searchDomain.Cols-1 || output[o] <
0 || output[i] < 0 {
    iterations += 1
    continue
}

```

```

        } else {
            break
        }
    }

    // return final output
    return output
}

/*
directedwalk generates a new directed walk connecting
a source subscript to a destination subscript within
the context of an input search domain
*/
func DirectedWalk(sourceSubs, destinationSubs []int,
searchDomain *Domain, searchParameters *Parameters,
basisSolution *Basis) (subs [][]int) {

    // initialize chromosomal 2D slice with source
    // subscript as first element
    output := make([][]int, 1, basisSolution.MaxLen)
    output[0] = make([]int, 2)
    output[0][0] = sourceSubs[0]
    output[0][1] = sourceSubs[1]

    // enter unbounded for loop
    for {

```

```

// initialize new tabu matrix
tabu := mat64.NewDense(searchDomain.Rows,
searchDomain.Cols, nil)
for i := 0; i < searchDomain.Rows; i++ {
    for j := 0; j < searchDomain.Cols; j++ {

        if i == 0 ||
i == searchDomain.Rows-1
|| j == 0 ||
j == searchDomain.Cols-1 {
            tabu.Set(i, j, 0.0)
        } else {
            tabu.Set(i, j, 1.0)
        }
    }
}

//tabu.Clone(searchDomain.Matrix)
tabu.Set(sourceSubs[0], sourceSubs[1], 0.0)

// initialize current subscripts, distance,
// try, and iteration counter
curSubs := make([]int, 2)
var curDist float64
var try []int

```

```

// enter bounded for loop
for i := 0; i < basisSolution.MaxLen; i++ {

    // get current subscripts
    curSubs = output[len(output)-1]

    // validate tabu neighborhood
    if ValidateTabu(curSubs, tabu) == false {
        break
    }

    // compute current distance
    curDist =
    basisSolution.Matrix.At(curSubs[0],
    curSubs[1])

    // generate new try
    try = NewSubs(curSubs, destinationSubs,
    curDist, searchParameters, searchDomain)

    // apply control conditions
    if try[0] == destinationSubs[0] && try[1]
    == destinationSubs[1] {
        output = append(output, try)
        break
    } else if
    tabu.At(try[0], try[1]) == 0.0 {

```

```

        continue
    } else {
        output = append(output, try)
        tabu.Set(try[o], try[i], 0.0)
    }
}

// repeat walk if destination not reached
if output[len(output)-1][0] ==
destinationSubs[o] && output[len(output)-1][1]
== destinationSubs[i] {

    // break unbounded for loop
    break
} else {

    // re-initialize chromosomal 2D
    // slice with source subscript
    // as first element
    output := make([][]int, 1,
basisSolution.MaxLen)
    output[o] = make([]int, 2)
    output[o][0] = sourceSubs[o]
    output[o][1] = sourceSubs[i]

    // restart process
    continue
}

```

```

        }
    }

    // return final output
    return output
}

/*
mutationwalk generates a new directed walk connecting
a source subscript to a destination subscript within
the context of an input mutation search domain
*/
func MutationWalk(sourceSubs, destinationSubs []int,
searchDomain *Domain, searchParameters *Parameters,
basisSolution *Basis) (subs [][]int, tabuTest bool) {

    // initialize chromosomal 2D slice with source
    // subscript as first element
    output := make([][]int, 1, basisSolution.MaxLen)
    output[0] = make([]int, 2)
    output[0][0] = sourceSubs[0]
    output[0][1] = sourceSubs[1]

    // initialize new tabu matrix
    tabu := mat64.NewDense(searchDomain.Rows,
searchDomain.Cols, nil)
    tabu.Clone(searchDomain.Matrix)

```

```

tabu.Set(sourceSubs[0], sourceSubs[1], 0.0)

// initialize current subscripts, distance, try,
// and iteration counter
curSubs := make([]int, 2)
var curDist float64
var try []int
var test bool

// enter un-bounded for loop
for {

    // get current subscripts
    curSubs = output[len(output)-1]

    // compute current distance
    curDist = basisSolution.Matrix.At(curSubs[0],
    curSubs[1])

    // generate new try
    try = NewSubs(curSubs,
    searchParameters.DstSubs, curDist,
    searchParameters, searchDomain)

    // apply control conditions
    if try[0] == destinationSubs[0] && try[1] ==
    destinationSubs[1] {

```

```

        output = append(output, try)
        break
    } else if tabu.At(try[o], try[1]) == o.o {
        continue
    } else {
        output = append(output, try)
        tabu.Set(try[o], try[1], o.o)
    }

    // validate tabu matrix
    test = ValidateMutationSubDomain(try,
    destinationSubs, tabu)

    // reset if tabu is invalid
    if test == false {
        break
    }
}

// return final output
return output, test
}

```

/*
newnodesubs generates an poutput slice of new
intermediate destination nodes that are progressively
further, in terms of euclidean distance, from


```

a given input source location and are orientation
towards a given destination location
*/
func NewNodeSubs(searchDomain *Domain,
searchParameters *Parameters) (nodeSubs [][]int) {

    // initialize output
    output := make([][]int, 1)
    output[0] = searchParameters.SrcSubs

    // check band count against input distance matrix
    // size
    if searchDomain.BndCnt < 3 {

        // assign node subscripts
        output = append(output,
            searchParameters.DstSubs)
    } else if searchDomain.BndCnt >= 3 {

        // generate distance matrix from source
        // subscripts
        distMat :=
            AllDistance(searchParameters.SrcSubs,
                searchDomain.Matrix)

        // encode distance bands
        bandMat := DistanceBands(searchDomain.BndCnt,

```

```

distMat)

if bandMat.At(searchParameters.SrcSubs[o],
searchParameters.SrcSubs[1]) ==
bandMat.At(searchParameters.DstSubs[o],
searchParameters.DstSubs[1]) {

    // assign node subscripts
    output = append(output,
searchParameters.DstSubs)
} else {

    // seed random number generator
    rand.Seed(time.Now().UnixNano())

    // loop through band vector and generate
    // band value subscripts
    for i := 1; i <
searchDomain.BndCnt-1; i++
    {

        // generate band mask
        bandMaskMat :=
        BandMask(
        float64(i),
        bandMat)

        // break loop if the

```

```

// destination is in
// the current band mask
if
(searchParameters.DstSubs[0],
searchParameters.DstSubs[1])
== 1.0 {
    break
}

// generate orientation mask
orientMaskMat :=
OrientationMask(output[i-1],
searchParameters.DstSubs,
searchDomain.Matrix)

// initialize final mask
finalMaskMat :=
mat64.NewDense(searchDomain.Rows,
searchDomain.Cols, nil)

// compute final mask through
// elementwise multiplication
finalMaskMat.MulElem(bandMaskMat,
orientMaskMat)

// generate subs from final mask
finalSubs :=

```

```

NonZeroSubs( finalMaskMat )

// generate random number of length
// interval
randInd :=
finalSubs [
rand.Intn( len( finalSubs ))]

// break out of loop if
// final mask is empty
if randInd[0] == 0 &&
randInd[1] == 0 {
    break
}

// extract randomly selected
// value and write to output
output = append( output , randInd)
}

// set the final subscript to the
// destination
output = append( output ,
searchParameters.DstSubs)
}
}

```

```

        // return output
        return output
    }

    /*
    multipartdirectedwalk generates a new multipart
    directed walk from a given set of input problem
    parameters
    */
    func MultiPartDirectedWalk(nodeSubs [][]int,
    searchDomain *Domain, searchParameters *Parameters)
    (subs [][]int) {

        // generate basis solution
        basisSolution := NewBasis(nodeSubs[0],
        nodeSubs[1], searchDomain)

        // initialize output
        output := make([][]int, basisSolution.MaxLen)

        // catch single part walk case
        if len(nodeSubs) == 2 {

            // generate output as a single part directed
            // walk
            output = DirectedWalk(nodeSubs[0],
            nodeSubs[1], searchDomain, searchParameters,

```

```

basisSolution)

} else if len(nodeSubs) > 2 {

    // generate output as multi part directed walk
    output = DirectedWalk(nodeSubs[0],
nodeSubs[1], searchDomain, searchParameters,
basisSolution)

    // loop through the band count to generate sub
    // walk parts
    for i := 1; i < len(nodeSubs)-1; i++ {

        // generate sub domain
        subSearchDomain, subSource,
subDestination := SubDomain(nodeSubs[i],
nodeSubs[i+1], searchDomain.Matrix)

        // generate basis solution
        basisSolution = NewBasis(subSource,
subDestination, subSearchDomain)

        // generate initial output slice and then
        // append subsequent slices
        curWalk := DirectedWalk(subSource,
subDestination, subSearchDomain,
searchParameters, basisSolution)

```

```

// translate subscripts
transWalk :=
TranslateWalkSubs(nodeSubs[i], curWalk)

// append subscripts to output
for j := 1; j < len(transWalk); j++ {
    output = append(output,
        transWalk[j])
}
}

// return output
return output
}

```

<types.go>

```
/*
Copyright ©2015 The corridor Authors. All rights
reserved. Use of this source code is governed by a
BSD-style license that can be found in the LICENSE
file.
*/

package corridor

import (
    "github.com/gonum/matrix/mat64"
    "github.com/satori/go.uuid"
)

/* parameters are comprised of fixed input avlues
that are unique to the problem specification that are
referenced by the algorithm at various stage of the
solution process
*/

type Parameters struct {
    SrcSubs []int
    DstSubs []int
    RndCoef float64
    PopSize int
    SelFrac float64
}
```



```

        SelProb float64
        MutaCnt int
        MutaFrc float64
        EvoSize int
        ConSize int
    }

    /*
    domains are comprised of boolean arrays which
    indicate the feasible locations for the search
    algorithm
    */
    type Domain struct {
        Rows int
        Cols int
        Matrix *mat64.Dense
        BndCnt int
    }

    /*
    objectives are comprised of matrices which use
    location indices to key to floating point fitness
    values within the search domain
    */
    type Objective struct {
        Id int
        Matrix *mat64.Dense
    }

```

```

}

/*
multiObjective objects are comprised of a channel of
individual independent objectives that are used for
the evaluation of chromosome and population level
fitness values
*/
type MultiObjective struct {
    ObjectiveCount int
    Objectives      []*Objective
}

/*
a basis solution is comprised of the subscript
indices forming the euclidean shortest path
connecting the source to the destination
*/
type Basis struct {
    Matrix *mat64.Dense
    Subs   [][]int
    MaxLen int
}

/*
chromosomes are comprised of genes which are
distinct row column indices to some spatially

```

```

reference search domain
*/
type Chromosome struct {
    Id          uuid.UUID
    Subs        [][]int
    Fitness     [][]float64
    TotalFitness []float64
    AggregateFitness float64
}

/*
populations are comprised of a fixed number of
chromosomes. This number corresponds to the
populationSize.
*/
type Population struct {
    Id          int
    Chromosomes chan *Chromosome
    MeanFitness []float64
    AggregateMeanFitness float64
}

/*
evolutions are comprised of a stochastic number of
populations. This number is determined by the
convergence rate of the algorithm.
*/

```

```
type Evolution struct {  
    Populations      chan *Population  
    FitnessGradient []float64  
}
```

```
<visualize.go>
```

```
/*
Copyright ©2015 The corridor Authors. All rights
reserved. Use of this source code is governed by a
BSD-style license that can be found in the LICENSE
file.package main
*/

package corridor

import (
    "fmt"

    "github.com/gonum/matrix/mat64"
)

/*
function to print the properties of a search domain
to the command line
*/
func ViewDomain(searchDomain *Domain) {

    // get search domain matrix dimensions
    rows, _ := searchDomain.Matrix.Dims()

    // print domain values to command line
```

```

fmt.Printf("Search Domain Values = \n")
for i := 0; i < rows; i++ {
    rawRowVals :=
        searchDomain.Matrix.RawRowView(i)
    fmt.Printf("\%I.0f\n", rawRowVals)
}
}

/*
function to print the properties of a basis solution
to the command line
*/
func ViewBasis(basisSolution *Basis) {

    // get basis solution matrix dimensions
    rows, _ := basisSolution.Matrix.Dims()

    // print domain values to command line
    fmt.Printf("Basis Solution Values = \n")
    for i := 0; i < rows; i++ {
        rawRowVals :=
            basisSolution.Matrix.RawRowView(i)
        fmt.Printf("\%I.0f\n", rawRowVals)
    }
}

/*

```

```

function to print the properties of a chromosome to
the command line
*/
func ViewChromosome(searchDomain *Domain,
searchParameters *Parameters, inputChromosome
*Chromosome) {

    // get search domain matrix dimensions and empty
    // value slice
    domainSize := searchDomain.Rows *
searchDomain.Cols
    v := make([]float64, domainSize)

    // allocate new empty matrix
    blankMat := mat64.NewDense(searchDomain.Rows,
searchDomain.Cols, v)

    // assign chromosome values to the empty matrix
    for i := 0; i < len(inputChromosome.Subs); i++ {
        blankMat.Set(inputChromosome.Subs[i][0],
inputChromosome.Subs[i][1], 1.0)
    }

    // print chromosome values to command line
    fmt.Printf("Chromosome = \n")
    for i := 0; i < searchDomain.Rows; i++ {
        rawRowVals := blankMat.RawRowView(i)

```

```

        fmt.Printf("%I.0f\n", rawRowVals)
    }

    // print output to the command line
    fmt.Printf("Chromosome Length = %d\n",
        len(inputChromosome.Subs))
    fmt.Printf("Chromosome Total Fitness = %1.5f\n",
        inputChromosome.TotalFitness)
}

/*
functions to print the frequency of chromosomes in a
search domain to the command line
*/
func ViewPopulation(searchDomain *Domain,
    searchParameters *Parameters, inputPopulation
    *Population) {

    // allocate new empty matrix
    mat := mat64.NewDense(searchDomain.Rows,
        searchDomain.Cols, nil)

    // accumulated visited subscripts in new empty
    // matrix
    for i := 0; i < searchParameters.PopSize; i++ {

        // extract current chromosome from channel

```



```

    curChrom := <-inputPopulation.Chromosomes
    curInd := curChrom.Subs
    lenCurInd := len(curInd)

    // iterate over subscript indices
    for j := 0; j < lenCurInd; j++ {
        curSubs := curInd[j]
        curVal := mat.At(curSubs[0], curSubs[1])
        newVal := curVal + 1
        mat.Set(curSubs[0], curSubs[1], newVal)
    }

    // repopulate channel
    inputPopulation.Chromosomes <- curChrom
}

// print matrix values to command line
fmt.Printf("Population Size = %d\n",
searchParameters.PopSize)
fmt.Printf("Population Frequency = \n")
for q := 0; q < searchDomain.Rows; q++ {
    rawRowVals := mat.RawRowView(q)
    fmt.Printf("%*.0f\n",
DigitCount(searchParameters.PopSize)+1,
rawRowVals)
}
}

```

References

- [1] Adams, B., Dajani, J., & Gemmell, R. (1973). On the Centralization of Wastewater Treatment Facilities. *Journal of the American Water Resources Association*, 9(5), 1065–1065.
- [2] Aissi, H., Chakhar, S., & Mousseau, V. (2012). GIS-based multicriteria evaluation approach for corridor siting. *Environment and Planning B: Planning and Design*, 39(2), 287–307.
- [3] Angelakis, A. N. & Rose, J. B. (2014). *Evolution of Sanitation and Wastewater Technologies Through the Centuries*. IWA Publishing.
- [4] Asano, T., Burton, F., Leverenz, H., Tsuchihashi, R., & Tchobanoglous, G. (2007). *Water Reuse: Issues, Technologies, and Applications*. Boston, MA: McGraw-Hill Professional, 1 edition edition.
- [5] Association, W. R. (2011). *National Database of Water Reuse Facilities Summary Report*. Technical report.
- [6] Averyt, K., Macknick, J., Rogers, J., Madden, N., Fisher, J., Meldrum, J., & Newmark, R. (2013). Water use for electricity in the United States: an analysis of reported and calculated water use information for 2008. *Environmental Research Letters*, 8(1), 015001.
- [7] Bennett, D. A., Xiao, N., & Armstrong, M. P. (2004). Exploring the geographic consequences of public policies using evolutionary algorithms. *Annals of the Association of American Geographers*, 94(4), 827–847.
- [8] Bixio, D., Thoeye, C., Wintgens, T., Ravazzini, a., Miska, V., Muston, M., Chikurel, H., Aharoni, a., Joksimovic, D., & Melin, T. (2008). Water reclamation and reuse: implementation and management issues. *Desalination*, 218(1-3), 13–23.
- [9] Bolstad, P. (2005). *GIS Fundamentals: A First Text on Geographic Information Systems*. Eider Press.
- [10] Bouwer, H. (1999). Artificial Recharge of Groundwater: Systems, Design, and Management. In L. W. Mays (Ed.), *Hydraulic Design Handbook* chapter 24, (pp. 1–44). New York, USA: McGraw-Hill Professional, 1 edition.

- [11] Bresenham, J. (1977). A linear algorithm for incremental digital display of circular arcs. *Communications of the ACM*, 20(2), 100–106.
- [12] California Department of Health Services Division of Drinking Water and Environmental Management (2001). *California Health Laws Related to Recycled Water: "The Purple Book"*. Technical Report June, State of California-Health and Human Services Agency, Sacramento, California.
- [13] California Department of Health Services Division of Drinking Water and Environmental Management (2011). *Title 22*. Technical report, State of California-Health and Human Services Agency, Sacramento, California.
- [14] California Department of Water Resources Recycled Water Task Force (2003). *Water Recycling 2030*. Technical report, California Department of Water Resources.
- [15] CH2M Hill (2004). *Recycled Water Project Implementation Strategies Technical Memorandum*. Technical report, The United States Bureau of Land Reclamation, Santa Ana, California.
- [16] Chakhar, S. & Martel, J.-M. (2003). Enhancing geographical information systems capabilities with multi-criteria evaluation functions. *Journal of Geographic Information and Decision Analysis*, 7(2), 47–71.
- [17] Cherkassky, B. V., Goldberg, A. V., & Radzik, T. (1996). Shortest paths algorithms: Theory and experimental evaluation. *Mathematical programming*, 73(2), 129–174.
- [18] Church, R. L. (2002). Geographical information systems and location science. *Computers & Operations Research*, 29(6), 541–562.
- [19] Church, R. L., Loban, S. R., & Lombard, K. (1992). An interface for exploring spatial alternatives for a corridor location problem. *Computers & Geosciences*, 18(8), 1095–1105.
- [20] Coello, C., Lamont, G., & Veldhuisen, D. V. (2007). *Evolutionary Algorithms for Solving Multi-Objective Problems*. New York, NY: Springer, second edition.
- [21] Coello, C. A. C., Aguirre, A. H., & Zitzler, E. (2001). Evolutionary multi-criterion optimization.
- [22] Collins, M. G., Steiner, F. R., & Rushman, M. J. (2001). Land-use suitability analysis in the United States: Historical development and promising technological achievements. *Environmental Management*, 28(5), 611–621.
- [23] Committee on Sustainable Underground Storage of Recoverable Water, N. R. C. (2008). *Prospects for Managed Underground Storage of Recoverable Water*. Washington D.C.: National Academies Press.

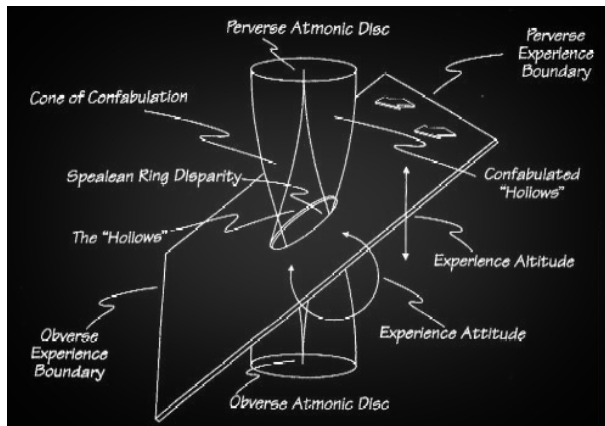
- [24] Daughton, C. G. (2004). Ground Water Recharge and Chemical Contaminants: Challenges in Communicating the Connections and Collisions of Two Disparate Worlds. *Ground Water Monitoring & Remediation*, 24(2), 127–138.
- [25] Deb, K. (2001). *Multi-Objective Optimization using Evolutionary Algorithms*. New York, New York, USA: Wiley.
- [26] Deb, K. (2014). *Search Methodologies*. Boston, MA: Springer US.
- [27] Dolničar, S. & Saunders, C. (2006). Recycled water for consumer markets — a marketing research review and agenda. *Desalination*, 187(1-3), 203–214.
- [28] Dreyfus, S. E. (1969). An appraisal of some shortest-path algorithms. *Operations research*, 17(3), 395–412.
- [29] Fonseca, C. M. & Fleming, P. J. (1995). An overview of evolutionary algorithms in multiobjective optimization. *Evolutionary computation*, 3(1), 1–16.
- [30] Freeman, G., Poghosyan, M., & Lee, M. (2008). *Where Will We Get the Water? Assessing Southern California's Future Water Strategies*. Technical report, Los Angeles County Economic Development Corporation (LACEDC), Los Angeles, California.
- [31] Goldberg, D. E. (1989). *Genetic Algorithms in Search, Optimization, and Machine Learning*, volume Addison-Wesley of *Artificial Intelligence*. Addison-Wesley.
- [32] Goldberg, D. E. & Holland, J. H. (1988). Genetic Algorithms and Machine Learning. *Machine Learning*, 3(2), 95–99.
- [33] Goodchild, M. F. (1977). An evaluation of lattice solutions to the problem of corridor location. *Environment and Planning A*, 9(7), 727–738.
- [34] Grübler, A. (2003). *Technology and global change*. Cambridge University Press.
- [35] Grübler, A. (2010). *Technological change and the environment*. Routledge.
- [36] Hallam, C., Harrison, K. J., & Ward, J. A. (2001). A multiobjective optimal path algorithm. *Digital Signal Processing*, 11(2), 133–143.
- [37] Hart, P. E., Nilsson, N. J., & Raphael, B. (1968). A formal basis for the heuristic determination of minimum cost paths. *Systems Science and Cybernetics, IEEE Transactions on*, 4(2), 100–107.
- [38] Hopkins, L. D. (1977). Methods for Generating Land Suitability Maps: A Comparative Evaluation. *Journal of the American Institute of Planners*, 43(4), 386–400.
- [39] Horton, M. B. (2009). *Treatment Technology Report for Recycled Water*. Technical Report 805, State of California-Health and Human Services Agency, Sacramento, California.

- [40] Horvath, A. (2005). *Life Cycle Energy Assessment of Alternative Water Supply Systems in California*. Technical Report July, California Energy Commission, Public Interest Energy Research Program, Berkeley, CA.
- [41] Huber, D. L. & Church, R. L. (1985). Transmission corridor location modeling. *Journal of Transportation Engineering*, 111(2), 114–130.
- [42] Jankowski, P. (1995). Integrating geographical information systems and multiple criteria decision-making methods. *International journal of geographical information systems*, 9(3), 251–273.
- [43] Jaynes, E. (1988). The evolution of Carnot's principle. *Maximum-entropy and bayesian methods in science ...*, 1, 1–17.
- [44] Johnson, N. L., Kotz, S., & Balakrishnan, N. (2002). *Continuous Multivariate Distributions, volume 1, Models and Applications*, volume 59. New York: John Wiley & Sons.
- [45] Kennedy, L. A. & Tsuchihashi, R. (2005). Is Water Reuse Sustainable? Factors Affecting its Sustainability. *The Arabian Journal for Science and Engineering*, 30(2), 3–15.
- [46] Klein, G., Krebs, M., Hall, V., O'Brien, T., & Blevins, B. B. (2005). *California's Water – Energy Relationship*. Technical Report November, California Energy Commission (CEC), Sacramento, California.
- [47] Lautze, J., Stander, E., Drechsel, P., da Silva, A. K., & Keraita, B. (2014). *Global experiences in water reuse*. International Water Management Institute (IWMI); CGIAR Research Program on Water, Land and Ecosystems (WLE).
- [48] Levine, A. D. & Asano, T. (2004). Recovering Sustainable Water from Wastewater. *Environmental science & technology*, 38(11), 201A–208A.
- [49] Liu, H. (2003). *Pipeline engineering*. CRC Press.
- [50] Lofman, D., Petersen, M., & Bower, A. (2010). Water, Energy and Environment Nexus: The California Experience. *International Journal of Water Resources Development*, 18(1), 73–85.
- [51] Lombard, K. & Church, R. L. (1993). The gateway shortest path problem: generating alternative routes for a corridor location problem. *Geographical systems*, 1(1), 25–45.
- [52] Malczewski, J. (2006). GIS-based multicriteria decision analysis: a survey of the literature. *International Journal of Geographical Information Science*, 20(7), 703–726.

- [53] McKay, M. D., Beckman, R. J., & Conover, W. J. (1979). Comparison of three methods for selecting values of input variables in the analysis of output from a computer code. *Technometrics*, 21(2), 239–245.
- [54] Metcalf, E., Eddy, H. P., & Tchobanoglous, G. (1991). Wastewater engineering: treatment, disposal, and reuse. *Water Resources and Environmental Engineering*.
- [55] Mooney, P. & Winstanley, A. (2006). An evolutionary algorithm for multicriteria path optimization problems. *International Journal of Geographical Information Science*, 20(4), 401–423.
- [56] Mousseau, V., Aissi, H., & Chakhar, S. (2010). A Three-Phase Approach and a Fast Algorithm to Compute Efficient Corridors within GIS Framework. *CER*, 10(7), 1–18.
- [57] Neema, M. & Ohgai, a. (2010). Multi-objective location modeling of urban parks and open spaces: Continuous optimization. *Computers, Environment and Urban Systems*, 34(5), 359–376.
- [58] NRC (2012). *Water Reuse: Potential for Expanding the Nation's Water Supply Through Reuse of Municipal Wastewater*. National Academies Press.
- [59] Pangilinan, J. M. A. & Janssens, G. K. (2007). Evolutionary algorithms for the multi-objective shortest path problem. *International Journal of Applied Science, Engineering, and Technology*, 4(1), 205–210.
- [60] Pate, R., Hightower, M., Cameron, C., & Einfeld, W. (2007). *Overview of Energy-Water Interdependencies and the Emerging Energy Demands on Water Resources*. Technical Report March 2007, Sandia National Laboratory, Albuquerque, New Mexico.
- [61] Pennington, D. W., Potting, J., Finnveden, G., Lindeijer, E., Jolliet, O., Rydberg, T., & Rebitzer, G. (2004). Life cycle assessment part 2: current impact assessment practice. *Environment International*, 30(5), 721–39.
- [62] Rebitzer, G., Ekvall, T., Frischknecht, R., Hunkeler, D., Norris, G., Rydberg, T., Schmidt, W.-P., Suh, S., Weidema, B. P., & Pennington, D. W. (2004). Life cycle assessment part 1: framework, goal and scope definition, inventory analysis, and applications. *Environment international*, 30(5), 701–20.
- [63] Roberts, S. a., Hall, G. B., & Calamai, P. H. (2010). Evolutionary Multi-objective Optimization for landscape system design. *Journal of Geographical Systems*, 13(3), 299–326.

- [64] Rodrigo, D., Calva, E. J. L., Cannan, A., Roesner, L., & O'Conner, T. P. (2012). *Total Water Management*. Technical Report July, United States Environmental Protection Agency: National Risk Management Research Laboratory Office of Research and Development, Cincinnati, Ohio.
- [65] Romero-Hernandez, O. (2004). Applying Life Cycle Tools and Process Engineering to Determine the Most Adequate Treatment Process Conditions. A Tool in Environmental Policy. *The International Journal of Life Cycle Assessment*, 10(5), 355–363.
- [66] Scaparra, M. P., Church, R. L., & Medrano, F. A. (2014). Corridor location: the multi-gateway shortest path model. *Journal of Geographical Systems*, 16(3), 287–309.
- [67] Schwarzenegger, A., Chrisman, M., & Snow, L. A. (2005). *California Water Plan Update 2005: Highlights*. Technical report, California Department of Water Resources, Sacramento, California.
- [68] Seaber, P. R., Kapinos, F. P., & Knapp, G. L. (1987). *Hydrologic Unit Maps: US Geological Survey Water Supply Paper 2294*. USGS.
- [69] Seiler, K.-P. & Gat, J. R. (2007). *Man's Impact on the Groundwater Recharge*. Springer.
- [70] Stander, A. G. J., Vuuren, L. R. J. V., & Stander, G. J. (1969). The Reclamation of Potable Water from Wastewater. *Journal (Water Pollution Control Federation)*, 41(3), 355–367.
- [71] Stefanakis, E. & Kavouras, M. (1995). On the determination of the optimum path in space. In *Spatial Information Theory A Theoretical Basis for GIS* (pp. 241–257). Springer.
- [72] Stokes, J. & Horvath, A. (2006). LCA Methodology and Case Study Life Cycle Energy Assessment of Alternative Water Supply Systems. *International Journal of Life Cycle Assessment*, 11(5), 335–343.
- [73] Stokes, J. & Horvath, A. (2011). Life-Cycle Assessment of Urban Water Provision : Tool and Case Study in California. *Journal of Infrastructure Systems*, (March), 15–24.
- [74] Stokes, J. R., Hendrickson, T. P., & Horvath, A. (2014). Save water to save carbon and money: developing abatement costs for expanded greenhouse gas reduction portfolios. *Environmental science & technology*, 48(23), 13583–91.
- [75] Stokes, J. R. & Horvath, A. (2010). Supply-chain environmental effects of wastewater utilities. *Environmental Research Letters*, 5(1), 014015.
- [76] Tchobanoglous, G., Burton, F., & Stensel, H. D. (2003). *Wastewater Engineering (Treatment and Reuse)*. McGraw-Hill Science/Engineering/Math, 4 edition.

- [77] Tomlin, C. (1994). Map algebra: one perspective. *Landscape and Urban Planning*, 30(1-2), 3-12.
- [78] Tomlin, C. & Berry, J. (1979). A Mathematical Structure for Cartographic Modeling in Environmental Analysis. In *Proceedings of the 39th Symposium of the American Conference on Surveying and Mapping* (pp. 269-283).
- [79] Tsai, C.-C., Huang, H.-C., & Chan, C.-K. (2011). Parallel elite genetic algorithm and its application to global path planning for autonomous robot navigation. *Industrial Electronics, IEEE Transactions on*, 58(10), 4813-4821.
- [80] USEPA (2012). *2012 Guidelines for Water Reuse*. Technical Report September, United States Environmental Protection Agency, Office of Wastewater Management, Washington D.C.
- [81] Wilkinson, R. C. (2007). *Analysis of the Energy Intensity of Water Supplies for West Basin Municipal Water District*. Technical report, West Basin Municipal Water District, Carson, CA.
- [82] World Health Organization (2006). *WHO Guidelines for the Safe Use of Wastewater, Excreta and Greywater: Volume 1, Policy and regulatory aspects*. Technical report, World Health Organization.
- [83] Ye, K. Q. (1998). Orthogonal column Latin hypercubes and their application in computer experiments. *Journal of the American Statistical Association*, 93(444), 1430-1439.
- [84] Younos, T. & Caitlin A, G., Eds. (2014). *Potable Water: Emerging Global Problems and Solutions*. Springer.
- [85] Zhang, X. & Armstrong, M. P. (2008). Genetic algorithms and the corridor location problem: multiple objectives and alternative solutions. *Environment and Planning B: Planning and Design*, 35(1), 148-168.
- [86] Zhou, A., Qu, B.-Y., Li, H., Zhao, S.-Z., Suganthan, P. N., & Zhang, Q. (2011). Multiobjective evolutionary algorithms: A survey of the state of the art. *Swarm and Evolutionary Computation*, 1(1), 32-49.
- [87] Zhou, J. & Civco, D. (1996). Using genetic learning neural networks for spatial decision making in GIS. *Photogrammetric Engineering and Remote Sensing*, 62(11), 1287-1295.
- [88] Zitzler, E. & Thiele, L. (1998). Multiobjective optimization using evolutionary algorithms—a comparative case study. In *Parallel problem solving from nature—PPSN V* (pp. 292-301).: Springer.



WE, AMNESIACS ALL, condemned to live in an eternally fleeting present, have created the most elaborate of human constructions, memory, to buffer ourselves against the intolerable knowledge of the irreversible passage of time and the irretrievability of its moments and events.

- Geoffrey Sonnabend